

POWER FLOW IN STRUCTURES DURING STEADY-STATE FORCED VIBRATION

by

JEROME ANTONIO

BSc, MSc, DIC

Thesis submitted in fulfilment of the requirements
for the degree of Doctor of Philosophy
of the University of London

Department of Mechanical Engineering
Imperial College of Science and Technology
London SW7

April 1984

To Patricia and Sika

ABSTRACT

A study is presented of the flow of vibrational power in linear structures during steady-state forced vibration. The main thrust of the work is directed towards an assessment of some applications proposed in the literature for vibrational power flow, and the identification of other areas where power flow methods are applicable.

With the help of basic Electrical Engineering concepts, the vibration analysis of spring-mass-damper systems is used as a vehicle for clarifying the basic relationships between power, energy and motion response in vibrating structures. The structures under consideration are presumed to be composed of substructures connected together at joints. The expressions for power flow are derived in terms of the frequency response matrices, and the nature of energy flow via the coordinate directions at the joints between substructures is examined.

A vibration isolation method proposed in the literature aims at minimising the time-average power flow to the structure which is to be isolated. An evaluation of the proposed method is presented. It is shown that under certain circumstances a reduction of the time-average power flow will not necessarily result in lower vibration amplitudes and, therefore, the proposed method must be employed with caution.

One object of the present work is to explore other areas of vibration analysis, outside the context of Statistical Energy Analysis, where the concept of power flow could be usefully employed. To this end, a method is proposed for assessing the relative importance of coordinates in the vibration analysis of connected structures by the Impedance Coupling technique. The method is based on the assumption that the relative importance of any coordinate at a joint depends on the magnitude of the energy transferred per cycle via that coordinate direction. The method is applied to a range of test structures, and the results show that the underlying assumption is sound and that the method works.

The flow of vibrational power in a simple beam structure is measured using a method proposed in the literature. The accuracy of the measuring technique is assessed, and some of the difficulties encountered in its application are discussed.

Acknowledgements

The research described in this thesis was carried out under the joint supervision of Professor P. Grootenhuis and Professor D.J. Ewins. Their guidance and encouragement ensured that I derived the greatest possible benefit from the conduct of my research. I am very pleased to acknowledge my debt to them.

I am indebted to Professor B.S. Berger (visiting from University of Maryland, USA) who also read the draft of this thesis and offered many suggestions for improvement.

I wish to record my sincere thanks to my colleagues in the Dynamics Group at Imperial College who have always been prepared to lend me a helping hand. Special thanks are due to my former colleagues Dr. H.D. Afolabi, Dr. J. Sidhu, Dr. B. Hillary and Dr. M. Imregun. I would also like to thank Dr. P. Cawley and Mr. D.A. Robb for the interest shown in my work, and Mr. R. Gunn, our Laboratory Technician, for his kind assistance during the course of vibration testing.

I am also indebted to *Bruel&Kjaer* who kindly agreed to provide on loan some of the equipment required for my experimental work.

Finally, I would like to acknowledge the financial support provided under the Commonwealth Scholarship and Fellowship Plan and the Overseas Research Students (ORS) Awards scheme.

J. ANTONIO

Contents

	Page
Abstract	3
Acknowledgements	4
Nomenclature	9
Chapter 1: Introduction	12
Chapter 2: Power and energy relations for spring-mass-damper systems subjected to sinusoidal force excitation	21
2.1 Introduction	21
2.2 The simple one-degree-of-freedom system	22
2.2.1 Kinetic and potential energy	22
2.2.2 Instantaneous power and energy	24
2.2.3 The concept of complex power	29
2.2.4 Frequency response functions in terms of energy functions	32
2.2.5 Variation of time-average power with excitation frequency and damping coefficient	34
2.2.6 Relationships between time-average power, velocity amplitude and force transmissibility	37
2.3 Multi-degree-of-freedom spring-mass-damper systems	40
2.3.1 Instantaneous power and the energy functions for the general N-degree-of-freedom system	40
2.3.2 The undamped dynamic vibration absorber	47
2.4 Discussion	51

Chapter 3:Power flow and energy transfer in connected structures	53
3.1 Introduction	53
3.2 Power input to elastic structures	54
3.3 General expressions for time-average power flow in connected structures	56
3.3.1 Power flow when coupling is in a single coordinate direction	56
3.3.2 The general case of power flow	60
3.3.3 Some consequences of power balance considerations	62
3.3.4 Random excitation	65
3.4 Energy flow via coordinate directions at joints between substructures	71
3.5 Discussion	74
Chapter 4: A method for assessing the relative importance of coordinates in the vibration analysis of connected structures by the Impedance Coupling technique	75
4.1 Introduction	75
4.2 The Impedance Coupling Technique	76
4.2.1 Single-coordinate coupling	77
4.2.2 Coupling in more than one coordinate	79
4.2.3 The general case	80
4.2.4 Coordinate elimination	83
4.3 Proposed method for assessing the relative importance of coordinates	85
4.4 Some illustrative examples	87
4.4.1 Example I	87
4.4.2 Example II	91
4.4.3 Example III	94
4.4.4 Example IV	100
4.5 Discussion	105

Chapter 5: An evaluation of the power flow approach to vibration isolation problems	108
5.1 Introduction	108
5.2 Expressions for time-average power flow, velocity amplitudes and force transmitted to the foundation	110
5.3 Influence of changes in the machine-isolator subsystem	110
5.4 Influence of changes in the characteristics of the foundation	112
5.4.1 One-degree-of-freedom approximation for foundation characteristics	112
5.4.2 Semi-infinite beam approximation for foundation characteristics	118
5.5 Discussion	123
Chapter 6: Measurement of time-average power flow along a simple beam structure	127
6.1 Introduction	127
6.2 Theory and measuring method	128
6.3 Theoretical study of test structure	133
6.3.1 The test structure and its model	133
6.3.2 Computed results	136
6.4 Experimental results	137
6.4.1 Set-up for vibration intensity measurements	137
6.4.2 Variation of intensity with distance from driving point	141
6.4.3 Variation of intensity with excitation frequency	143
6.5 Discussion	144
Chapter 7: Conclusions	150

References	155
Appendix 1: Determination of various areas under instantaneous power curve	159
Appendix 2: The influence of damping on the mobility of the simple oscillator	161
Appendix 3: Analysis of vibration intensity in uniform beams	164

Nomenclature

Most of the symbols used in this thesis have been defined in the text. The following list includes some of the more important symbols and those that have not been defined explicitly in the text.

- a Acceleration
 - b Width of beam
 - A Cross-section area; also, a constant
 - [C] Viscous damping matrix
 - D A constant; also, Rayleigh's Dissipation Function
 - E Modulus of Elasticity
 - f,F Force
 - F_t Transmitted force
 - f_i Force applied to Structure A
 - $\{f\}_A$ Vector of force amplitudes relating to Structure A
 - I Second moment of area
 - I_0 Second moment of area per unit width of a beam
 - k Stiffness; also, wavenumber
 - K Stiffness
 - [K] Stiffness matrix
 - iii Mass per unit length
 - m Mass
 - M Mass; also, bending moment
 - [M] Mass matrix
 - P(t) Instantaneous power as a function of time
 - \bar{P} Complex power
 - P_{av} Time-average power
 - P_{alt} Alternating component of instantaneous power
 - \hat{P}_{alt} Amplitude of alternating component of instantaneous power
-

Q Shear force

Q_{av} Imaginary part of complex power

$Q_i^{(A)}$ Force transmitted to Substructure A in direction of coordinate i

$R_{f,v}(\tau)$ Cross-correlation function between the stationary random processes f and v. The cross-correlation function between two random processes, x and y, is defined as

$$R_{xy}(\tau) = E [x(t)y(t + \tau)] = \int_{-\infty}^{\infty} S_{xy}(\omega) e^{j\omega\tau} d\omega$$

$S_{f,v}(\omega)$ Cross-spectral density between force f and velocity v. The cross-spectral density $S_{xy}(\omega)$ of a pair of random processes, x and y, is defined by

$$S_{xy}(\omega) = \frac{1}{2\pi} \int_{-\infty}^{\infty} R_{xy}(\tau) e^{-j\omega\tau} d\tau$$

where $R_{f,v}(\tau)$ is the cross-correlation function.

T Kinetic energy

T_{av} Time-average kinetic energy

T_r Force transmissibility

$[T_{ij}(\omega)]$ Force transmissibility matrix

U Potential energy

U_{av} Time-average potential energy

v,V Velocity

w_{in} Vibration intensity calculated from input power measurements

w_x Vibration intensity at position x

w_{xf} Force component of vibration intensity at position x

w_{xm} Moment component of vibration intensity at position x

w'_{xm} Moment component of vibration intensity obtained from measurement

x,X Displacement

$\{x\}_A$ Displacement vector relating to Structure A

Y Mobility

$[Y^{(A)}]$ Mobility matrix of Structure A

$Y_{ij}^{(A)}$ Element in the i^{th} row and j^{th} column of the mobility matrix of Structure A

$[Z^{(A)}]$ Impedance matrix of Structure A

$Z_{ij}^{(A)}$ Element in the i^{th} row and j^{th} column of the impedance matrix of Structure A. Note that in general $Z_{ij}^{(A)} \neq 1/Y_{ij}^{(A)}$

$E[\]$ Denotes the ensemble averaged value of the quantity in square brackets

$\text{Re}(\)$ Denotes real part of complex quantity in brackets

$\text{Im}(\)$ Denotes imaginary part of complex quantity in brackets

$\langle \dots \rangle_t$ Denotes time-averaging

\oplus Denotes the addition of two component impedance matrices, the addition being restricted to those coordinates that are common to both components

Greek letters

α, β Constants; also used as indices

ζ Viscous damping ratio

η Damping loss factor

θ Phase angle; also, rotational motion

ξ Transverse displacement of uniform beam vibrating in flexure

ρ Mass density

τ Time-period of vibration

ϕ Phase angle

ω Angular frequency

ω_n Natural frequency

A A constant

Superscripts

H Hermitian transpose of a matrix

T Transpose of a matrix

* Denotes the complex conjugate

Chapter 1
INTRODUCTION

The last two decades have seen a steady growth of interest in the use of the concept of power flow in vibration problems. The bulk of the published work has been in connection with the development of an approach to vibration problems which is now generally known as *Statistical Energy Analysis* (SEA). The primary variable of interest in SEA is energy rather than one of the usual vector quantities. Applications of the concept of power flow have also been proposed in other areas of vibration analysis. These include the identification of vibration transmission paths, nondestructive testing of structural components and vibration isolation. The work described in this thesis is a contribution to the literature on the use of power flow considerations in vibration problems involving steady-state forced excitation.

Statistical Energy Analysis

SEA provides a set of procedures for calculating the average responses of the component parts of a vibrating system in the high frequency regime. Energy is the primary variable of interest in SEA, and this accounts for the fact that most of the published theoretical and experimental work involving power flow has been in connection with SEA. The original formulation of the SEA procedure is based on the observation that the time-average power flow between two lightly-coupled oscillators, randomly excited by independent forces, is directly proportional to the energy difference between the oscillators [1]. From this basis the theory was gradually developed to enable the proportionality between power flow and energy to be applied to

multi-modal structural and acoustic systems.

Since the development of the SEA approach in the early 1960's the literature has grown quite rapidly. A number of surveys and reviews have been published for various audiences [eg 2 - 7]; but perhaps the most complete exposition of the subject to date is the work by Lyon [8] whose book also contains a very extensive list of references of earlier work.

Although SEA is now a well-established method, there are still several analytical and experimental problems to be overcome [7]. The validity of SEA techniques depends on a number of fundamental assumptions, and the extent to which these are justified in various practical situations is often difficult to determine. Also, some of the parameters required in the application of SEA are difficult to obtain in certain situations. Recent additions to the literature indicate that efforts are continuing to extend the theoretical basis of SEA, and to develop some of its theoretical and experimental techniques in a more systematic way. See, for example, references 9 - 12.

Other applications of the concept of power flow

Outside the context of SEA, not much has been published concerning the use of power flow in vibration problems. Goyder and White [13,14,15] have studied the flow of power from machines to built-up structures, and have proposed a vibration isolation method which aims at minimising the power flow to the foundation. They examined the nature of typical flexible foundations and obtained simple formulae for approximating the behaviour of the foundations. They then used these approximations to study the flow of

power through single- and two-stage isolators to the supporting foundation. As a follow-up, Pinnington and White [16] have studied the flow of power through machine isolators to resonant and non-resonant beams. These works represent a significant contribution to the literature on power flow in vibrating structures.

Recently, Verheij [17] has also published the results of a study of the multi-path sound transfer in resiliently-mounted machinery on board ships. He describes the development of several experimental techniques for measuring the power flow from shipboard machinery to the surroundings via various transmission paths.

A question that arises from a study of the literature on the use of power flow in vibration analysis, outside the SEA framework, is this: Does the time-average power flow to a component of a vibrating structure provide a good indication of its level of vibration? A similar question does not arise with SEA because the underlying assumptions of the SEA procedure are very clearly stated. These assumptions concern, among other things, the nature of the exciting forces, the characteristics of the components and the nature of the coupling between adjacent components. There is a need for other users of the concept of power flow to state their assumptions very clearly, and to examine the conditions under which these assumptions are valid. The proposal to use the reduction of time-average power flow as a criterion for assessing the effectiveness of vibration isolation appears to be based on the assumption that a reduction of power flow will always be accompanied by a reduction of the vibration transmitted to the foundation. The validity of this assumption requires examination, and this is one object of the work described in this thesis.

The underlying principle of the use of power flow in nondestructive testing is quite simple. Since a flaw or damage in a structural component acts as a location of increased dissipation, it should be possible to detect the flaw by monitoring the flow of dissipated power in the component when it is set in vibration. However, the translation of this basic principle into practice is fraught with many problems, the most significant of which is the difficulty of measuring power (or dissipation) very accurately. Although some measure of success has been reported in the literature [eg. 18,19], the use of dissipation measurements for flaw detection is not yet well-established. Brownjohn and Steele [20] have reported an unsuccessful attempt to monitor the power flow along a steel bar as a possible means of locating the site of structural damage on the bar. A similar experiment carried out recently did not yield encouraging results [21]. The use of the concept of power flow in nondestructive testing is an area that urgently requires further research.

Measurement of input power and power flow in vibrating structures

The growth of interest in the use of methods based on power flow has been accompanied by the need to measure power. In principle the input power to a structure from a vibration generator may be obtained by measuring the input force and the velocity at the driving-point, and calculating the time-average value of the product. In practice the measurement of input power presents several problems. The accurate measurement of force and velocity at the same point on a structure is difficult. Studies by Brownjohn *et al.* [22] have shown that the acceleration measured with an impedance head has an inevitable error which is proportional to the input force and the square

of the frequency, and is inversely proportional to the series combination of the stiffness of the force crystal and its attachment to the structure.

A major difficulty with input power measurements by direct multiplication of force and velocity signals is that accuracy depends heavily on the correct determination of phase angles. Ottesen and Vigran [23] have proposed a method for measuring input power by direct analogue multiplication and integration of force and velocity signals whereby the influence of phase errors is controlled through the measurement of both real and imaginary power components. Swift and Bies [24] have also described a power injection device which reduces phase angle errors by matching the mechanical impedance of the driver to that at the point of power input. The use of this power flow transducer for the measurement of input power to a plate has been reported by Bies and Hamid [25].

In the determination of power from force and velocity, the velocity may be obtained by electronically integrating the signal from the acceleration transducer. The velocity signal obtained in this way is much smaller than the acceleration signal, and is consequently more prone to the influence of noise. To overcome this problem in the case of random excitation, Fahy [26] proposed a method by which input power may be determined from the integration of the cross-correlation between the force and acceleration signals.

Many attempts have been made to measure power flow through vibrating structures with varying degrees of success. Noiseux [27] proposed a method for measuring vibrational intensity (power flow per unit width of cross-section) in uniform beams and plates vibrating in flexure. Simple elasticity

theory was used to obtain expressions for the vibrational intensity. The application of the method is limited by the fact that it requires the measurement of rotation, a measurement which is quite difficult to make. Rasmussen [28] has recently reported the use of Noiseux's method to measure the vibration intensity in a steel plate loaded with two viscous dampers. Rotation was obtained from the difference of the signals from two accelerometers mounted on a block. His results, judged against input power measurements, were reasonable. However, there is still the need to examine the accuracy of the method more closely.

Pavic [29] has also formulated methods for making wave intensity measurements similar to Noiseux's. The intensities are calculated from data obtained purely from measurements of kinematic quantities. Spatial derivatives of displacement are required for the calculations, and these are obtained by finite differences. The inevitable errors associated with the application of finite differences to measured data constitute one of the main shortcomings of the method.

It is analytically possible to determine the power flow through a built-up structure by using the velocity responses of the assembled structure and the mechanical impedances of the individual components. However, it is unlikely that experimentally-determined data will be sufficiently accurate to enable reliable calculation of power flow. Moreover, for a structure which has already been assembled it is not easy to obtain the frequency response data for the individual components unless these have been determined previously. Goyder [30] has reported an unsuccessful attempt to determine power flow in a simple connected structure by this method.

The increased availability of digital equipment appears to have stimulated the formulation and application of spectral density methods for the measurement of input power and power flow in structures; see, for example, references **31, 32 and 33**. In their study of power flow from machines to resonant and non-resonant beams, Pinnington and White **[16]** also proposed a method for measuring the power transmission through spring-like isolators, using the isolator dynamic stiffness and the cross-spectrum of the acceleration signals above and below the isolator. One limitation of the method is that it considers motion in one direction only. Indeed, this is a limitation which is shared by many of the methods proposed for the measurement of power flow in vibrating structures. Very often it is assumed that the structure moves only in translation at the point of measurement. Consequently, any power flow due to rotational motion is not accounted for. In real structures the magnitude of energy transmission due to rotational motion is seldom negligible. The tendency to assume pure translation is probably due to the difficulty of measuring rotation accurately.

Object and scope of present study

The initial Chapters of this thesis are concerned with setting out clearly the basic relations governing the flow of vibrational energy in structures during steady-state forced vibration. The discussion of the basic relations begins in Chapter 2 with the classical problem of the vibration of simple spring-mass-damper systems excited by sinusoidal forces. In Chapter 3 the flow of power and the transfer of energy in connected structures is considered. The general expressions for the time-average power flow to the components of a connected structure are derived, and the flow of energy in the coordinate directions at the joints between substructures is examined.

One object of the present study is to explore other areas of vibration analysis, outside the context of Statistical Energy Analysis, where power flow considerations could be usefully employed. Thus, in Chapter 4 a method is proposed for assessing the relative importance of coordinates in the vibration analysis of connected structures by the Impedance or Receptance Coupling technique [34].

The vibration isolation method proposed by Goyder and White [13,14,15] and further studied by Pinnington and White [16] is based on the tacit assumption that a reduction of the time-average power flow to a structure will automatically lead to a reduction of the vibration transmitted to the structure. One object of the present study is to assess the validity of this assumption for the case of steady-state forced vibration. An evaluation of the power flow approach to vibration isolation is presented in Chapter 5.

The flow of power along a simple beam structure has been studied experimentally, and the results are presented in Chapter 6. Power was measured using the method proposed by Noiseux [27]. The accuracy of the measuring method is assessed and some of the difficulties involved in its use are discussed.

A substructure approach is adopted in analysing the vibrating systems under consideration in this thesis. The discussions are generally based on steady-state forced excitation, although reference is made to random excitation from time to time. Wherever **possible** the vibrating systems are described by their frequency response functions. These functions may be in any one of six related forms: *Receptance*, *Dynamic Stiffness*, *Mobility*, *Impedance*,

Inertance and Apparent Mass. Since there is some confusion in the literature concerning the precise definition of some of these terms, it is necessary to state here that the usage adopted throughout this thesis follows that by Ewins [35].

Chapter 2

POWER AND ENERGY RELATIONS FOR SPRING-MASS-DAMPER SYSTEMS SUBJECTED TO SINUSOIDAL FORCE EXCITATION

2.1 Introduction

The vibration analysis of spring-mass-damper systems excited by sinusoidal forces offers a particularly suitable vehicle for introducing the relationships between power, energy and response in vibrating systems. This chapter introduces a discussion of the power and energy relations for vibrating systems made up of a finite number of masses, springs and dampers.

The discussion begins with the classical problem of the vibration of a simple one-degree-of-freedom system consisting of a spring-mounted mass and a viscous damper. The expressions for energy and instantaneous power provide an insight into the transfer of energy back and forth between the source and the oscillator. The relationships between time-average power, velocity amplitude and force transmissibility are also examined. It is shown that, in general, the time-average power input to the oscillator is not a reliable indicator of the amplitude of response and the magnitude of the force transmitted to the support.

The discussion is concluded by examining the power and energy relations for multi-degree-of-freedom spring-mass-damper systems. The relationships between instantaneous power and vibration response are examined for the undamped dynamic vibration absorber as a simple example of a multi-DOF spring-mass system.

2.2 The Simple One-degree-of-freedom System

2.2.1 Kinetic and Potential Energy

Under steady state conditions the velocity response of the **one-degree-of-freedom** system in Fig.2.1 is sinusoidal, and may be written as

$$v(t) = |V| \cos \omega t \quad (2.1)$$

The instantaneous kinetic energy, T , is

$$T = \frac{1}{2} m v^2(t) = \frac{1}{2} m |V|^2 \cos^2 \omega t$$

This may be written as

$$T = \frac{1}{4} m |V|^2 (1 + \cos 2\omega t) \quad (2.2)$$

This result is shown graphically in Fig.2.2.

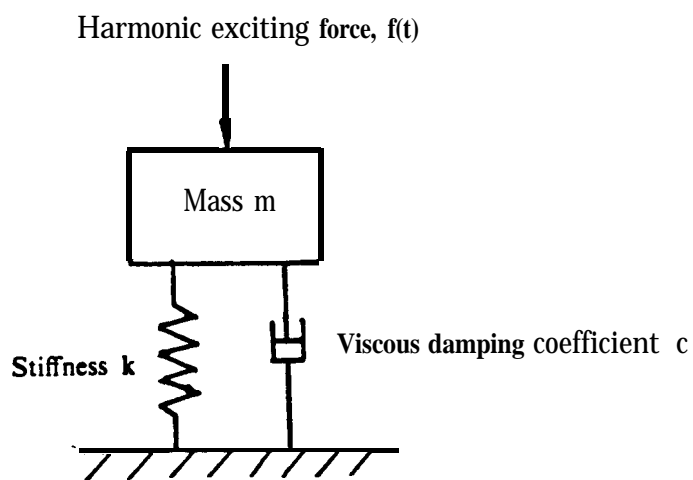


Fig.2.1 One-degree-of-freedom system

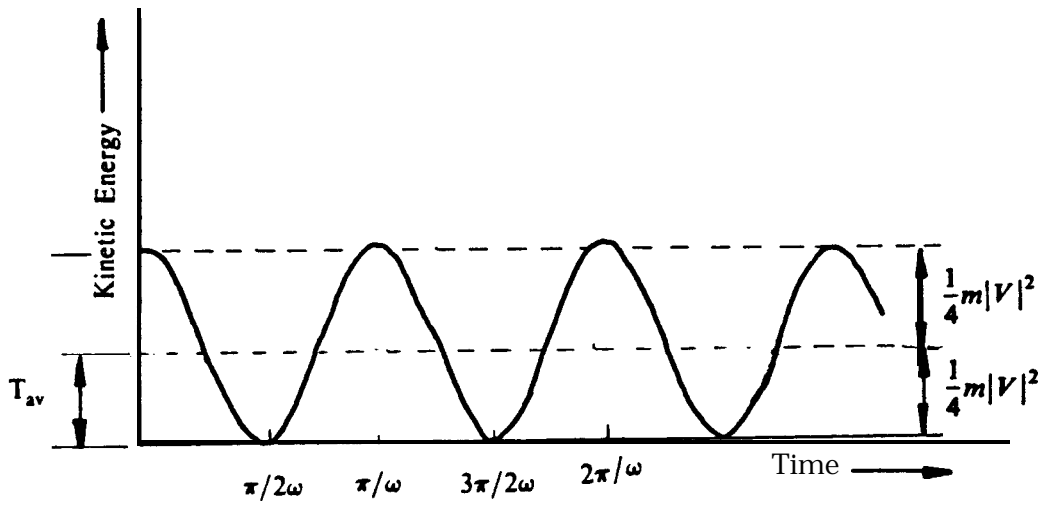


Fig.22 Instantaneous kinetic energy of one-degree-of-freedom system

The kinetic energy is seen to vary sinusoidally between zero and a maximum value of $\frac{1}{2}m|V|^2$, with a frequency which is twice that of the velocity $v(t)$. The kinetic energy as a function of time consists of a constant component

$$T_{av} = \frac{1}{4}m|V|^2 \quad (2.3)$$

plus an alternating component whose average value is zero. The average value of kinetic energy is therefore equal to the constant component, T_{av} .

The power taken by the mass m is given by the time rate of change of T . From equation (2.2). we have

$$\frac{dT}{dt} = -\frac{\omega}{2}m|V|^2 \sin 2\omega t \quad (2.4)$$

which is a sinusoid with twice the excitation frequency and zero average value. Thus, the time-average energy consumed by the inertia element is zero.

The time variation of potential **energy**, U , is similar to that for kinetic energy. If we let

$$x(t) = |X| \cos(\omega t + \theta) \quad (2.5)$$

where θ is a phase angle, we have the result

$$U = \frac{1}{4}k|X|^2[1 + \cos 2(\omega t + \theta)] \quad (2.6)$$

The average potential energy is

$$U_{av} = \frac{1}{4}k|X|^2 \quad (2.7)$$

The time rate of change of potential energy is

$$\frac{dU}{dt} = -\frac{\omega}{2}k|X|^2 \sin 2(\omega t + \theta) \quad (2.8)$$

which has zero average value. A plot of U against time is of a similar form to that in Fig.2.2 for kinetic energy.

2.2.2 Instantaneous power and energy

The well-known equation of motion for the one-degree-of-freedom system shown in Fig.2.1 is

$$m\ddot{x} + c\dot{x} + kx = f(t) \quad (2.9)$$

If each term in this equation is multiplied by the velocity, $v(t)$, we have

$$m\ddot{x} + cv^2 + kxv = f(t)v(t) \quad (2.10)$$

Now,
$$m\dot{x}v = \frac{d}{dt}\left(\frac{1}{2}mv^2\right) = \frac{dT}{dt} \quad (2.11)$$

and
$$kvx = \frac{d}{dt}\left(\frac{1}{2}kx^2\right) = \frac{dU}{dt} \quad (2.12)$$

The equation of motion (2.9) is therefore equivalent to

$$cv^2 + \frac{d}{dt}(T + U) = f(t)v(t) \quad (2.13)$$

This expression is a statement of the conservation of energy. The quantity cv^2 represents the instantaneous rate of energy dissipation by the viscous damper; $\frac{d}{dt}(T+U)$ is the instantaneous rate of energy intake by the inertia and elastic elements; and $f(t)v(t)$ is the instantaneous power input to the system.

In the sinusoidal steady-state, we may write

$$f(t) = \frac{1}{2}(F e^{j\omega t} + F^* e^{-j\omega t}) \quad (2.14)$$

and
$$v(t) = \frac{1}{2}(V e^{j\omega t} + V^* e^{-j\omega t}) \quad (2.15)$$

where the force, F , and velocity, V , are complex quantities (with magnitude and phase) related through the system's frequency response functions. The superscript * indicates a complex conjugate value.

Integration of equation (2.15) gives the displacement as

$$x(t) = \frac{1}{2j\omega}(V e^{j\omega t} - V^* e^{-j\omega t}) \quad (2.16)$$

and the squares of velocity and displacement are given by

$$v^2(t) = \frac{1}{4}V^2 e^{j2\omega t} + \frac{1}{4}V^{*2} e^{-j2\omega t} + \frac{1}{2}V\dot{V} \quad (2.17)$$

and

$$x^2(t) = -\frac{1}{4\omega^2}(V^2 e^{j2\omega t} + V^{*2} e^{-j2\omega t} - 2V\dot{V}) \quad (2.18)$$

These equations may be written in the forms

$$v^2(t) = \frac{1}{2}|V|^2 + \frac{1}{2}R e\{V^2 e^{j2\omega t}\} \quad (2.19)$$

and

$$x^2(t) = \frac{1}{2\omega^2}|V|^2 - \frac{1}{2\omega^2}R e\{V^2 e^{j2\omega t}\} \quad (2.20)$$

The potential and kinetic energies thus become

$$T = \frac{m}{4}|V|^2 + \frac{m}{4}R e\{V^2 e^{j2\omega t}\} \quad (2.21)$$

and

$$U = \frac{k}{4\omega^2}|V|^2 - \frac{k}{4\omega^2}R e\{V^2 e^{j2\omega t}\} \quad (2.22)$$

The first terms in these equations are respectively T_{av} and U , as given by equations (2.3) and (2.7). The time derivatives are

$$\frac{dT}{dt} = \frac{1}{2}R e\{j\omega m V^2 e^{j2\omega t}\} \quad (2.23)$$

and

$$\frac{dU}{dt} = \frac{1}{2}R e\left\{\frac{k}{j\omega} V^2 e^{j2\omega t}\right\} \quad (2.24)$$

Substituting these into the equation of motion (2.13), we have

$$\frac{1}{2}c|V|^2 + \frac{1}{2}Re\left\{\left(\frac{k}{j\omega} + j\omega m + c\right)V^2 e^{j2\omega t}\right\} = f(t)v(t) \quad (2.25)$$

Using equations (2.14) and (2.15), the right hand side of equation (2.25) may be written as

$$f(t)v(t) = \frac{1}{2}Re(F^*V) + \frac{1}{2}Re(FV e^{j2\omega t}) \quad (2.26)$$

Since $(k/j\omega + j\omega m + c)$ is the impedance of the system, and the product $(k/j\omega + j\omega m + c)V$ equals the force F , equation (2.25) may be written as

$$f(t)v(t) = \frac{1}{2}c|V|^2 + \frac{1}{2}Re(FV e^{j2\omega t}) \quad (2.27)$$

The product $f(t)v(t)$ is the instantaneous power supplied to the system by the external force $f(t)$. Equation (2.27) shows that the instantaneous power consists of a constant component

$$P_{av} = \frac{1}{2}Re(F^*V) = \frac{1}{2}c|V|^2 \quad (2.28)$$

(which is the time-average value of input power) plus a double-frequency sinusoidal component which is given by the term

$$P_{alt} = \frac{1}{2}Re(FV e^{j2\omega t}) \quad (2.29)$$

With F as reference phasor, equation (2.28) may be written as

$$P_{av} = \frac{1}{2}|F||V|\cos\phi_v \quad (2.30)$$

where ϕ_v is the phase angle of the velocity response relative to the exciting force. Thus, in the language of vector algebra, the time-average power input may be said to be given by one-half the scalar product of the force and velocity vectors.

Equation (2.26) may also be written as

$$f(t)v(t) = \frac{1}{2}|F||V|\cos\phi_v + \frac{1}{2}|F||V|\cos(2\omega t + \phi_v) \quad (2.31)$$

A plot of the expression for instantaneous power is shown in Fig.2.3.

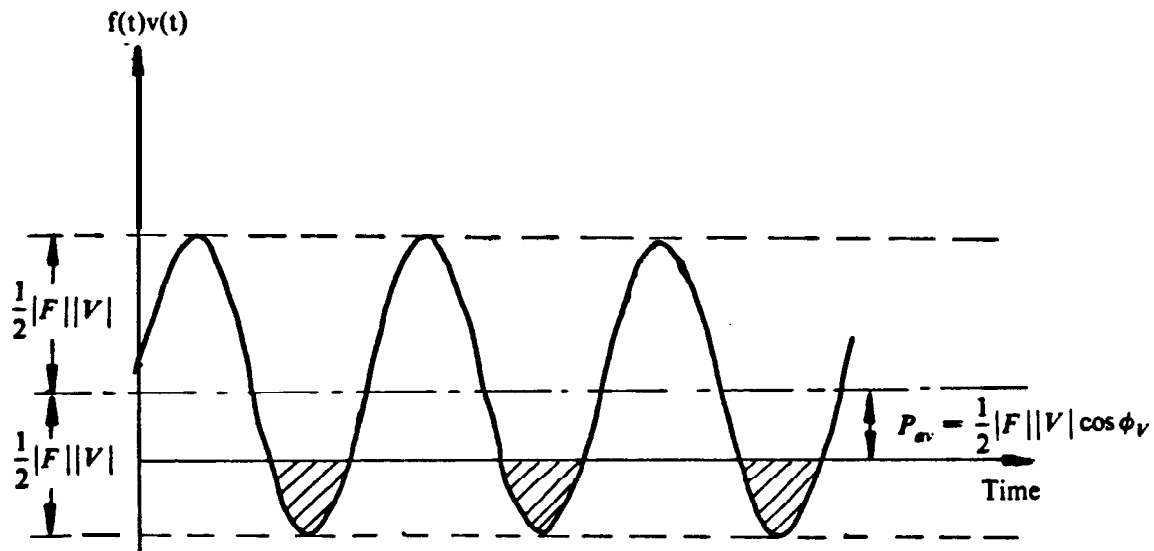


Fig.2.3 Instantaneous power as a function of time

Fig.2.3 shows that the instantaneous power is negative during some parts of each cycle. The area of each portion of the plot below the time axis represents an amount of energy that is being returned to the excitation source by the system, this energy having been stored as kinetic and potential energy. We must note that in general power flows in both

directions, and the power input to the system is not characterised by a uniform flow of energy. Since the system contains a dissipative element, more energy flows into the system than is returned to the excitation source. The net amount of energy supplied to the system is transferred at a rate equal to P .

The value of $\cos\phi_v$ characterises the extent to which the system is damped. We know that $\cos\phi_v$ is zero for $\phi_v = \pi/2$, and unity for $\phi_v = 0$. When the system is excited at the natural frequency, $\omega_n = \sqrt{k/m}$, the mobility is purely real. ϕ_v is zero and $\cos\phi_v$ is unity. The power input is then limited only by the damping in the system. The instantaneous power curve lies wholly above the zero axis so that the cross-hatched portions are just eliminated. Thus at the natural frequency none of the energy supplied to the system is returned to the source.

When an undamped system is excited at its natural frequency there is a net amount of energy gained by the system for each cycle, proportional to the amplitude of that cycle. Since the system contains no energy dissipating elements the amplitude builds up in each cycle. Steady-state conditions are never attained, and the system will ultimately 'explode' unless the frequency of excitation is changed. For an undamped system excited away from resonance, the mobility is purely imaginary and $\cos\phi_v$ becomes zero. The curve in Fig.2.3 then oscillates symmetrically about the zero axis, and the average power input is zero.

2.2.3 The Concept of Complex Power

We have seen that when a system is subjected to sinusoidal excitation in the steady-state, energy may be exchanged back and forth between excitation source and the system. The term *reactive power* or *wattless power*, borrowed from Electrical Engineering, may be used to refer to the

rate at which this energy exchange occurs.

The reactive power is defined to be equal to one-half the product of force F and the component of velocity at right-angles to the force. This definition is natural since the average power, P_{av} , is equal to one-half the product of force and the in-phase component of velocity. The average power, according to equation (2.28), is equal to the real part of $\frac{1}{2}(F^*V)$. Following the usage in Electrical Engineering we may regard the complex quantity $\frac{1}{2}(F^*V)$ as a *complex power*. The real part of this complex power is the average power input, which may be referred to as the *active power*. The magnitude of the complex power is equal to the amplitude of the double-frequency alternating component of instantaneous power.

We may write the complex power as

$$\bar{P} = P_{av} + jQ_{av} = \frac{1}{2}(F^*V) \quad (2.32)$$

where Q_{av} denotes the quadrature component of the complex power. Using the relationships $V = F/Z = FY$, we may write alternatively

$$\bar{P} = \frac{1}{2}F^*FY = \frac{1}{2}|F|^2Y \quad (2.33)$$

$$\bar{P} = \frac{1}{2}V^*VZ^* = \frac{1}{2}|V|^2Z^* \quad (2.34)$$

The power per root-mean-square force is

$$\bar{P}_{(F-rms\ value)} = Y \quad (2.35)$$

and the power per root-mean-square velocity is

$$\bar{P}_{(V-rms\ value)} = Z^* \quad (2.36)$$

Thus the complex power supplied per unit rms force is numerically equal to the mobility, Y; and the complex power supplied per unit rms velocity is numerically equal to the complex conjugate of impedance, Z.

Returning to equation (2.9). if we substitute $f(t) = Fe^{j\omega t}$ and $v(t) = Ve^{j\omega t}$, we have

$$cV + j\omega(mV - \frac{kV}{\omega^2}) = F \quad (2.37)$$

Taking the complex conjugate, we have

$$F^* = cV^* + j\omega(\frac{kV^*}{\omega^2} - mV^*) \quad (2.38)$$

The complex power may then be written as

$$\bar{P} = \frac{1}{2}(F^*V) = \frac{1}{2}c|V|^2 + j2\omega(\frac{k|V|^2}{4\omega^2} - \frac{m}{4}|V|^2) \quad (2.39)$$

$$\text{Now, from equation (2.7), } \frac{k|V|^2}{4\omega^2} = \frac{k}{4}|X|^2 = U_{av} \quad (2.40)$$

$$\text{and, according to equation (2.3), } \frac{1}{4}m|V|^2 = T_{av} \quad (2.41)$$

Also, $\frac{1}{2}c|V|^2 = P_{av}$. according to equation (2.28). and therefore equation (2.39) becomes

$$\bar{P} = P_{av} + jQ_{av} = \frac{1}{2}c|V|^2 + j2\omega(U_{av} - T_{av}) \quad (2.42)$$

Of particular interest to us here is the result

$$Q_{av} = 2\omega(U_{av} - T_{av}) \quad (2.43)$$

This result states that the reactive power is proportional to the difference between the average potential and kinetic energies. In other words, the reactive power is proportional to the time-average Lagrangian.

If the inertia and elastic elements in the system do not store equal amounts of energy, on the average, i.e if $U_{av} \neq T_{av}$, then some of the stored energy is continuously transferred back and forth between the excitation source and the system. On the other hand if $U_{av} = T_{av}$, then the inertia and elastic elements merely exchange a certain amount of energy between them, and the excitation source does not take part in this interplay. Thus we see that the reactive power is a measure of the extent to which the excitation source is called upon to participate in the exchange of stored energy.

2.2.4 Frequency response functions in terms of energy functions

Using the conventional definitions of mobility and Impedance, equation (2.42) may be written as

$$\bar{P} = \frac{1}{2}(F^* V) = \frac{1}{2}|F|^2 Y = \frac{1}{2}|V|^2 Z^* = P_{av} + j2\omega(U_{av} - T_{av}) \quad (2.44)$$

Thus we can express the mobility as

$$Y(\omega) = \frac{2P_{av} + j4\omega(U_{av} - T_{av})}{|F|^2} \quad (2.45)$$

and the impedance as

$$Z(\omega) = \frac{2P_{av} - j4\omega(U_{av} - T_{av})}{|V|^2} \quad (2.46)$$

Equations (2.45) and (2.46) express the mobility and impedance explicitly in terms of the power and energy functions if it is assumed that these expressions are evaluated for unit force and unit velocity respectively?

For a single-degree-of-freedom system, the mobility and impedance become purely real only when the system is excited at the natural frequency, $\sqrt{k/m}$. Since equations (2.45) and (2.46) become purely real only when $U_{av} = T_{av}$, equality of the time-average potential and kinetic energies implies a condition of resonance.

† The general definitions of mobility and impedance are:

$$\text{Mobility, } Y_{ij} = \left(\frac{V_i}{F_j} \right)_{F_k=0, k \neq j}$$

and

$$\text{Impedance, } Z_{ij} = \left(\frac{F_i}{V_j} \right)_{V_k=0, k \neq j}$$

The impedance matrix of a system is equal to the inverse of its mobility matrix:

$$[Z] = [Y]^{-1}$$

The mobility, Y_{ij} , relating the force and velocity response in any two coordinate directions, i and j , remains the same irrespective of the number of coordinates used to describe the system. However, the impedance Z_{ij} depends on the particular choice of coordinates, and therefore impedance data is meaningless unless complete information is given about the system of coordinates. For the case under consideration here, there is no ambiguity because there is only one degree of freedom.

2.2.5 Variation of time-average power with excitation frequency and damping coefficient

In terms of the system's parameters the time-average power input to the one-degree-of-freedom system in Fig.2.1 is

$$P_{av} = \frac{1}{2}|F|^2 \frac{\omega^2 c}{(k - \omega^2 m)^2 + \omega^2 c^2} \quad (2.47)$$

This may be written as

$$P_{av} = \frac{1}{2}|F|^2 \frac{\lambda c}{(k - \lambda m)^2 + \lambda c^2} \quad (2.48)$$

where $\lambda = \omega^2$.

Differentiating with respect to λ we have

$$\frac{dP_{av}}{d\lambda} = \frac{|F|^2 c [(k - \lambda m)^2 + \lambda c^2] - c[\lambda c^2 - 2m\lambda(k - \lambda m)]}{2 [(k - \lambda m)^2 + \lambda c^2]^2} \quad (2.49)$$

At the frequency for maximum power input, $\partial P_{av}/\partial \lambda = 0$, ie

$$c[(k - \lambda m)^2 + \lambda c^2] - c[\lambda c^2 - 2m\lambda(k - \lambda m)] = 0$$

$$\text{or} \quad c(k - \lambda m)(k + \lambda m) = 0 \quad (2.50)$$

Equation (2.50) is satisfied if $k = \lambda m$, i.e when excitation is at the natural frequency. At this frequency the mobility is purely real, and the power input is

$$P_{av}(\omega = \omega_n) = \frac{|F|^2}{2c} \quad (2.51)$$

The variation of time-average input power with excitation frequency is shown in Fig.2.4.

The magnitude of average power input depends to a large extent on the system's capacity to dissipate energy. It is therefore necessary to investigate the influence of damping. Differentiating equation (2.47) with respect to the damping coefficient, we have

$$\frac{dP_{av}}{dc} = \frac{|F|^2}{2} \left[\frac{\omega^2}{(k - \omega^2 m)^2 + \omega^2 c^2} - \frac{2\omega^4 c^2}{[(k - \omega^2 m)^2 + \omega^2 c^2]^2} \right] \quad (2.52)$$

The damping coefficient for maximum power input may be obtained by equating $\partial P_{av}/\partial c$ to zero. This leads to the condition

$$(k - \omega^2 m)^2 = \omega^2 c^2 \quad (2.53)$$

Thus, if excitation is at a fixed frequency, maximum power is supplied when the damping coefficient satisfies equation (2.53). ie when

$$c = \left| \frac{k - \omega^2 m}{\omega} \right| \quad (2.54)$$

We see from equation (2.54) that the damping coefficient for maximum power depends on the excitation frequency. If the system is excited at the undamped natural frequency, maximum power is supplied when damping is zero. At other excitation frequencies the damping coefficient for maximum power is given by equation (2.54). The variation of power input with damping is shown graphically in Fig.2.5 for the two excitation cases.

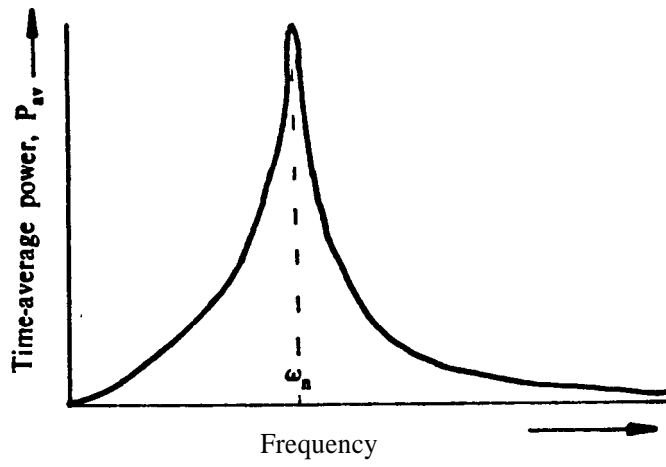


Fig.2.4 Variation of average power with frequency

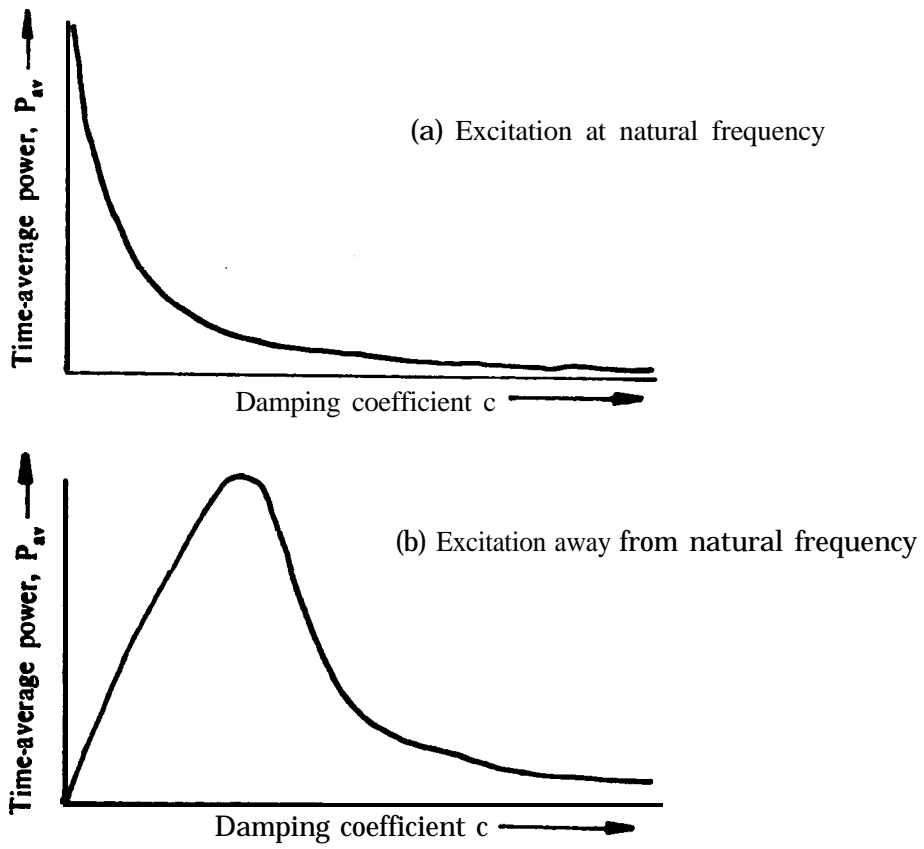


Fig.25 Variation of average power with damping

An expression for the maximum power may be obtained by substituting the damping coefficient from equation (2.54) into the expression for input power, equation (2.47) :

$$P_{av(max)} = \frac{\omega}{4} |F|^2 \frac{1}{|k - \omega^2 m|} \quad (2.55)$$

2.2.6 Relationships between time-average power, velocity amplitude and force transmissibility

Equation (2.28) gives the relationship between time-average power and velocity amplitude:

$$P_{av} = \frac{1}{2} c |V|^2$$

If damping is kept constant the average power input is proportional to the square of velocity amplitude. Thus power and velocity amplitude have a similar dependence on excitation frequency. A plot of velocity amplitude versus frequency is similar in shape to that shown in Fig.2.4 for time-average input power.

The expression for velocity amplitude is

$$|V| = \frac{\omega |F|}{\sqrt{(k - \omega^2 m)^2 + \omega^2 c^2}} \quad (2.56)$$

The variation of velocity amplitude with damping is shown graphically in Fig.2.6. For all excitation frequencies $|V|$ decreases continuously as damping is increased. Thus, except for excitation at the natural frequency, power and velocity amplitude do not have a similar dependence on damping.

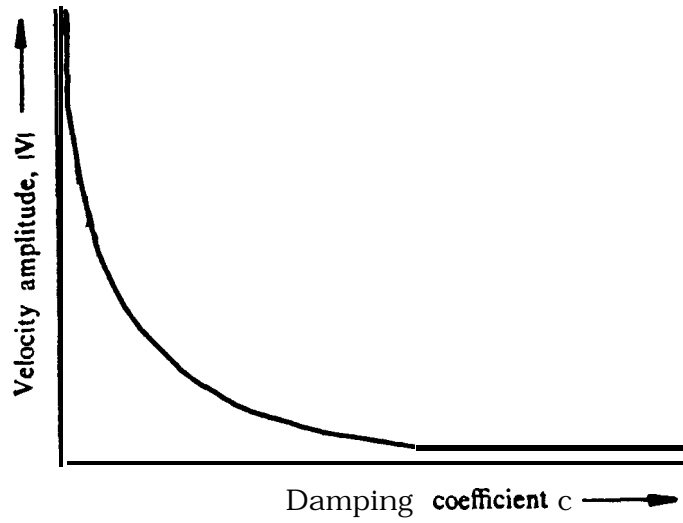


Fig.2.6 Variation of velocity amplitude with damping

The force transmissibility is

$$T_r = \sqrt{\frac{1 + (2\zeta\frac{\omega}{\omega_n})^2}{(1 - \frac{\omega^2}{\omega_n^2})^2 + (2\zeta\frac{\omega}{\omega_n})^2}} \quad (2.57)$$

The usual plot of transmissibility as a function of frequency ratio is shown in Fig.2.7 for various values of damping ratio.

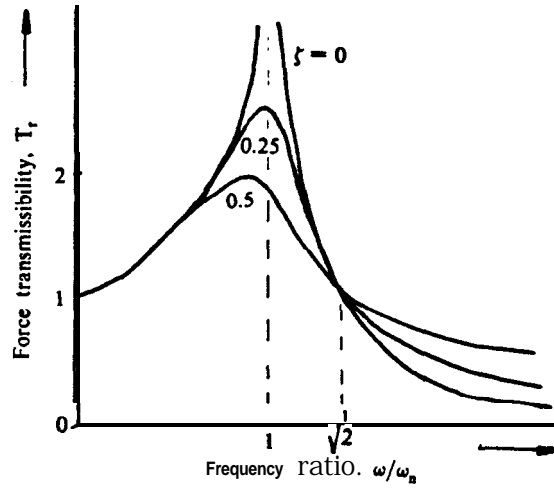


Fig.2.7 Force transmissibility as a function of frequency ratio

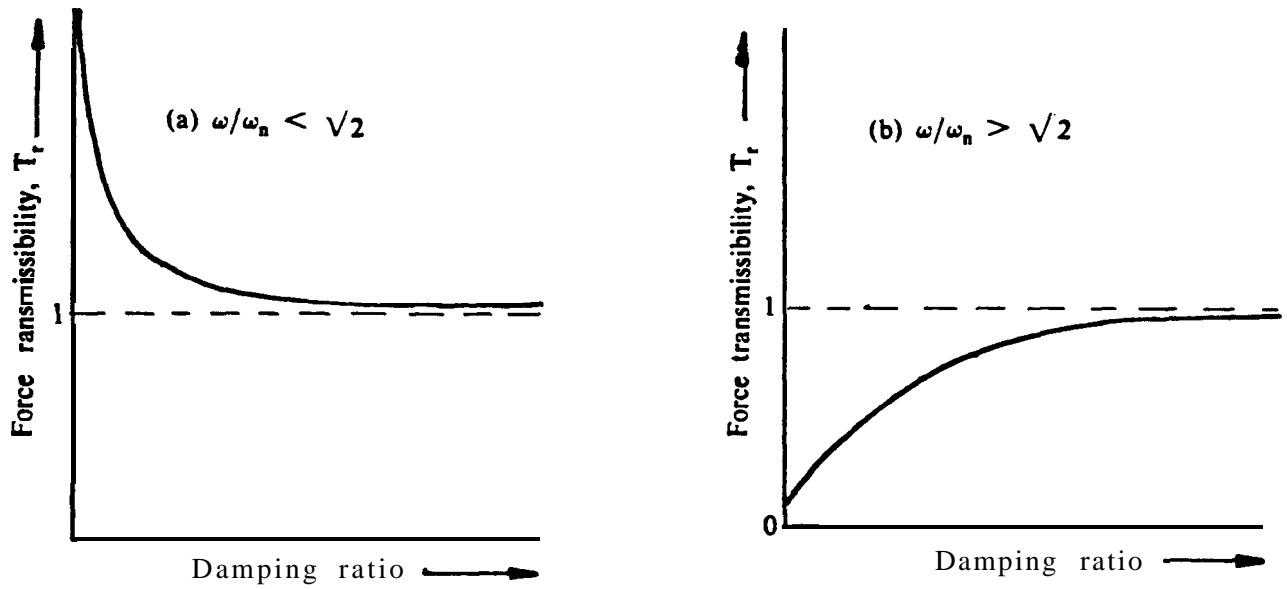


Fig.2.8 Variation of force transmissibility with damping

We see that except for an undamped system the force transmissibility is maximum at a frequency which is less than the undamped natural frequency. This contrasts with the average power input which always has its peak at the natural frequency, $\omega_n = \sqrt{(k/m)}$.

The variation of T_r with damping is shown graphically in Fig.2.8. If the excitation frequency is kept constant the effect of variations in damping depends on the excitation frequency. In the region where $(\omega/\omega_n) < \sqrt{2}$, increased damping reduces the force transmissibility. Where $(\omega/\omega_n) > \sqrt{2}$, increased damping increases the transmissibility. Thus, force transmissibility and average power input do not have a similar dependence on damping.

2.3 Multi-degree-of-freedom spring-mass-damper systems

23.1 Instantaneous power and energy functions for the general **N-degree-of-freedom** system

The equation of motion for a system with N degrees of freedom may be written as

$$[M]\{\ddot{x}\} + [C]\{\dot{x}\} + [K]\{x\} = \{f\} \quad (2.58)$$

where [M], [K] and [C] are the inertia, stiffness and viscous damping matrices respectively, and {f} is the excitation force vector. It is assumed that the system possesses a finite number of degrees of freedom, and that the displacements are completely specified by N independent coordinates. We are also assuming that the conditions leading to symmetric inertia, stiffness and damping matrices are satisfied [36].

The instantaneous power input to the system by the N forces is

$$P(t) = f_1\dot{x}_1 + f_2\dot{x}_2 + \dots + f_N\dot{x}_N = \sum_{q=1}^N f_q\dot{x}_q \quad (2.59)$$

If we premultiply the matrix equation (2.56) by the transpose of the velocity vector, {v}^T = {ẋ}^T, we have

$$\{v\}^T[M]\{\ddot{x}\} + \{v\}^T[C]\{\dot{x}\} + \{v\}^T[K]\{x\} = \{v\}^T\{f\} = \sum_{q=1}^N f_q v_q \quad (2.60)$$

The energy functions are defined as follows:

$$D = \frac{1}{2}\{v\}^T[C]\{v\} = \frac{1}{2}\sum_{q=1}^N \sum_{r=1}^N v_q c_{qr} v_r \quad (2.61)$$

$$T = \frac{1}{2} \{v\}^T [M] \{v\} = \frac{1}{2} \sum_{q=1}^N \sum_{r=1}^N v_q m_{qr} v_r \quad (2.62)$$

and

$$U = \frac{1}{2} \{x\}^T [K] \{x\} = \frac{1}{2} \sum_{q=1}^N \sum_{r=1}^N x_q k_{qr} x_r \quad (2.63)$$

Now,

$$\begin{aligned} \frac{dU}{dT} &= \frac{1}{2} \sum_{q=1}^N \sum_{r=1}^N k_{qr} \frac{d}{dt} (x_q x_r) \\ &= \frac{1}{2} \sum_{q=1}^N \sum_{r=1}^N k_{qr} x_q \frac{dx_r}{dt} + \frac{1}{2} \sum_{q=1}^N \sum_{r=1}^N k_{qr} x_r \frac{dx_q}{dt} \\ &= \sum_{q=1}^N \sum_{r=1}^N k_{qr} x_q v_r \\ &= \{v\}^T [K] \{x\} \end{aligned} \quad (2.64)$$

By a similar process we find that

$$\frac{dT}{dt} = \{\dot{v}\}^T [M] \{v\} \quad (2.65)$$

Using equations (2.61), (2.64) and (2.65), equation (2.66)

may be written in the equivalent form

$$P(t) = 2D + \frac{d}{dt} (T + U) = \sum_{q=1}^N f_q v_q \quad (2.66)$$

The expression in equation (2.66) is a generalisation of the result obtained for the simple one-degree-of-freedom system. The functions $2D$, T and U are respectively the instantaneous rate of energy dissipation, the instantaneous kinetic energy and the instantaneous potential energy. The function D is the well-known Rayleigh's Dissipation Function [37].

For steady-state sinusoidal excitation we may write

$$v_q(t) = \frac{1}{2}(V_q e^{j\omega t} + V_q^* e^{-j\omega t}) \quad (2.67)$$

and

$$x_q(t) = \frac{1}{2j\omega}(V_q e^{j\omega t} - V_q^* e^{-j\omega t}) \quad (2.66)$$

Now,

$$\begin{aligned} v_q v_r &= \frac{1}{4}(V_q e^{j\omega t} + V_q^* e^{-j\omega t})(V_r e^{j\omega t} + V_r^* e^{-j\omega t}) \\ &= \frac{1}{2} R e(V_q V_r^*) + \frac{1}{2} R e(V_q V_r e^{j2\omega t}) \end{aligned} \quad (2.69)$$

and similarly
$$x_q x_r = \frac{1}{2\omega^2} R e(V_q V_r^*) - \frac{1}{2\omega^2} R e(V_q V_r e^{j2\omega t}) \quad (2.70)$$

Substituting into equations (2.61), (2.62) and (2.63), we have for the energy functions

$$\begin{aligned} D &= \frac{1}{4} \sum_{q=1}^N \sum_{r=1}^N c_{qr} V_q V_r^* + \frac{1}{4} R e(e^{j2\omega t} \sum_{q=1}^N \sum_{r=1}^N c_{qr} V_q V_r) \\ &= \frac{1}{4} (\{V\}^H [C] \{V\}) + \frac{1}{4} R e(e^{j2\omega t} \{V\}^T [C] \{V\}) \end{aligned} \quad (2.71)$$

$$\begin{aligned} T &= \frac{1}{4} \sum_{q=1}^N \sum_{r=1}^N m_{qr} V_q V_r^* + \frac{1}{4} R e(e^{j2\omega t} \sum_{q=1}^N \sum_{r=1}^N m_{qr} V_q V_r) \\ &= \frac{1}{4} (\{V\}^H [M] \{V\}) + \frac{1}{4} R e(e^{j2\omega t} \{V\}^T [M] \{V\}) \end{aligned} \quad (2.72)$$

$$\begin{aligned} U &= \frac{1}{4\omega^2} \sum_{q=1}^N \sum_{r=1}^N k_{qr} V_q V_r^* - \frac{1}{4\omega^2} R e(e^{j2\omega t} \sum_{q=1}^N \sum_{r=1}^N k_{qr} V_q V_r) \\ &= \frac{1}{4\omega^2} (\{V\}^H [K] \{V\}) - \frac{1}{4\omega^2} R e(e^{j2\omega t} \{V\}^T [K] \{V\}) \end{aligned} \quad (2.73)$$

where the superscripts H and T are used to indicate respectively the Hermitian and the ordinary transpose of the vectors to which they are appended. We see that each of the energy functions is made up of a constant term plus a double-frequency sinusoid. In each case the constant term is the average value of the function. Thus we have

$$D_{av} = \frac{1}{4}(\{V\}^H[C]\{V\}) \quad (2.74)$$

$$T_{av} = \frac{1}{4}(\{V\}^H[M]\{V\}) \quad (2.75)$$

$$U_{av} = \frac{1}{4\omega^2}(\{V\}^H[K]\{V\}) \quad (2.76)$$

For reasons of energy conservation the amplitude of the sinusoidal component of each energy function must not be greater than its average value. If this were not so, a physically impossible condition would arise whereby the instantaneous value of the function would be negative during some time interval.

Differentiating equations (2.72) and (2.73) with respect to time, and substituting the results into equation (2.66), we have

$$\begin{aligned} P &= \frac{1}{2} \sum_{q=1}^N \sum_{r=1}^N c_{qr} V_q V_r^* + \frac{1}{2} R e^{j2\omega t} \sum_{q=1}^N \sum_{r=1}^N (c_{qr} + j\omega m_{qr} + \frac{k_{qr}}{j\omega}) V_q V_r \\ &= P_{av} + \frac{1}{2} R e^{j2\omega t} \sum_{q=1}^N F_q V_q \end{aligned} \quad (2.77)$$

As in the case of the simple one-degree-of-freedom system, the instantaneous power input to the system equals a constant plus an alternating component of twice the excitation frequency.

In §2.2.3 the complex power input due to a single excitation force, F , was defined to be equal to the complex quantity $\frac{1}{2}F^*V$. This definition is maintained here; but since there are now N forces, the total complex power is represented by the summation $\frac{1}{2}\sum F_q^*V_q$.

Now, under steady-state conditions we may write

$$\begin{aligned} \{f\} &= \{F\}e^{j\omega t} \\ \{v\} &= \{V\}e^{j\omega t} \end{aligned} \quad (2.78)$$

Substituting these into the equilibrium equation (2.58) and cancelling the exponential factor, we have

$$(j\omega[M] + [C] + \frac{1}{j\omega}[K])\{V\} = \{F\} \quad (2.79)$$

Extracting the q^{th} row from this matrix equation, we have

$$\sum_{r=1}^N (j\omega m_{qr} + c_{qr} + \frac{k_{qr}}{j\omega})V_r = F_q \quad (2.80)$$

Taking the complex conjugate and rearranging, we have

$$F_q^* = \sum_{r=1}^N [c_{qr} - j\omega(m_{qr} - \frac{k_{qr}}{\omega^2})]V_r^* \quad (2.81)$$

Multiplication by $V_q/2$, and summation over the index q gives the complex power:

$$\begin{aligned} \bar{P} &= \frac{1}{2} \sum_{q=1}^N F_q^* V_q \\ &= \frac{1}{2} \sum_{q=1}^N \sum_{r=1}^N c_{qr} V_q V_r^* - \frac{j\omega}{2} \left(\sum_{q=1}^N \sum_{r=1}^N m_{qr} V_q V_r^* - \frac{1}{\omega^2} \sum_{q=1}^N \sum_{r=1}^N k_{qr} V_q V_r^* \right) \end{aligned} \quad (2.82)$$

Using equations (2.74), (2.75) and (2.76). we may write equation (2.62) in the form

$$\bar{P} = P_{av} + jQ_{av} = 2D_{av} + j2\omega(U_{av} - T_{av}) \quad (2.63)$$

from which we have

$$P_{av} = 2D_{av} \quad (2.64)$$

and

$$Q_{av} = 2\omega(U_{av} - T_{av}) \quad (2.65)$$

These results are identical to those obtained for the simple **one-degree-of-freedom** system. The real part of the complex power is the time-average power dissipated by the system, and the imaginary part or the reactive *power* is proportional to the difference between the average potential and kinetic energies. When the average potential and kinetic energies are equal, the reactive power is zero, and the excitation sources do not take part in the interchange of stored energy. It can be shown that in the case of single-point excitation, the amplitude of the alternating component of instantaneous power is equal to the magnitude of complex power. Consider the result in equation (2.77) if the system is excited by a single force, F_i . We have

$$P = P_{av} + \operatorname{Re}\left(\frac{F_i V_i}{2} e^{j2\omega t}\right) \quad (2.66)$$

This may be written as

$$P = P_{av} + \frac{|F_i V_i|}{2} \cos(2\omega t + \phi_i) \quad (2.87)$$

where ϕ_i is the phase angle of the velocity phasor V_i , relative to the force, F_i . Now from equations (2.82) and (2.83), we have

$$\frac{|F_i V_i|}{2} = \frac{|F_i^* V_i|}{2} = \sqrt{(P_{av}^2 + Q_{av}^2)} \quad (2.88)$$

Therefore equation (2.87) may be written as

$$P = P_{av} + \sqrt{(P_{av}^2 + Q_{av}^2)} \cos(2\omega t + \phi_i) \quad (2.89)$$

and thus the amplitude of the double-frequency sinusoidal component of instantaneous power equals the magnitude of the complex power.

As in the case of the simple oscillator, there is a simple correlation between the driving-point frequency response functions and the energy functions. Suppose there is only a single excitation force, F_i . Then equation (2.83) may be written as

$$\bar{P} = \frac{1}{2} F_i V_i = 2D_{av} + j2\omega(U_{av} - T_{av}) \quad (2.90)$$

or

$$F_i^* V_i = 4D_{av} + j4\omega(U_{av} - T_{av}) \quad (2.91)$$

Taking the complex conjugate of both sides of equation (2.91) we have

$$F_i V_i^* = 4D_{av} - j4\omega(U_{av} - T_{av}) \quad (2.92)$$

Dividing both sides of equation (2.91) by $F_i F_i^* = |F_i|^2$, we obtain the

result

$$\frac{V_i}{F_i} = Y_{ii}(\omega) = \frac{4D_{av} + j4\omega(U_{av} - T_{av})}{|F_i|^2} \quad (2.93)$$

and, dividing both sides of equation (2.92) by $V_i V_i^* = |V_i|^2$, we get

$$\frac{F_i}{V_i} = Z_{ii}(\omega) = \frac{4D_{av} - j4\omega(U_{av} - T_{av})}{|V_i|^2} \quad (2.94)$$

If the functions D_{av} , U_{av} and T_{av} are evaluated for unit force then equation (2.93) expresses the driving-point mobility explicitly in terms of these energy functions. A similar interpretation may be given to the Impedance expression (2.94) on the understanding that the functions D_{av} , U_{av} and T_{av} are evaluated for unit velocity response. (Here, the system is being described by a single coordinate, i. so that $Z_{ii} = 1/Y_{ii}$.)

2.3.2 The undamped dynamic vibration absorber

We shall now examine briefly the classical problem of the undamped dynamic vibration absorber, Fig.2.9, from the point of view of power flow.

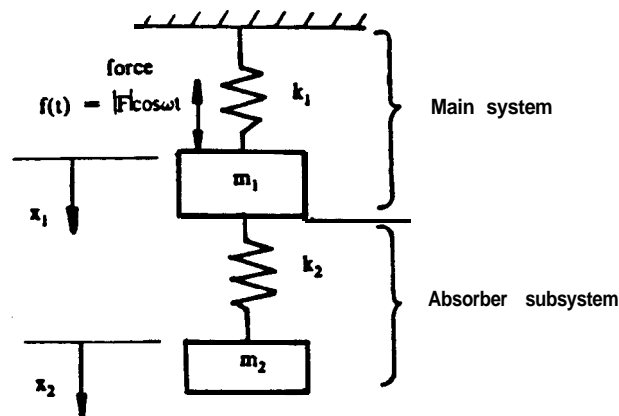


Fig.2.9 Undamped dynamic vibration absorber

The velocity responses are:

for the main mass:

$$v_1(t) = -\frac{|F|}{\Delta}(k_2 - m_2\omega^2)\omega \sin \omega t \quad (2.95)$$

and for the absorber mass:

$$v_2(t) = -\frac{|F|}{\Delta}k_2\omega \sin \omega t \quad (2.96)$$

where

$$A = (k_1 + k_2 - \omega^2 m_1)(k_2 - \omega^2 m_2) - k_2^2 \quad (2.97)$$

The instantaneous power input to the system by the exciting force is

$$P_{total}(t) = -\frac{1}{2} \frac{|F|^2}{\Delta} \omega (k_2 - \omega^2 m_2) \sin 2\omega t \quad (2.98)$$

By employing the general expressions derived in Chapter 3, the instantaneous power flow to the main system is found to be

$$P_{main}(t) = -\frac{1}{2} \frac{|F|^2}{\Delta^2} \omega (k_1 - \omega^2 m_1)(k_2 - \omega^2 m_2)^2 \sin 2\omega t \quad (2.99)$$

and that for the absorber subsystem to be

$$P_{abs}(t) = \frac{1}{2} \frac{|F|^2}{\Delta^2} \omega k_2 m_2 (k_2 - \omega^2 m_2) \sin 2\omega t \quad (2.100)$$

The power expressions in equations (2.98), (2.99) and (2.100) are pure sinusoids with twice the excitation frequency. The absence of a constant component is due to the fact that the system is not damped.

The untuned absorber

For an untuned system, $k_1/m_1 \neq k_2/m_2$. When the excitation frequency is equal to the natural frequency of the absorber spring-mass subsystem, i.e. $\omega^2 = k_2/m_2$, the instantaneous power input is zero, according to equation (2.98). The power flow to each of the subsystems is also zero according to

equations (2.99) and (2.100). Equations (2.95) and (2.96) show that the main mass remains stationary, while the absorber mass vibrates with an amplitude which is determined by the magnitude of the exciting force and the stiffness of the absorber spring.

When the excitation frequency coincides with the natural frequency of the main system, i.e. $\omega^2 = k_1/m_1$, the instantaneous power flow to the main system is zero. The energy input is taken up entirely by the absorber subsystem. Although the main system does not take any energy the motion of the main mass is not zero. The vibration of the main mass is maintained by energy being transferred back and forth between the mass m , and the spring k .

The tuned absorber

If the system is tuned, so that $\omega_1^2 = \omega_2^2$, i.e. $k_1/m_1 = k_2/m_2$, then at this tuned frequency the instantaneous power input is zero. The main system remains stationary while the absorber mass vibrates as a result of the interplay of stored energy between the mass m_2 and the spring k .

Fig.2.10 is a plot of the amplitude of the instantaneous power flow to the subsystems of a vibration absorber system with the following parameters: $m_1 = 20.0\text{kg}$, $m_2 = 1.0\text{kg}$, $k_1 = 5.78 \times 10^5 \text{N/m}$, $k_2 = 2.25 \times 10^4 \text{N/m}$.[†] The driving-point and the transfer mobilities are also shown in Fig.2.11. The point of interest here is that there is a frequency range, between the two resonances, in which the velocity response of the main system increases as the instantaneous power flow decreases. This result shows that we cannot rely on the instantaneous power flow to a subsystem as a sole indicator of its response amplitude.

[†] Note that the vibration absorber system being considered here is untuned, i.e. $\omega_1 \neq \omega_2$. Here, $\omega_1 = 170\text{rad/s}$ and $\omega_2 = 150\text{rad/s}$.

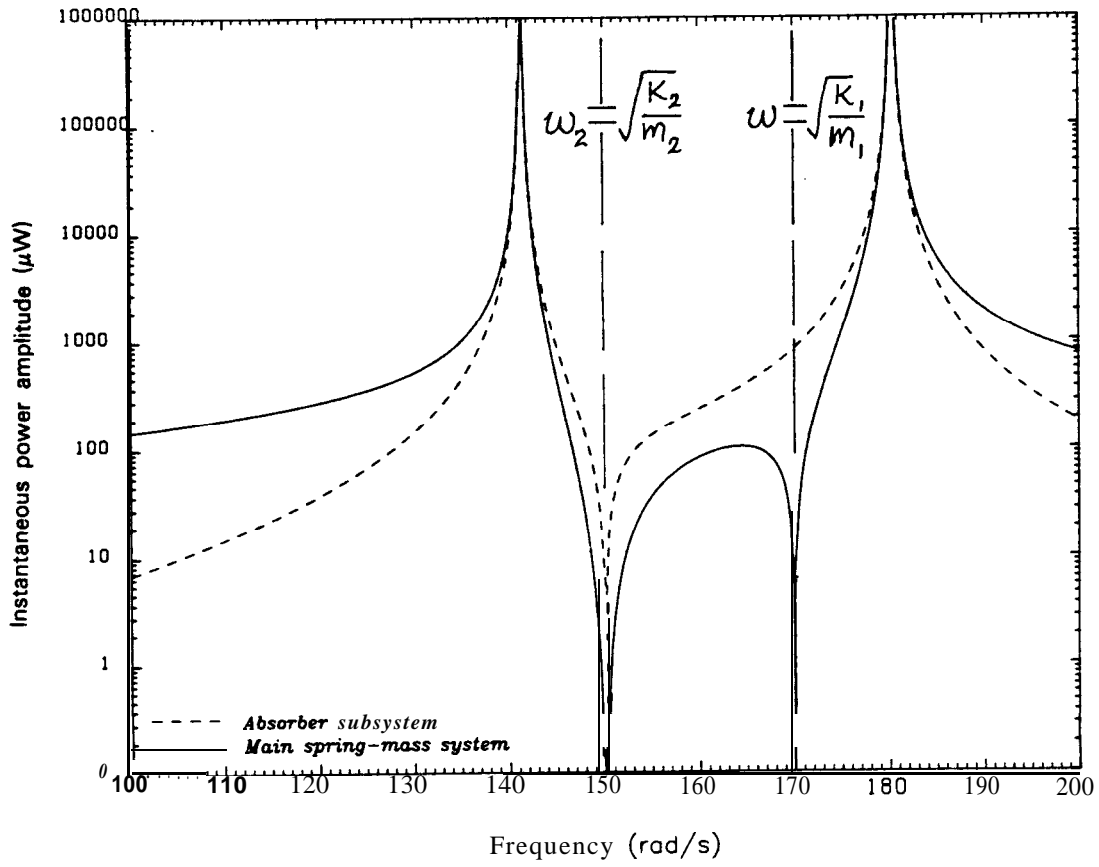


Fig.2.10 Instantaneous power flow to subsystems of dynamic absorber

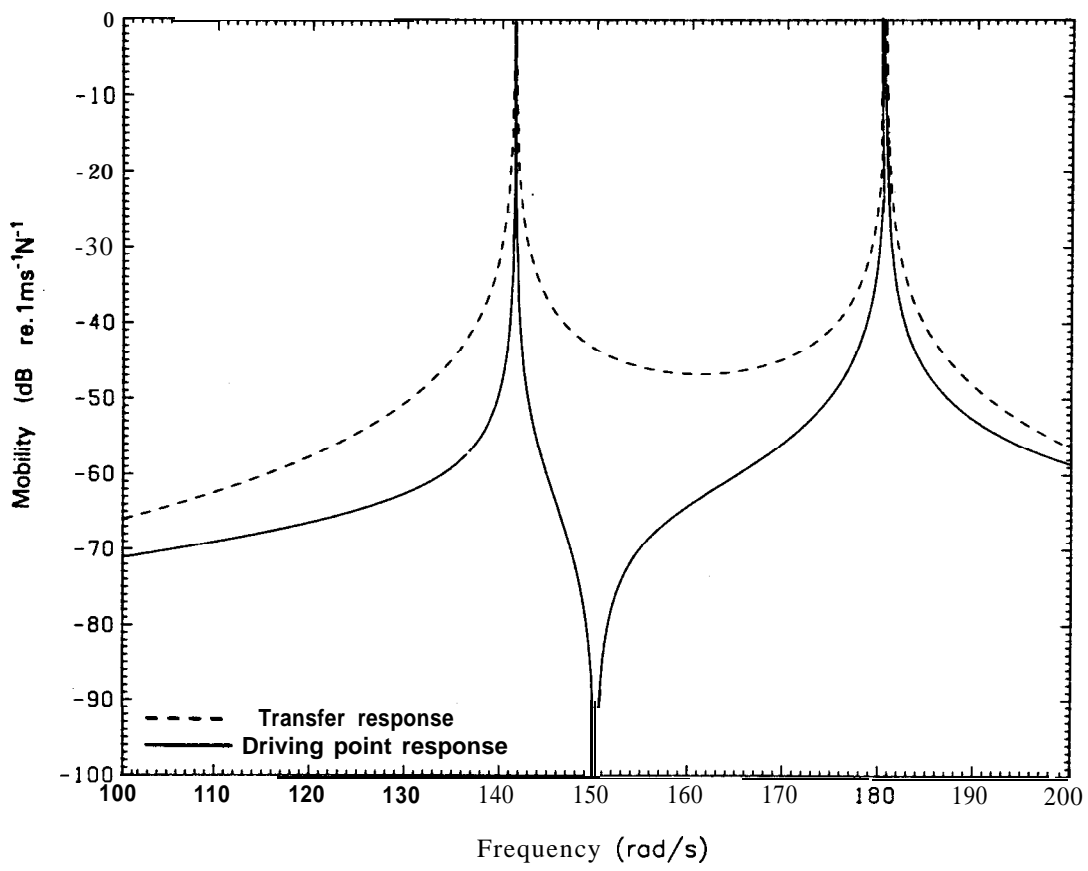


Fig.2.11 Driving-point and Transfer Mobilities of dynamic absorber

2.4 Discussion

In this chapter the vibration of simple spring-mass-damper systems has been examined from the point of view of power flow and energy transfer. The power and energy relations for these systems have been derived and discussed, drawing heavily on concepts that are already well established in Electrical Circuit Theory; see, for example, ref 38.

The study of the one-degree-of-freedom system provides insight into the nature of energy transfer back and forth between the source of excitation and the system. By employing the concept of complex power, it has been shown that the driving-point frequency response functions may be expressed in terms of the energy functions. This relationship, though notable, is limited because it applies only to driving-point data and only if unit force or unit velocity is assumed. By investigating the dependence of time-average power, velocity amplitude and force transmissibility on frequency and damping, we have also shown that time-average power is not always a suitable indicator of vibration levels.

Broadly speaking, the power and energy relations discussed for the simple one-degree-of-freedom system are also applicable to more complex systems. The brief study of the undamped dynamic vibration absorber shows that a reduction in the instantaneous power flow to a part of a structure could be accompanied by an increase of the vibration amplitude of that part of the structure. This result, which provides further evidence of the unsuitability of power flow for assessing vibration amplitudes, is not unexpected for undamped systems since such systems do not require an external supply of

energy to maintain their vibration. Thus it is easy to conceive of a situation where the vibration of a particular subsystem is maintained purely by the interchange of kinetic and potential energy within the subsystem.

Chapter 3

POWER FLOW AND ENERGY TRANSFER IN CONNECTED STRUCTURES

3.1 Introduction

In Chapter 2 the basic power and energy relations for vibrating systems were introduced with a discussion of the vibration of simple systems having a finite number of degrees of freedom. Such systems are composed solely of rigid bodies which have mass and inertia, and are capable of acquiring kinetic energy, and **massless** bodies which can store only potential energy. The potential and dissipative forces are due to the relative motion between pairs of rigid bodies. However, vibrating systems made up of components that are perfectly rigid or without inertia are idealisations of real systems. The components of real engineering structures have **continuously** distributed mass and elasticity. This chapter concerns the flow of power and the transfer of energy in real elastic structures which are presumed to be composed of subsystems connected together at joints. First, the expressions for input power are examined briefly for both single-point and multi-point excitation, and the general expressions for the power flowing to the components of connected structures are derived. Then some consequences of power balance considerations are discussed and, finally, the nature of energy flow in the various coordinate directions at the joints between connected structures is examined very closely.

3.2 Power **input to elastic structures**

When a structure is excited by a single force the instantaneous power input is given by

$$P(t) = f(t)v(t) \quad (3.1)$$

where $f(t)$ and $v(t)$ are the instantaneous values of force and velocity respectively. If the exciting force is sinusoidal, then in the steady-state we may write

$$f(t) = \frac{1}{2}[F e^{j\omega t} + F^* e^{-j\omega t}] \quad (3.2)$$

and

$$v(t) = \frac{1}{2}[V e^{j\omega t} + V^* e^{-j\omega t}] \quad (3.3)$$

where F and V are complex quantities. Substituting these into equation (3.1), we have

$$P(t) = \frac{1}{2} \text{Re}\{F^* V\} + \frac{1}{2} \text{Re}\{F V e^{j2\omega t}\} \quad (3.4)$$

This equation may also be written as

$$P(t) = \frac{1}{2}|F||V| \cos \phi + \frac{1}{2}|F||V| \cos(2\omega t + \phi) \quad (3.5)$$

where ϕ is the phase angle of the velocity phasor relative to the force.

When a structure is subjected to sinusoidal force excitation in more than

one coordinate direction the instantaneous power input is given by the summation

$$\begin{aligned}
 P(t) &= \sum_{q=1}^N f_q(t)v_q(t) \\
 &= \frac{1}{2} \sum_{q=1}^N (\operatorname{Re}\{F_q^*V_q\} + \operatorname{Re}\{F_qV_qe^{j2\omega t}\}) \\
 &= \frac{1}{2} \operatorname{Re}\left[\sum_{q=1}^N (F_q^*V_q + e^{j2\omega t}F_qV_q)\right]
 \end{aligned} \tag{3.6}$$

Now

$$\begin{aligned}
 V_q &= Y_{q1}F_1 + Y_{q2}F_2 + \dots + Y_{qN}F_N \\
 &= \sum_{r=1}^N Y_{qr}F_r
 \end{aligned} \tag{3.7}$$

Therefore

$$\begin{aligned}
 P(t) &= \frac{1}{2} \operatorname{Re}\left[\sum_{q=1}^N \sum_{r=1}^N F_q^*Y_{qr}F_r + e^{j2\omega t} \sum_{q=1}^N \sum_{r=1}^N F_qY_{qr}F_r\right] \\
 &= \frac{1}{2} \operatorname{Re}\{ \{F\}^H [Y] \{F\} \} + \frac{1}{2} \operatorname{Re}\{ e^{j2\omega t} \{F\}^T [Y] \{F\} \} \}
 \end{aligned} \tag{3.8}$$

where [Y] is the NxN mobility matrix relating to the coordinate directions in which excitation forces are applied, and {F} is the excitation force vector. Equations (3.4) and (3.8) show that, for both single-point and multi-point excitation, the instantaneous power as a function **of time consists** of a constant component and a double-frequency sinusoid.

By using the relationship

$$F_q = Z_{q1}V_1 + Z_{q2}V_2 + \dots + Z_{qN}V_N$$

and noting that $\mathbf{Re}\{\mathbf{F}_q^* \mathbf{V}_q\} = \mathbf{Re}\{\mathbf{F}_q \mathbf{V}_q^*\}$, equation (3.6) may also be written in terms of the velocities and the impedances:

$$P(1) = \frac{1}{2} \mathbf{Re}\left(\{\mathbf{V}\}^H [\mathbf{Z}] \{\mathbf{V}\}\right) + \frac{1}{2} \mathbf{Re}\left(e^{j2\omega t} \{\mathbf{V}\}^T [\mathbf{Z}] \{\mathbf{V}\}\right) \quad (3.9)$$

3.3 General expressions for time-average power flow in connected structures

3.3.1 Power flow when coupling is in a single coordinate direction

In Fig.3.1 the two substructures are connected in coordinate j . One external force is applied in coordinate i . The velocity response of the coupled system may be written in terms of the system's mobility matrix and the force F_i :

$$\begin{Bmatrix} V_j \\ V_j \end{Bmatrix} = \begin{bmatrix} Y_{ii}^{(C)} & Y_{ij}^{(C)} \\ Y_{ji}^{(C)} & Y_{jj}^{(C)} \end{bmatrix} \begin{Bmatrix} F_i \\ 0 \end{Bmatrix} \quad (3.10)$$

We may also write

$$\begin{Bmatrix} F_i \\ 0 \end{Bmatrix} = \begin{bmatrix} Z_{ii}^{(C)} & Z_{ij}^{(C)} \\ Z_{ji}^{(C)} & Z_{jj}^{(C)} \end{bmatrix} \begin{Bmatrix} V_j \\ V_j \end{Bmatrix} \quad (3.11)$$

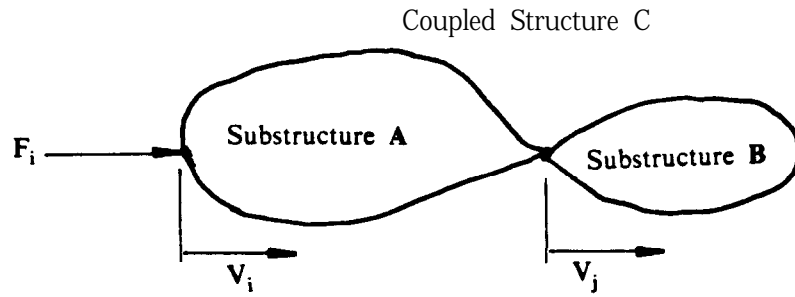


Fig.3.1 Two substructures coupled in a single coordinate

The time-average power flow from substructure A to substructure B is the time-average value of the product of the velocity at j and the internal force exerted on B by A. The velocity V_j can be obtained directly from equation (3.10). However, the internal force exerted on B must be determined indirectly. We separate the coupled structure into its component parts and apply equal and opposite forces on the substructures in such a way that force balance and motion compatibility are satisfied, Fig.3.2.

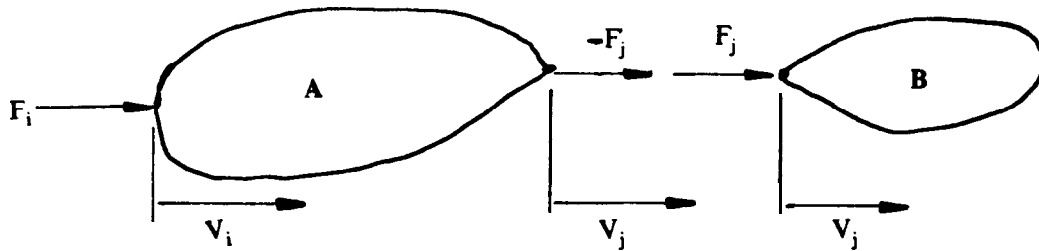


Fig.3.2 Coupled Structure separated into component parts

The systems shown in Fig.3.1 and Fig.3.2 are dynamically equivalent since

the velocities and the resultant forces are the same in both cases. Therefore we may consider each of the substructures separately. Considering B alone, we may write

$$F_j = \frac{V_j}{Y_{jj}^{(B)}} \quad (3.12)$$

and, taking A alone we have

$$\begin{Bmatrix} V_j \\ V_j \end{Bmatrix} = \begin{bmatrix} Y_{ii}^{(A)} & Y_{ij}^{(A)} \\ Y_{ji}^{(A)} & Y_{jj}^{(A)} \end{bmatrix} \begin{Bmatrix} F_i \\ -F_j \end{Bmatrix} \quad (3.13)$$

The time-average power flow to substructure B is the average of the product $f_i(t)v_j(t)$, and is given by

$$P_{av}^{(B)} = \frac{1}{2} \text{Re} \{ F_j V_j^* \} \quad (3.14)$$

Using the expression for F_j from equation (3.12) we have

$$P_{av}^{(B)} = \frac{1}{2} |V_j|^2 \text{Re} \left\{ \frac{1}{Y_{jj}^{(B)}} \right\} \quad (3.15)$$

Where there is an external exciting force in the coupling coordinate we may still follow the same analysis as above. However, when the structure is broken up into its component parts the forces to be applied to the two substructures are not equal in magnitude.

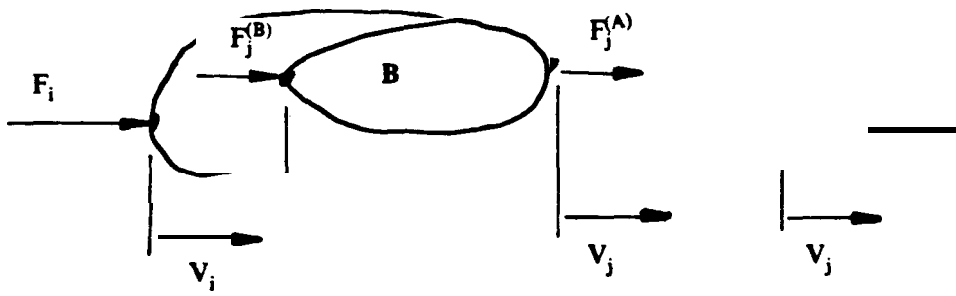


Fig.3.3 Power flow when there is external force in coupling coordinate

In Fig.3.3 the forces $F_j^{(A)}$ and $F_j^{(B)}$ must satisfy the condition

$$F_j^{(A)} + F_j^{(B)} = F_j \quad (3.16)$$

where F_j is the force externally applied in the coupling coordinate. As before, we obtain the force $F_j^{(B)}$ from the mobility of B and the velocity response v_j :

$$F_j^{(B)} = \frac{v_j}{Y_{jj}^{(B)}} \quad (3.17)$$

The time-average power flow from A to B is then given by

$$\begin{aligned} P_{av}^{(B)} &= \frac{1}{2} \text{Re}\{F_j^{(B)} v_j^*\} \\ &= \frac{1}{2} \text{Re}\{v_j v_j^* \frac{1}{Y_{jj}^{(B)}}\} \\ &= \frac{1}{2} |v_j|^2 \text{Re}\{\frac{1}{Y_{jj}^{(B)}}\} \end{aligned} \quad (3.18)$$

This is, in fact, the same equation as that derived for the case where there is no excitation force in the coupling coordinate. We note also that

the velocity V , is obtained from the mobilities of the coupled system and the external excitation forces:

$$V_j = Y_{jj}^{(C)} F_j + Y_{ji}^{(C)} F_i \quad (3.19)$$

3.3.2 The general case of power flow

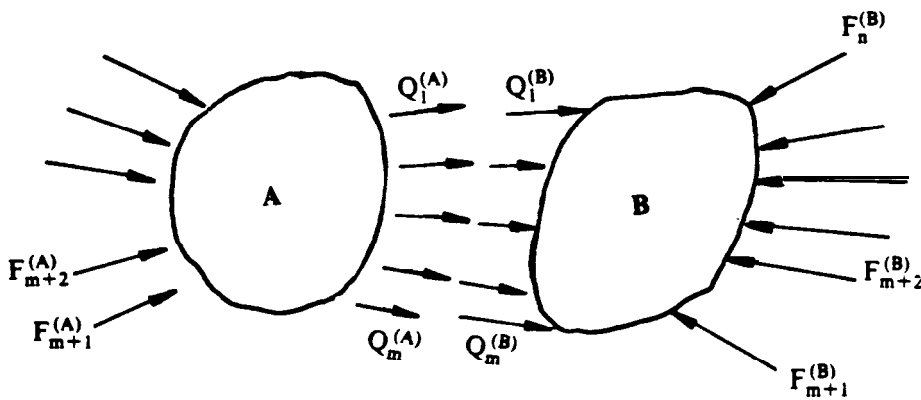


Fig.3.4 Time-average power flow in the general case

Fig.3.4 shows a coupled structure which has been separated into its two component parts. Forces $Q_1^{(A)}, Q_2^{(A)}, \dots, Q_m^{(A)}$ and $Q_1^{(B)}, Q_2^{(B)}, \dots, Q_m^{(B)}$ have been applied in the m coupling coordinates so that the resultant force in each coordinate is equal to the externally-applied force on the coupled structure. There are n coordinates on substructure B, m of which are coupling coordinates. Taking substructure B alone, we may write

$$\begin{Bmatrix} Q_1^{(B)} \\ Q_2^{(B)} \\ \vdots \\ Q_m^{(B)} \\ \vdots \\ F_n^{(B)} \end{Bmatrix} = \begin{bmatrix} Z_{11}^{(B)} & Z_{12}^{(B)} & \cdot & \cdot & \cdot & \cdot & Z_{1n}^{(B)} \\ Z_{21}^{(B)} & Z_{22}^{(B)} & \cdot & \cdot & \cdot & \cdot & Z_{2n}^{(B)} \\ \cdot & \cdot & \cdot & \cdot & \cdot & \cdot & \cdot \\ Z_{m1}^{(B)} & Z_{m2}^{(B)} & \cdot & \cdot & \cdot & \cdot & Z_{mn}^{(B)} \\ \cdot & \cdot & \cdot & \cdot & \cdot & \cdot & \cdot \\ \cdot & \cdot & \cdot & \cdot & \cdot & \cdot & \cdot \\ Z_{n1}^{(B)} & Z_{n2}^{(B)} & \cdot & \cdot & \cdot & \cdot & Z_{nn}^{(B)} \end{bmatrix} \begin{Bmatrix} V_1 \\ V_2 \\ \vdots \\ V_m \\ \vdots \\ V_n \end{Bmatrix} \quad (3.20)$$

The total time-average power flowing from A to B via the coupling coordinate directions is given by

$$P_{av}^{(AB)} = \sum_{k=1}^m \frac{1}{2} \text{Re} \{ Q_k^{(B)} V_k^* \} \quad (3.21)$$

Now

$$\begin{aligned} Q_k^{(B)} &= Z_{k1}^{(B)} V_1 + Z_{k2}^{(B)} V_2 + \dots + Z_{kn}^{(B)} V_n \\ &= \sum_{l=1}^n Z_{kl}^{(B)} V_l \end{aligned}$$

Therefore.

$$\begin{aligned} P_{av}^{(AB)} &= \frac{1}{2} \sum_{k=1}^m \text{Re} \left\{ V_k^* \sum_{l=1}^n Z_{kl}^{(B)} V_l \right\} \\ &= \frac{1}{2} \text{Re} \left\{ \sum_{k=1}^m \sum_{l=1}^n V_k^* Z_{kl}^{(B)} V_l \right\} \end{aligned}$$

Also,

$$\sum_{k=1}^m \sum_{l=1}^n V_k^* Z_{kl}^{(B)} V_l = \{ V_1^* \ V_2^* \ \dots V_m^* \} \begin{bmatrix} Z_{11}^{(B)} & Z_{12}^{(B)} & \cdot & \cdot & Z_{1n}^{(B)} \\ Z_{21}^{(B)} & Z_{22}^{(B)} & \cdot & \cdot & Z_{2n}^{(B)} \\ \cdot & \cdot & \cdot & \cdot & \cdot \\ \cdot & \cdot & \cdot & \cdot & \cdot \\ Z_{m1}^{(B)} & Z_{m2}^{(B)} & \cdot & \cdot & Z_{mn}^{(B)} \end{bmatrix} \begin{Bmatrix} V_1 \\ V_2 \\ \vdots \\ V_n \end{Bmatrix} \quad (3.22)$$

Therefore,
$$P_{av}^{(AB)} = \frac{1}{2} R e(\{V_R\}^H [Z_R^{(B)}] \{V\}) \quad (3.23)$$

where $\{V\}$ is the $n \times 1$ column matrix of the velocity responses in all the n coordinates of substructure B, and $\{V_R\}$ is the $m \times 1$ column matrix obtained by taking only the first m rows of $\{V\}$. The matrix $[Z_R^{(B)}]$ is the $m \times n$ matrix obtained by taking the first m rows of the impedance matrix of B.

The total time-average power flowing into substructure B can be obtained by summing the contributions due to all the forces $Q_1^{(B)}, Q_2^{(B)}, \dots, Q_m^{(B)}, F_{m+1}^{(B)}, \dots, F_n^{(B)}$:

$$P_{av}^{(B)} = \frac{1}{2} R e(\{V\}^H [Z^{(B)}] \{V\}) \quad (3.24)$$

3.3.3 Some consequences of power balance considerations

Consider a structure C which is made up of two subsystems A and B. Subsystem A has α coordinates and B has β coordinates, and the two subsystems are connected such that the total number of coordinates required to describe the coupled structure is N . The time-average power flow to the coupled structure C may written as

$$P_{av}^{(C)} = \frac{1}{2} R e(\{V\}_{1 \times N}^H [Z^{(C)}]_{N \times N} \{V\}_{N \times 1}) \quad (3.25)$$

The matrix $[Z^{(C)}]$ is the $N \times N$ impedance matrix obtained by inverting the mobility matrix, $[Y^{(C)}]$, of the coupled structure, and $\{V\}_{N \times 1}$ is the column vector of the velocity responses.

We may also write a similar expression for the time-average power flow to each of the subsystems:

$$P_{av}^{(A)} = \frac{1}{2} R e(\{V\}_{1 \times \alpha}^H [Z^{(A)}]_{\alpha \times \alpha} \{V\}_{\alpha \times 1}) \quad (3.26a)$$

and
$$P_{av}^{(B)} = \frac{1}{2} R e(\{V\}_{1 \times \beta}^H [Z^{(B)}]_{\beta \times \beta} \{V\}_{\beta \times 1}) \quad (3.26b)$$

where $[Z^{(A)}] = [Y^{(A)}]^{-1}$, and $[Z^{(B)}] = [Y^{(B)}]^{-1}$, and the vectors $\{V\}_{\alpha x_1}$ and $\{V\}_{\beta x_1}$ are velocity vectors relating to the coordinates on each subsystem. Now, equations (3.26a) and (3.26b) may be written as

$$P_{av}^{(A)} = \frac{1}{2} Re \left(\begin{Bmatrix} V_1 \\ V_2 \\ \vdots \\ V_N \end{Bmatrix}^H \left[\begin{array}{c|c} [Z^{(A)}]_{\alpha \times \alpha} & 0 \\ \hline 0 & 0 \end{array} \right] \begin{Bmatrix} V_1 \\ V_2 \\ \vdots \\ V_N \end{Bmatrix} \right) \quad (3.27a)$$

and

$$P_{av}^{(B)} = \frac{1}{2} Re \left(\begin{Bmatrix} V_1 \\ V_2 \\ \vdots \\ V_N \end{Bmatrix}^H \left[\begin{array}{c|c} 0 & 0 \\ \hline 0 & [Z^{(B)}]_{\beta \times \beta} \end{array} \right] \begin{Bmatrix} V_1 \\ V_2 \\ \vdots \\ V_N \end{Bmatrix} \right) \quad (3.27b)$$

The sum of equations (3.27a) and (3.27b) is

$$P_{av}^{(A)} + P_{av}^{(B)} = \frac{1}{2} Re \left(\begin{Bmatrix} V_1 \\ V_2 \\ \vdots \\ V_N \end{Bmatrix}^H \left[\begin{array}{c|c} [Z^{(A)}] & 0 \\ \hline 0 & [Z^{(B)}] \end{array} \right] \begin{Bmatrix} V_1 \\ V_2 \\ \vdots \\ V_N \end{Bmatrix} \right) \quad (3.28)$$

The matrix addition implied in equation (3.26) is restricted to those coordinate directions in which the two subsystems are connected. For the rest of this section we shall use the symbol \oplus to denote this type of matrix addition.

Now, power balance considerations require that the time-average power flow to the coupled structure be equal to the sum of the power flow to each of the subsystems, i.e

$$P_{av}^{(C)} = P_{av}^{(A)} + P_{av}^{(B)} \quad (3.29)$$

Consequently we may write

$$Re \left(\{V\}^H [Z^{(C)}] \{V\} \right) = Re \left(\{V\}^H [Z^{(A)} \oplus Z^{(B)}] \{V\} \right) \quad (3.30)$$

Although we know from Impedance Coupling theory (Chapter 4) that the matrix $[Z^{(A)} \oplus Z^{(B)}]$ is equal to the impedance matrix of the coupled system, $[Z^{(C)}]$,

this fact cannot be deduced from equation (3.30). If equation (3.30) is expanded and the individual terms are examined it will be found that the equation relates only the real parts of the matrices. The condition $\text{Re}(\{Z^{(c)}\}) = \text{Re}(\{Z^{(a)} \oplus Z^{(b)}\})$ is, in fact, sufficient for equation (3.30) to be satisfied.

The fact that time-average power balance considerations lead to a relationship involving only the real parts of the coupled and subsystem matrices reveals a limitation on the information obtainable from time-average power. This limitation is more obvious if the time-average power input to the structure is written in terms of the mobilities and the exciting forces:

$$P_{av}^{(c)} = \frac{1}{2} \text{Re}(\{F\}^H \{Y^{(c)}\} \{F\}) \quad (3.31)$$

For a given excitation force vector, any alteration to the system which does not affect the real parts of the elements in the mobility matrix will leave the time-average power unchanged. However, we know that the motion response depends on both the real and imaginary parts of mobility, and therefore the time-average power flowing to a system does not define its motion responses uniquely.

By following a similar recipe but starting with the alternating component of power, another equation may be derived relating the coupled impedance matrix to the subsystem matrices. The alternating component of instantaneous power input to the coupled structure is

$$P_{alt}^{(c)} = \frac{1}{2} \text{Re}(\{V\}_{1 \times N}^T [Z^{(c)}]_{N \times N} \{V\}_{N \times 1} e^{j2\omega t}) \quad (3.32)$$

Similarly- we may- write for the subsystems

$$P_{alt}^{(A)} = \frac{1}{2} \operatorname{Re}(\{V\}^T [Z^{(A)}] \{V\} e^{j2\omega t}) \quad (3.33a)$$

and

$$P_{alt}^{(B)} = \frac{1}{2} \operatorname{Re}(\{V\}^T [Z^{(B)}] \{V\} e^{j2\omega t}) \quad (3.33b)$$

The sum of equations (3.33a) and (3.33b) is then

$$P_{alt}^{(A)} + P_{alt}^{(B)} = \frac{1}{2} \operatorname{Re}(\{V\}^T [Z^{(A)} \diamond Z^{(B)}] \{V\} e^{j2\omega t}) = P_{alt}^{(C)} \quad (3.34)$$

and we may therefore write

$$\operatorname{Re}(\{V\}^T [Z^{(C)}] \{V\} e^{j2\omega t}) = \operatorname{Re}(\{V\}^T [Z^{(A)} \diamond Z^{(B)}] \{V\} e^{j2\omega t}) \quad (3.35)$$

It is not possible to deduce from equation (3.35) that the matrices $[Z^{(C)}]$ and $[Z^{(A)} \diamond Z^{(B)}]$ are equal. Unlike equation (3.30), however, it represents a relationship involving both the real and imaginary parts of the matrices. We may infer from this that the alternating component of power contains more information than the time-average power.

3.3.4 Random Excitation

Expressions for power input

Let a force, $f(t)$, of spectral density $\mathbf{S}_{FF}(\omega)$, act on a structure to produce a velocity response $v(t)$. The time-average power input to the structure may be written as

$$P_{av} = E [f(t)v(t)] \quad (3.36)$$

Now, by definition, the input-output cross-correlation function is

$$R_{FV}(\tau) = E [f(t)v(t + \tau)] = \int_{-\infty}^{\infty} S_{FV}(\omega) e^{j\omega\tau} d\omega \quad (3.37)$$

where $S_{FV}(\omega)$ is the input-output cross-spectral density. Thus the power input may be written as

$$\begin{aligned} P_{av} &= R_{FV}(\tau = 0) \\ &= \int_{-\infty}^{\infty} S_{FV}(\omega) d\omega \\ &= \int_{-\infty}^{\infty} Y(\omega) S_{FF}(\omega) d\omega \end{aligned} \quad (3.38)$$

where $Y(\omega)$ is the driving-point mobility of the structure.

An alternative expression for the power input may be obtained by using the output-input cross-correlation function and its corresponding cross-spectral density:

$$P_{av} = R_{VF}(\tau = 0) = \int_{-\infty}^{\infty} S_{VF}(\omega) d\omega \quad (3.39)$$

From equations (3.38) and (3.39) we may write

$$\begin{aligned} P_{av} &= \frac{1}{2} \int_{-\infty}^{\infty} [S_{FV}(\omega) + S_{VF}(\omega)] d\omega \\ &= \frac{1}{2} \int_{-\infty}^{\infty} [S_{FV}(\omega) + S_{FV}^*(\omega)] d\omega \\ &= \int_{-\infty}^{\infty} \text{Re}[S_{FV}(\omega)] d\omega \\ &= \int_{-\infty}^{\infty} \text{Re}[Y(\omega) S_{FF}(\omega)] d\omega \\ &= \int_{-\infty}^{\infty} S_{FF}(\omega) \text{Re}\{Y(\omega)\} d\omega \end{aligned} \quad (3.40)$$

When a structure is subjected to random excitation in more than one coordinate, the time-average power input may be written as

$$P_{av} = \sum_{r=1}^m E [f_r(t)v_r(t)] \quad (3.4.1)$$

where m is the number of coordinate directions in which forces are applied.

Now,

$$E [f_r(t)v_r(t)] = R_{F_r, V_r}(\tau = 0) = \int_{-\infty}^{\infty} S_{F_r, V_r}(\omega) d\omega$$

Therefore,

$$P_{av} = \sum_{r=1}^m \int_{-\infty}^{\infty} S_{F_r, V_r}(\omega) d\omega = \sum_{r=1}^m \int_{-\infty}^{\infty} Re \{ S_{F_r, V_r}(\omega) \} d\omega \quad (3.4.2)$$

Also,

$$S_{F_r, V_r}(\omega) = \sum_{s=1}^m S_{F_r, F_s}(\omega) Y_{rs}(\omega)$$

Therefore,

$$\begin{aligned} P_{av} &= \sum_{r=1}^m \int_{-\infty}^{\infty} Re \left(\sum_{s=1}^m S_{F_r, F_s}(\omega) Y_{rs}(\omega) \right) d\omega \\ &= \int_{-\infty}^{\infty} \left(\sum_{r=1}^m \sum_{s=1}^m Re \{ S_{F_r, F_s}(\omega) Y_{rs}(\omega) \} \right) d\omega \end{aligned} \quad (3.4.3)$$

If the excitation forces are uncorrelated then, for rfs, $S_{F_r, F_s}(\omega) = 0$, and the power input reduces to

$$P_{av} = \int_{-\infty}^{\infty} \left(\sum_{i=1}^m Re \{ S_{F_i, F_i}(\omega) Y_{ii}(\omega) \} \right) d\omega$$

and since the power spectral density, $S_{F_i, F_i}(\omega)$, is real, we have

$$P_{av} = \int_{-\infty}^{\infty} \left(\sum_{i=1}^m S_{F_i F_i}(\omega) \operatorname{Re} \{ Y_{ii}(\omega) \} \right) d\omega \quad (3.44)$$

Expressions for power flow

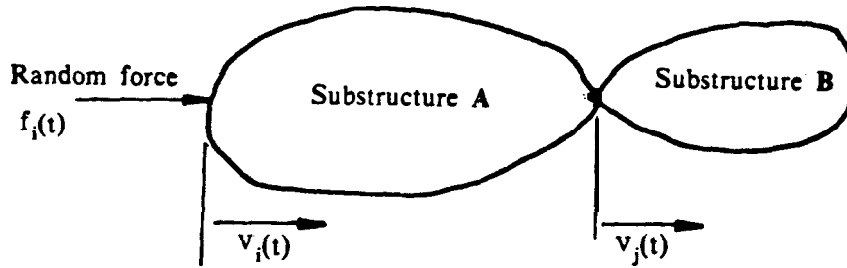


Fig.3.5 Power flow when coupling is in a single coordinate

Fig.3.5 shows two substructures, A and B, connected together in coordinate j to form a coupled structure C. A random force $f_i(t)$ of spectral density $S_{F_i F_i}(\omega)$ acts in coordinate i . The time-average power flow to substructure B is the average value of the product of the velocity $v_j(t)$ and the internal force, $f_i^{(B)}(t)$, exerted on B by A. We may write

$$P_{av}^{(B)} = E [f_i^{(B)}(t) v_j(t)] = \int_{-\omega}^{\omega} S_{F_i v_j}(\omega) d\omega \quad (3.45)$$

where $S_{F_i v_j}(\omega)$ is the cross-spectral density between the velocity $v_j(t)$ and the transmitted force $f_i^{(B)}(t)$. We may define a force transmissibility function, $T_{ij}^{(B)}$, to relate the transmitted force to the excitation force:

$$T_{ij}^{(B)}(\omega) = \frac{F_i^{(B)}(\omega)}{F_i(\omega)} = \frac{Y_{ji}^{(C)}(\omega)}{Y_{jj}^{(B)}(\omega)} \quad (3.46)$$

The spectral density of the transmitted force is

$$S_{F_i F_i}(\omega) = S_{F_i F_i}(\omega) |T_{ji}^{(B)}(\omega)|^2 \quad (3.47)$$

and the cross-spectral density between transmitted force, $\mathbf{f}_i^{(B)}(t)$, and velocity, $v_j(t)$ is

$$\begin{aligned} S_{F_i v_j}(\omega) &= S_{F_i F_i}(\omega) Y_{jj}^{(B)}(\omega) \\ &= S_{F_i F_i}(\omega) |T_{ji}^{(B)}(\omega)|^2 Y_{jj}^{(B)}(\omega) \\ &= S_{F_i F_i}(\omega) \left| \frac{Y_{ji}^{(C)}(\omega)}{Y_{jj}^{(B)}(\omega)} \right|^2 Y_{jj}^{(B)}(\omega) \end{aligned} \quad (3.48)$$

The time-average power flow to substructure B is then given by

$$\begin{aligned} P_{av}^{(B)} &= \int_{-\infty}^{\infty} \left(S_{F_i F_i}(\omega) \left| \frac{Y_{ji}^{(C)}(\omega)}{Y_{jj}^{(B)}(\omega)} \right|^2 Y_{jj}^{(B)}(\omega) \right) d\omega \\ &= \int_{-\infty}^{\infty} \left(S_{F_i F_i}(\omega) \left| \frac{Y_{ji}^{(C)}(\omega)}{Y_{jj}^{(B)}(\omega)} \right|^2 \text{Re} \{ Y_{jj}^{(B)}(\omega) \} \right) d\omega \end{aligned} \quad (3.49)$$

Consider a connected structure, C, which has been separated into its component parts, A and B. The coupled structure is described by a total of m coordinates, and there are n coordinates on substructure B. Let the forces $\mathbf{f}_1^{(B)}, \mathbf{f}_2^{(B)}, \dots, \mathbf{f}_n^{(B)}$ be the resultant forces exerted on B due to coupling to A as well to as external excitation. The total power flow to substructure B is then

$$\begin{aligned} P_{av}^{(B)} &= \sum_{r=1}^n E [f_r^{(B)}(t) v_r(t)] \\ &= \int_{-\infty}^{\infty} \left(\sum_{r=1}^n \text{Re} \{ S_{F_i F_i}^{(B)}(\omega) Y_{rs}^{(B)}(\omega) \} \right) d\omega \end{aligned} \quad (3.50)$$

where $S_{F_i F_i}^{(B)}(\omega)$ is the cross-spectral density between the transmitted forces f_i and f_i .

The matrix of transmitted force spectral densities may be determined as follows. Consider the situation where the excitation forces are sinusoidal. Then, we may write

$$\{F_i\}_{n \times 1} = [Z^{(B)}(\omega)]_{n \times n} \{V^{(B)}\}_{n \times 1} \quad (3.51)$$

where $\{F_i\}_{n \times 1}$ is a column vector of the resultant forces transmitted to B in its n coordinates, $[Z^{(B)}(\omega)]$ is the $n \times n$ impedance matrix of B, and $\{V^{(B)}\}$ is a column vector of the corresponding n velocities. Equation (3.51) may be written as

$$\begin{aligned} \{F_i\}_{n \times 1} &= [Z^{(B)}(\omega)]_{n \times n} [Y_R^{(C)}(\omega)]_{n \times m} \{F_i^{(C)}\}_{m \times 1} \\ &= [T_{ij}^{(B)}(\omega)]_{n \times m} \{F_i^{(C)}\}_{m \times 1} \end{aligned} \quad (3.52)$$

$[T_{ij}^{(B)}(\omega)]$ is a force transmissibility matrix relating the resultant forces to the m external excitation forces. $[Y_R^{(C)}(\omega)]$ is the reduced mobility matrix obtained by deleting from the overall system mobility matrix those rows which do not relate to substructure B. $\{F_i^{(C)}\}$ is the column vector of the external sinusoidal forces acting on the coupled structure. The matrix of transmitted force spectral densities is then given by

$$[S_{F_i F_i}^{(B)}(\omega)]_{n \times n} = [T_{ij}^{(B)}(\omega)]_{n \times m}^* [S_{F_i F_i}(\omega)]_{m \times m} [T_{ij}^{(B)}(\omega)]_{m \times n}^T \quad (3.53)$$

where $[S_{F_r F_r}(\omega)]$ is the spectral density matrix of the external excitation forces.

3.4 Energy flow via coordinate directions at joints between substructures

In §3.2 it was shown that the instantaneous power input to a structure by N sinusoidal forces is given by

$$P(t) = \frac{1}{2} R e(\{F\}^H [Y] \{F\}) + \frac{1}{2} R e(e^{j2\omega t} \{F\}^T [Y] \{F\}) \quad (3.54)$$

This expression represents a summation of the power due to the forces acting in each coordinate direction. The power input due to the force acting in the q^{th} coordinate may be obtained by extracting the corresponding terms from equation (3.54):

$$P^{(q)}(t) = \frac{1}{2} R e\left(\sum_{r=1}^N F_q^* Y_{qr} F_r\right) + \frac{1}{2} R e\left(e^{j2\omega t} \sum_{r=1}^N F_q Y_{qr} F_r\right) \quad (3.55)$$

Equation (3.55) shows that the instantaneous power input through any coordinate direction is made up of a constant term plus an alternating component of twice the excitation frequency.

The constant term is

$$P_{av}^{(q)} = \frac{1}{2} R e\left(\sum_{r=1}^N F_q^* Y_{qr} F_r\right) \quad (3.56)$$

and the alternating component is

$$P_{alt}^{(q)} = \frac{1}{2} R e\left(e^{j2\omega t} \sum_{r=1}^N F_q Y_{qr} F_r\right) \quad (3.57)$$

A plot of equation (3.55) is shown in Fig.3.6 In that figure. $\hat{P}_{alt}^{(q)}$ is the amplitude of the alternating component of power. and is given by

$$\hat{P}_{alt}^{(q)} = \frac{1}{2} \left| \sum_{r=1}^N F_q Y_{qr} F_r \right| \quad (3.58)$$

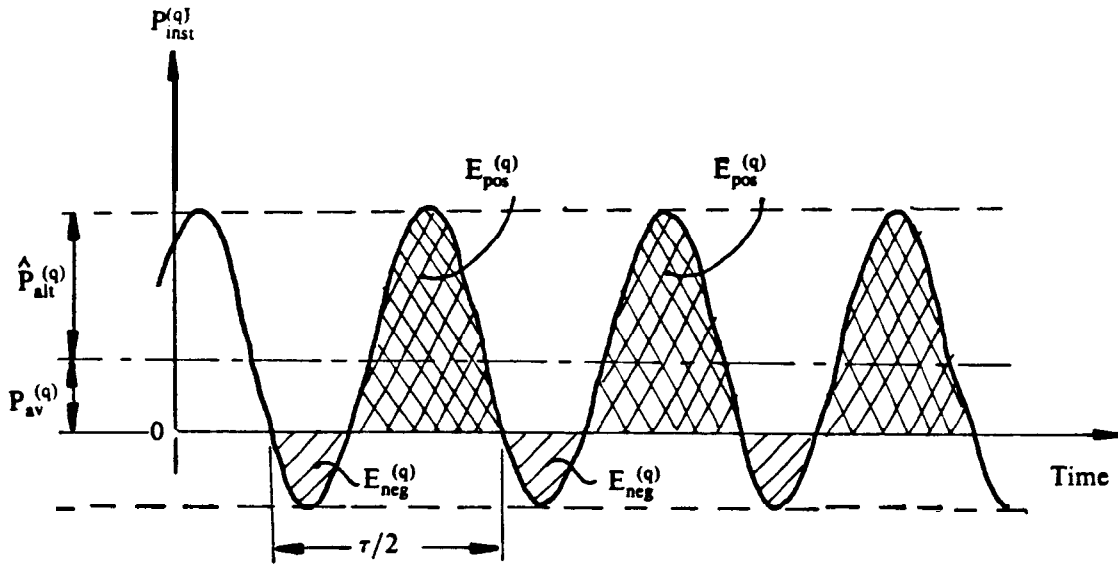


Fig.3. 6 Instantaneous power input in direction of coordinate q

The cross-hatched areas above the time axis, labelled $E_{pos}^{(q)}$, represent energy being delivered to the system by the force of excitation. The areas below the time axis labelled $E_{neg}^{(q)}$, represent energy that is returned to the source of excitation by the vibrating structure during each half-cycle. The difference between $E_{pos}^{(q)}$ and $E_{neg}^{(q)}$ is energy that is lost in the system through dissipation, such that the following relationship holds:

$$E_{pos}^{(q)} - E_{neg}^{(q)} = \frac{P_{av}^{(q)} \tau}{2} \quad (3.59)$$

where τ is the time period of vibration.

It is shown in Appendix 1 that

$$E_{\text{pos}}^{(q)} = \frac{\hat{P}_{\text{alt}}^{(q)}}{\omega}((\pi - \phi) \cos \phi + \sin \phi) \quad (3.60)$$

and

$$E_{\text{neg}}^{(q)} = \frac{\hat{P}_{\text{alt}}^{(q)}}{\omega}(\sin \phi - \phi \cos \phi) \quad (3.61)$$

where

$$\phi = \cos^{-1}\left(\frac{P_{\text{av}}^{(q)}}{\hat{P}_{\text{alt}}^{(q)}}\right) \quad (3.62)$$

The foregoing discussion refers to the flow of energy to a structure from external sources. When considering power input to a structure it is important to note that the time-average power is always positive. If this were not so a physically impossible situation would arise whereby the conservation of energy would be violated. In effect the system would be returning more energy than that being supplied to it. These remarks apply also to the total power flowing to any subsystem of a connected structure.

The situation is different when considering the flow of energy in any individual coordinate direction at a joint between subsystems. In this case negative values of time-average power are admissible. A negative value of time-average power in any coordinate implies that the subsystem returns more energy than that supplied to it in that coordinate direction. The instantaneous power flow via any coordinate direction is given by equation (3.55). with the proviso that the forces $F_1, F_2, \dots, F_q, \dots, F_N$ are the resultant forces (internal and external) exerted on the subsystem.

3.5 Discussion

One purpose of this chapter is to set out some of the general expressions concerning power flow in connected structures. The expressions derived in §3.3 are meant to indicate the general procedure by which the power flow to any component of a connected structure can be calculated if a substructure approach based on frequency response data is adopted. The examination in §3.4 of the nature of energy transfer in the coordinate directions at the joints between subsystems lays the foundation for a method, proposed in Chapter 4, for assessing the relative importance of coordinates when the Impedance Coupling technique is used in the vibration analysis of structures.

By using the requirement that the power input to a system be balanced by the sum of the power flow to each of the subsystems, two equations were obtained relating the system impedance matrix to the subsystem matrices. The fact that the basic Impedance Coupling relation (*i.e.* the addition of subsystem impedance matrices to obtain the overall system matrix) cannot be extracted from these equations reveals an important difference between the information contained in power flow data and that represented by frequency response data. The main ingredients in the derivation of the Impedance Coupling relation are the imposition of force balance and motion compatibility between the subsystems. Since power involves both force and motion (velocity) one might expect to be able to derive the Impedance Coupling relation by starting from a consideration of power balance. That this is not the case is not altogether surprising, since power flow contains information which is specific to the particular excitation forces imposed on the system. Frequency response data, on the other hand, indicate the input-output (force-motion) characteristics of the system, and are of a more general nature.

Chapter 4

A METHOD FOR ASSESSING THE RELATIVE IMPORTANCE OF COORDINATES IN THE VIBRATION ANALYSIS OF CONNECTED STRUCTURES BY THE IMPEDANCE COUPLING TECHNIQUE

4.1 Introduction

One of the commonly-used techniques for the vibration analysis of complex structures is the method of Receptance or Impedance Coupling [34]. The method involves the subdivision of the structure into a number of subsystems each of which is analysed separately to obtain its frequency response data. The frequency response properties of the complete structure are then obtained by combining the subsystem data in such a way that force balance and motion compatibility are satisfied at the connection points.

At the start of any Impedance Coupling analysis it is necessary to decide which coordinates are to be included in order to obtain an adequate description of the dynamic behaviour of each subsystem. In general, six coordinates are required to describe completely the motion of any point on a structure. However, inclusion of all six coordinates at each connection point is seldom practicable partly because it leads to very large system matrices which may be difficult to handle. Deleting unimportant coordinates reduces the size of the problem, and, where some of the subsystem data are to be obtained experimentally, big savings may be made in the time required for mobility measurements. In certain simple

cases (for example, where the structure is two-dimensional, and motion is known to be restricted to one plane) it is obvious which coordinates may be deleted. However, in more complex situations the coordinates to be used in the analysis are not at all obvious. Previous applications of the Impedance Coupling technique have shown the difficulties involved in deciding which coordinates may be excluded from the analysis without significant loss of accuracy [39]. Computational studies [40] have also indicated that the accuracy of the analysis may not be improved by merely increasing the number of coordinates included. The particular choice of coordinates to be used in the analysis has been found to be of considerable importance.

In this chapter a method is proposed for assessing the relative importance of coordinates in the analysis of connected structures by the Impedance Coupling technique. The method is based on the premise that the relative importance of any coupling coordinate depends on the magnitude of the energy transferred in that coordinate direction. Calculations on a number of simple structures are used to test the validity of this assumption.

4.2 The Impedance Coupling Technique

The practical application of the Impedance Coupling technique involves three main steps:

(i) *Division of the system into subsystems*

The determination of the best subdivision is not always obvious, and may require considerable judgement. Very often, it is convenient to divide the system into a series of components, each of which has a distinct geometry or function. It is useful to examine the system for

planes of symmetry which might permit a complete 3-dimensional analysis to be made in stages.

(ii) *Analysis of each individual component, by whatever means is best suited to it, to obtain the frequency response properties relating to all points of interest on the component.*

A theoretical analysis may be sufficient for simple components such as beams, springs, etc. In the case of more complex components, however, it might be necessary to resort to direct measurement. In such cases it would almost invariably be necessary to process the measured data by a modal analysis method [42] before inclusion in any subsequent analysis.

(iii) *Combination of the component response properties to obtain the properties of the complete system.*

The underlying theory of this final step is described in the following sections. A detailed exposition of the theory of Impedance or Receptance Coupling may be found in the work by Bishop and Johnson [34]. Examples of the practical application of the technique to real engineering structures may also be found in references 39 and 41.

4.2.1 Single- coordinate Coupling

The simplest case of Impedance Coupling arises where two subsystems are connected in a single coordinate. Consider two single-coordinate subsystems, A and B, which are to be connected to form a coupled system, C, as shown in Fig.4.1.

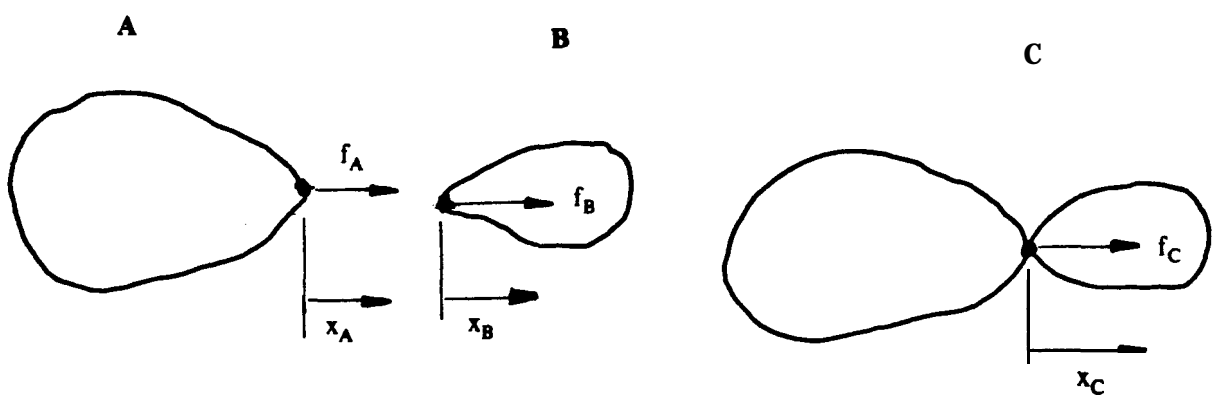


Fig.4.1 Single-coordinate coupling

For steady sinusoidal vibration at a given frequency, the velocities of the subsystems may be written as

$$V_A = Y_A f_A \quad \text{and} \quad V_B = Y_B f_B \quad (4.1)$$

where Y_A and Y_B are the driving-point mobilities of A and B respectively, relating to excitation in the coordinate x .

When the subsystems are connected together to form C, their velocities must be identical at the connection point, so that

$$V_A = V_B = V_C \quad (4.2)$$

Also, by considering force balance at the connection point we may write

$$f_C = f_A + f_B \quad (4.3)$$

Dividing through by V_C , and noting from equation (4.2) that V_C , V_A and V_B are identical, we have

$$\frac{f_C}{V_C} = \frac{f_A}{V_A} + \frac{f_B}{V_B} \quad (4.4)$$

Using the definition of mobility we have that

$$Y_C^{-1} = Y_A^{-1} + Y_B^{-1}$$

For steady sinusoidal vibration at a given frequency, the velocities of the subsystems may be written as

$$V_A = Y_A f_A \text{ and } V_B = Y_B f_B \quad (4.1)$$

where Y_A and Y_B are the driving-point mobilities of A and B respectively, relating to excitation in the coordinate x .

When the subsystems are connected together to form C, their velocities must be identical at the connection point, so that

$$V_A = V_B = V_C \quad (4.2)$$

Also, by considering force balance at the connection point we may write

$$f_C = f_A + f_B \quad (4.3)$$

Dividing through by V_C , and noting from equation (4.2) that V_C , V_A and V_B are identical, we have

$$\frac{f_C}{V_C} = \frac{f_A}{V_A} + \frac{f_B}{V_B} \quad (4.4)$$

Using the definition of mobility we have that

$$Y_C^{-1} = Y_A^{-1} + Y_B^{-1}$$

or. in terms of impedances,

$$Z_C = Z_A + Z_B \quad (4.5)$$

4.2.2 Coupling in more than one coordinate

For the case where the components A and B each has more than one coordinate, all of which are involved in the coupling process, the mobilities of each component may be expressed in matrix form, and the velocities of the components may be written as

$$\{V\}_A = [Y]_A \{f\}_A, \quad \{V\}_B = [Y]_B \{f\}_B \quad (4.6)$$

The compatibility equation (4.2) becomes

$$\{V\}_C = \{V\}_A = \{V\}_B \quad (4.7)$$

and, the equilibrium equation (4.3) becomes

$$\{f\}_C = \{f\}_A + \{f\}_B \quad (4.8)$$

Now, from equation (4.6). we have

$$\begin{aligned} \{f\}_A &= [Y]_A^{-1} \{V\}_A \\ \{f\}_B &= [Y]_B^{-1} \{V\}_B \\ \{f\}_C &= [Y]_C^{-1} \{V\}_C \end{aligned} \quad (4.9)$$

Substituting into equation (4.8). we have

$$[Y]_C^{-1} \{V\}_C = [Y]_A^{-1} \{V\}_A + [Y]_B^{-1} \{V\}_B$$

Using equation (4.7), we have the coupling equation

$$[Y]_C^{-1} = [Y]_A^{-1} + [Y]_B^{-1}$$

or, $[Z]_C = [Z]_A + [Z]_B$ (4.10)

4.2.3 The General Case

The most general case of Impedance Coupling arises where each component has several coordinates, not all of which are involved in the coupling process.

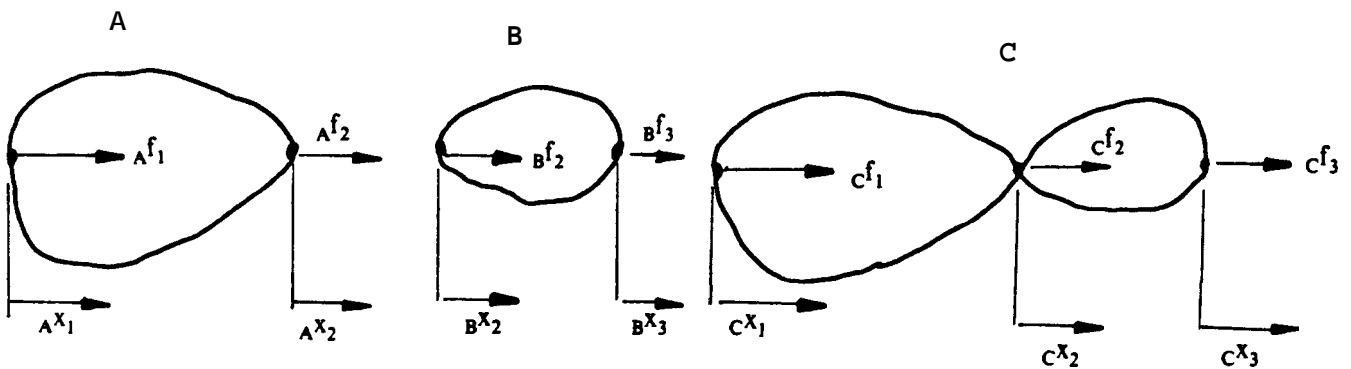


Fig.4.2 The general case of Impedance Coupling

Consider the simple case where two subsystems, each having two coordinates, are to be connected in one coordinate to form a 3-coordinate system as in Fig.4.2. The velocities of the subsystems are given by

$$\begin{Bmatrix} {}_A V_1 \\ {}_A V_2 \end{Bmatrix} = \begin{bmatrix} {}_A Y_{11} & {}_A Y_{12} \\ {}_A Y_{21} & {}_A Y_{22} \end{bmatrix} \begin{Bmatrix} {}_A f_1 \\ {}_A f_2 \end{Bmatrix} = [Y]_A \{f\}_A \quad (4.1 \text{ la})$$

and

$$\begin{Bmatrix} {}_B V_2 \\ {}_B V_3 \end{Bmatrix} = \begin{bmatrix} {}_B Y_{22} & {}_B Y_{23} \\ {}_B Y_{32} & {}_B Y_{33} \end{bmatrix} \begin{Bmatrix} {}_B f_2 \\ {}_B f_3 \end{Bmatrix} = [Y]_B \{f\}_B \quad (4.1 \text{ lb})$$

When the components are coupled together, compatibility requirements lead to the following equations:

$$\begin{aligned} {}_C V_1 &= {}_A V_1 \\ {}_C V_2 &= {}_A V_2 = {}_B V_2 \\ {}_C V_3 &= {}_B V_3 \end{aligned} \quad (4.12)$$

Also, considering force balance in the three coordinate directions we have

$$\begin{Bmatrix} {}_C f_1 \\ {}_C f_2 \\ {}_C f_3 \end{Bmatrix} = \begin{Bmatrix} \{f\}_A \\ \text{---} \\ 0 \end{Bmatrix} + \begin{Bmatrix} 0 \\ \text{---} \\ \{f\}_B \end{Bmatrix} \quad (4.13)$$

Now,

$$\begin{aligned} \{f\}_A &= [Y]_A^{-1} \{V\}_A = [Z]_A \{V\}_A \\ \{f\}_B &= [Y]_B^{-1} \{V\}_B = [Z]_B \{V\}_B \\ \{f\}_C &= [Y]_C^{-1} \{V\}_C = [Z]_C \{V\}_C \end{aligned}$$

So that, using equation (4.12) we have

$$\begin{aligned}
 \{V\}_c &= \begin{Bmatrix} [Z]_A \{V\}_A \\ 0 \end{Bmatrix} + \begin{Bmatrix} 0 \\ [Z]_B \{V\}_B \end{Bmatrix} \\
 &= \begin{bmatrix} A Z_{11} & A Z_{12} & 0 \\ A Z_{21} & A Z_{22} & 0 \\ 0 & 0 & 0 \end{bmatrix} \begin{Bmatrix} cV_1 \\ cV_2 \\ cV_3 \end{Bmatrix} + \begin{bmatrix} 0 & 0 & 0 \\ 0 & B Z_{22} & B Z_{23} \\ 0 & B Z_{32} & B Z_{33} \end{bmatrix} \begin{Bmatrix} cV_1 \\ cV_2 \\ cV_3 \end{Bmatrix} \\
 &= \begin{bmatrix} A Z_{11} & A Z_{12} & 0 \\ A Z_{21} & A Z_{22} + B Z_{22} & B Z_{23} \\ 0 & B Z_{32} & B Z_{33} \end{bmatrix} \begin{Bmatrix} cV_1 \\ cV_2 \\ cV_3 \end{Bmatrix} \\
 &= [Z]_c \{V\}_c \tag{4.14}
 \end{aligned}$$

Thus, in the general case the impedance matrices of the components have to be partitioned, all the coordinates at the joints between subsystems being grouped together. The impedance matrix of the complete system is then obtained by adding the component impedance matrices in the way suggested above.

4.2.4 Coordinate Elimination

By a simple extension of the coupling process described above, the frequency response properties of a multi-component structure may be “built up” by a sequential addition of its components. Any coordinates used in joining two subsystems which are of no further interest may be dropped from the mobility matrix of the coupled system by simply deleting the corresponding rows and columns. Consider again the case shown in Fig.4.2. For the coupled system C we may write

$$\{V\}_c = [Y]_c \{f\}_c$$

This may be expanded to give

$$\begin{aligned} cV_1 &= cY_{11}f_1 + cY_{12}f_2 + cY_{13}f_3 \\ cV_2 &= cY_{21}f_1 + cY_{22}f_2 + cY_{23}f_3 \\ cV_3 &= cY_{31}f_1 + cY_{32}f_2 + cY_{33}f_3 \end{aligned} \tag{4.15}$$

Now, if we are not interested in the response in coordinate cX_2 , we may delete the second of equations (4.15). Furthermore, if the external force f_2 applied in coordinate cX_2 is zero, the second term in each of equations (4.15) may be deleted. Thus, the reduced description of the frequency response properties of the coupled system may be written as

$$\begin{Bmatrix} cV_1 \\ cV_3 \end{Bmatrix} = \begin{bmatrix} cY_{11} & cY_{13} \\ cY_{31} & cY_{33} \end{bmatrix} \begin{Bmatrix} cf_1 \\ cf_3 \end{Bmatrix} \tag{4.16}$$

Coordinate elimination applied to a mobility matrix does not imply a reduction in the system's degrees of freedom. It merely results in a

reduced description of the system, and a reduction in the size of the matrices to be handled in any subsequent analysis.

When coordinate elimination is applied to the impedance matrix of a system the effect is rather different. Consider again the case shown in Fig.4.2. for which we may write

$$\begin{aligned} f_1 &= cZ_{11} cV_1 + cZ_{12} cV_2 + cZ_{13} cV_3 \\ f_2 &= cZ_{21} cV_1 + cZ_{22} cV_2 + cZ_{23} cV_3 \\ f_3 &= cZ_{31} cV_1 + cZ_{32} cV_2 + cZ_{33} cV_3 \end{aligned} \tag{4.17}$$

If, for example, we are not interested in the force f_2 applied in coordinate cX_2 , we may remove the second of equations (4.17). Since the impedance terms cZ_{12} , cZ_{22} and cZ_{32} are, in general, different from zero we may delete the second term of each equation only if the velocity cV_2 is zero. Thus, the elimination of coordinates from an Impedance matrix has the effect of grounding those particular coordinates.

It must be mentioned that the main subject of this chapter is not coordinate elimination in the sense that has been described in this section. We are concerned here with situations where some of the coordinates taking part in the coupling process must be excluded from the analysis in order to reduce the size of the problem. The exclusion of such coordinates will lead to some inaccuracy. The method proposed in the next section provides a basis for deciding which coordinates may be excluded from the analysis without severe loss of accuracy.

4.3 Proposed method for assessing the relative importance of coordinates

It was shown in Chapter 3 §3.4 that the instantaneous power flow through any coordinate at a joint between two subsystems is made up of a constant term, plus an alternating component of twice the excitation frequency. The constant term, P_{av} , is the time-average power flow in that coordinate direction, and is closely related to dissipation, although it is not entirely dependent upon it. (In an undamped system, for example, the time-average power flow in any coordinate direction at a joint could be non-zero if there is a closed circulation of energy, ie energy entering a subsystem in one coordinate direction and leaving via another in such a way that the total flow from adjacent subsystems is zero.) The alternating component of power, P_{alt} , is a measure of the rate at which energy is transferred reversibly between the subsystems via that coordinate direction. The instantaneous power as a function of time is shown in Fig.4.3.

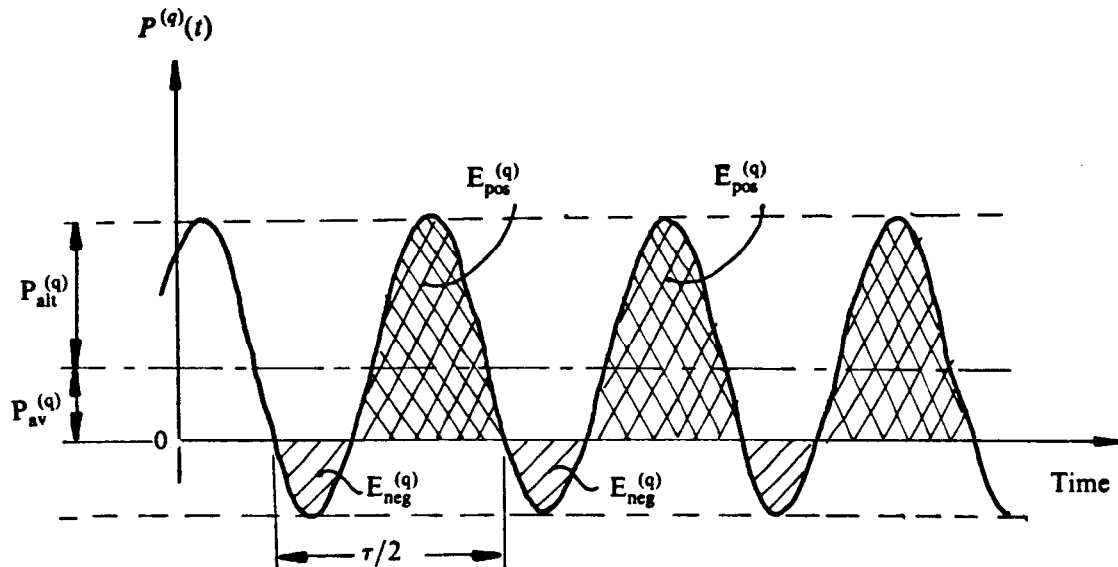


Fig.4.3 Instantaneous power flow in any coordinate direction

Since the transmission of vibration through a structure is the result of the propagation of energy-bearing waves, it seems reasonable to expect that the relative importance of any coordinate in the transmission path will be related to the extent to which it participates in the energy transmission process. It is proposed that the relative importance of the coordinates at a joint be assessed by comparing the magnitudes of the energy transferred via each coordinate direction. The energy transferred, $E^{(q)}$, is represented by the greater of the two quantities $E_{pos}^{(q)}$ and $E_{neg}^{(q)}$ in Fig.4.3. and is given by

$$E^{(q)} = \frac{\hat{P}_{alt}^{(q)}}{\omega} [(\pi - \phi) \cos \phi + \sin \phi] \quad (4.18)$$

where

$$\hat{P}_{alt}^{(q)} = \frac{1}{2} \left| \sum_{r=1}^N F_q Y_{qr} F_r \right| \quad (4.19)$$

$$\phi = \cos^{-1} \left| \frac{P_{av}^{(q)}}{\hat{P}_{alt}^{(q)}} \right| \quad (4.20)$$

and, F_q and F_r are the internal forces transmitted at the joints in the q and r coordinate directions respectively.

$E^{(q)}$ takes account of the energy that is irreversibly transferred, as well as the energy that is merely swapped back and forth between the subsystems.†

† The method proposed here is based on energy rather than time-average power partly because time-average power is very heavily dependent on the amount and distribution of damping. A method based on time-average power is likely to break down when it is applied to systems that are assumed to be undamped, whereas energy transfer always exists whether the system is damped or undamped.

4.4 Some illustrative examples

In order to test the underlying assumption of the proposed method a number of simple structures were analysed. For each structure a complete analysis† was first carried out, and the energy transfer in each coordinate direction was calculated over a chosen frequency range. Based on the energy calculations predictions were made about the relative importance of the coupling coordinates. Further analyses were then carried out in which various combinations of coupling coordinates were excluded, and the responses were compared with those for the complete analysis to see if the predictions were borne out. The Impedance Coupling computations were performed using the computer program **COUPLE1**[45,46].

4.4.1 Example I

The test structure here consists of two simple Bernoulli-Euler beams connected together as shown in Fig.4.4. The structure vibrates in one plane under the action of a sinusoidal force of unit amplitude. The coupling coordinates are x , y and θ . However, since the excitation is applied at right-angles to the structure there is no motion in the x coordinate direction, and therefore x is excluded from the analysis.

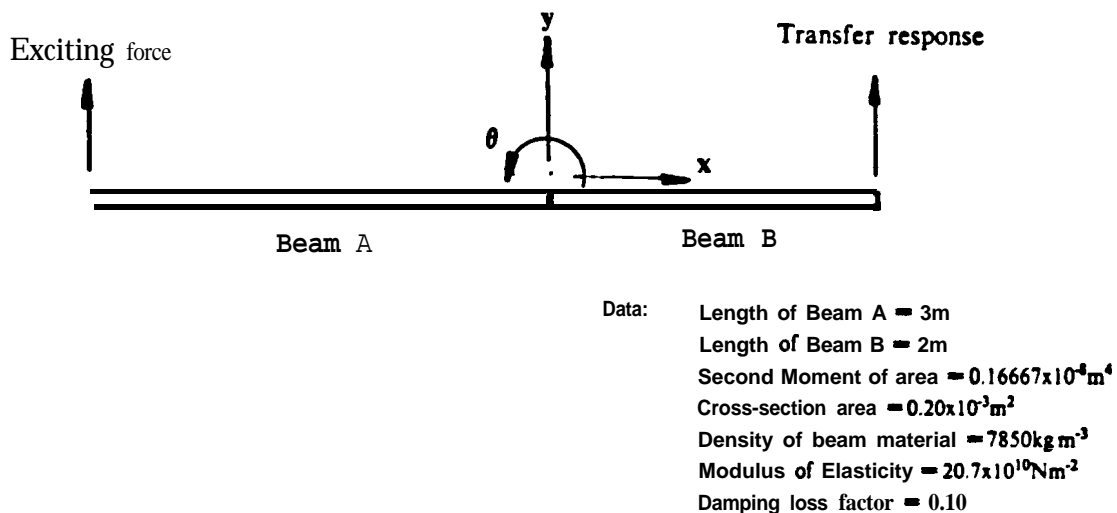


Fig.4.4 Test structure for Example I

† 'Complete analysis' refers to an analysis which includes all the coordinates at the joints between components.

The energy transfer for the two coordinates y and θ , are shown graphically in Fig.4.5(a) for the frequency range 0 - 1000Hz.[†] The time-average power and the amplitude of the alternating component of power are also shown in Figs.4.5(b) and 4.5(c). It is seen that the energy transfer via the two coordinate directions are roughly equal. The same is true of the time-average power and the alternating component of power. On the basis of the relative magnitudes of energy transfer we would expect that the two coordinates would be of roughly equal importance. This expectation is borne out by the fact that when either of the coordinates is excluded from the analysis the responses differ from the true values by similar amounts; see Figs.4.6(a) and 4.6(b). In the case of the driving-point responses, Fig.4.6(b), the deviations from the true responses become smaller as the frequency increases. It was found that at high frequencies the exclusion of both coordinates (ie completely uncoupling the two beams) has very little effect on the driving-point responses, Fig.4.6(c). These observations are explained by the fact that on a damped finite structure there is a frequency above which the driving-point characteristics are approximately the same as those of a similar structure of infinite extent [43,44]. At high frequencies the reflected waves returning to the driving-point are heavily attenuated, and the actual location at which the waves are reflected has only a small effect on the driving-point response. The implication of these observations is that when assessing the relative importance of coordinates misleading results could be obtained if attention is restricted to driving-point responses alone.

[†] Note that in Fig.4.5(a),(b) and (c) the energy or power flow via the coordinates at the joint is indicated for the individual coordinates. The total energy or power flow is not shown. In the response plots, Fig.4.6(a),(b) and (c), the responses are shown for the complete analysis as well as the responses based on various coupling conditions. Note that the legends used for the response plots are not meant to be related to those used for the energy plots. This note applies to all the plots in the rest of this chapter.

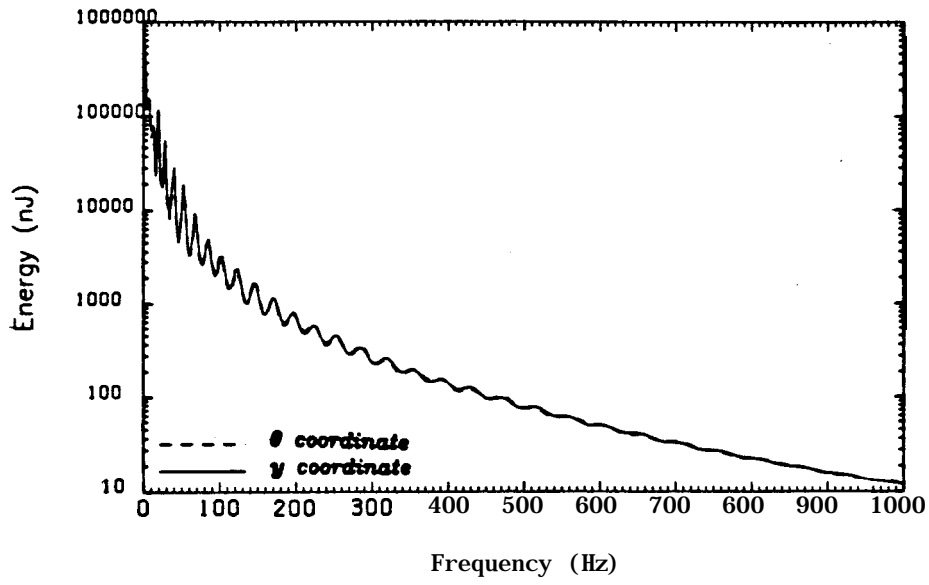


Fig.4.5(a) Example I - Energy flow in coordinate directions

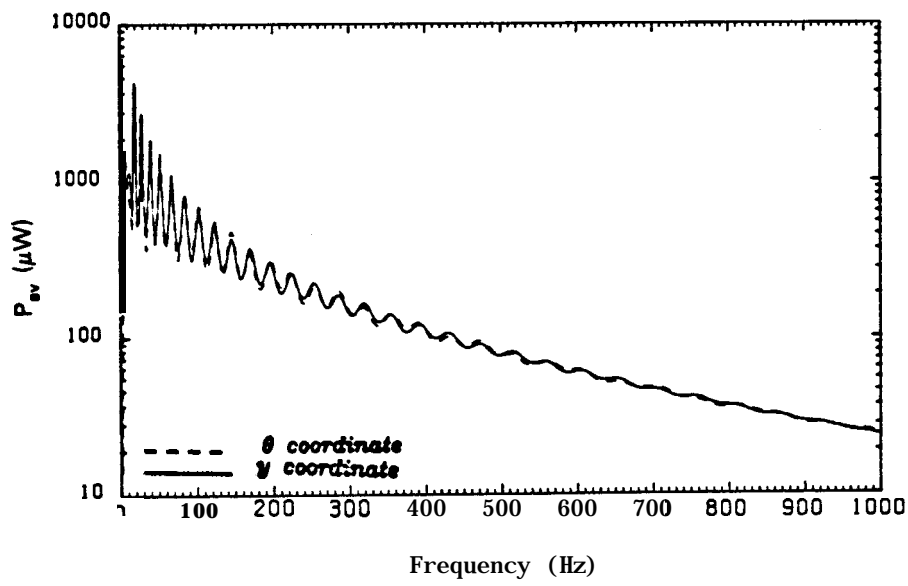


Fig.4.5(b) Example I - Time-average power flow in coordinate directions

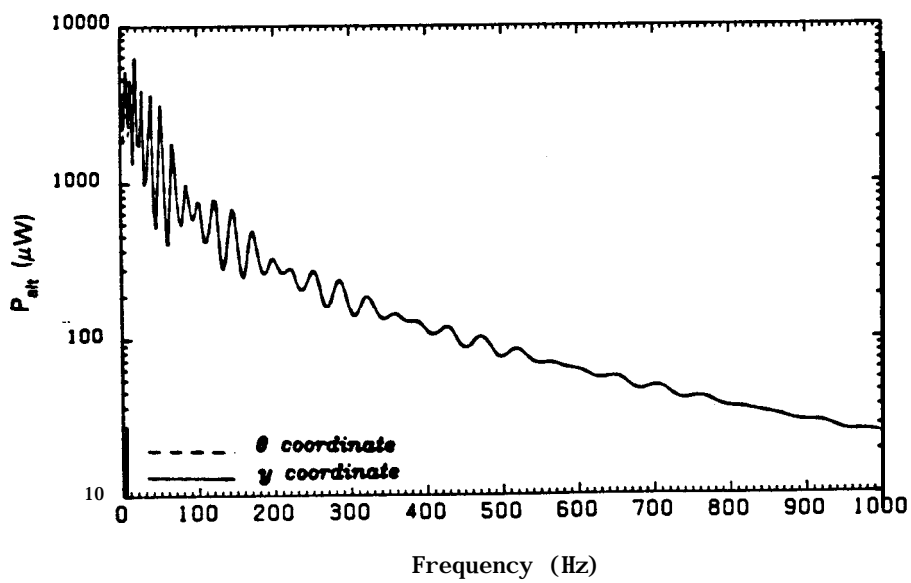


Fig.4.5(c) Example I - Amplitude of alternating component of power

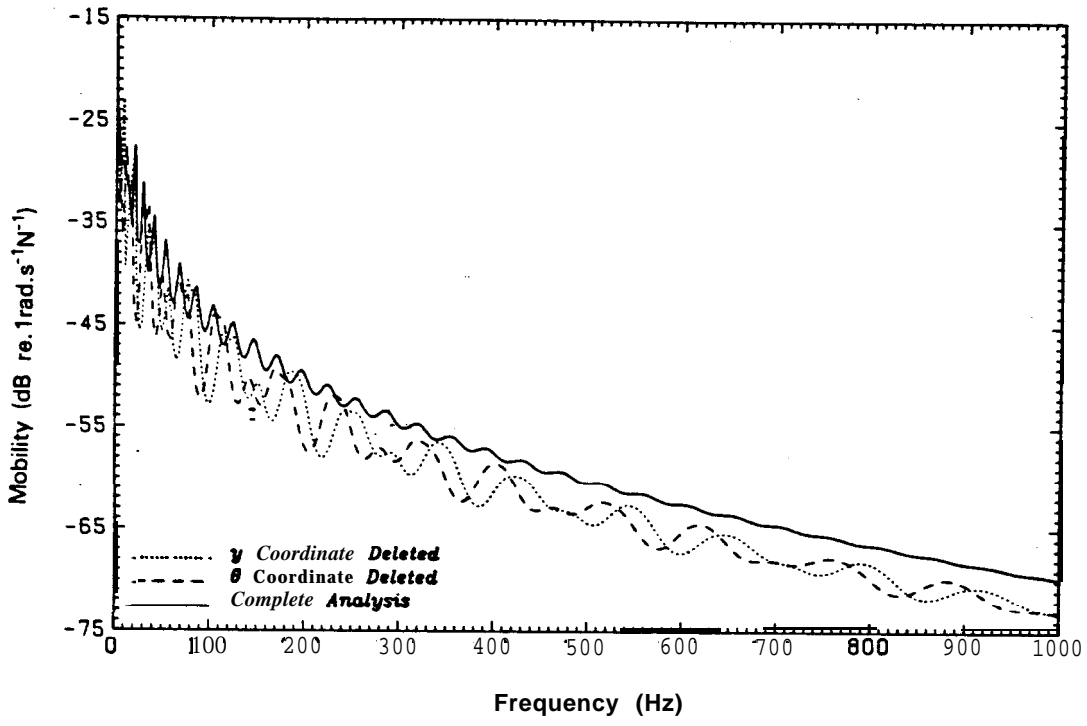


Fig.4.6(a) Example I - Transfer response

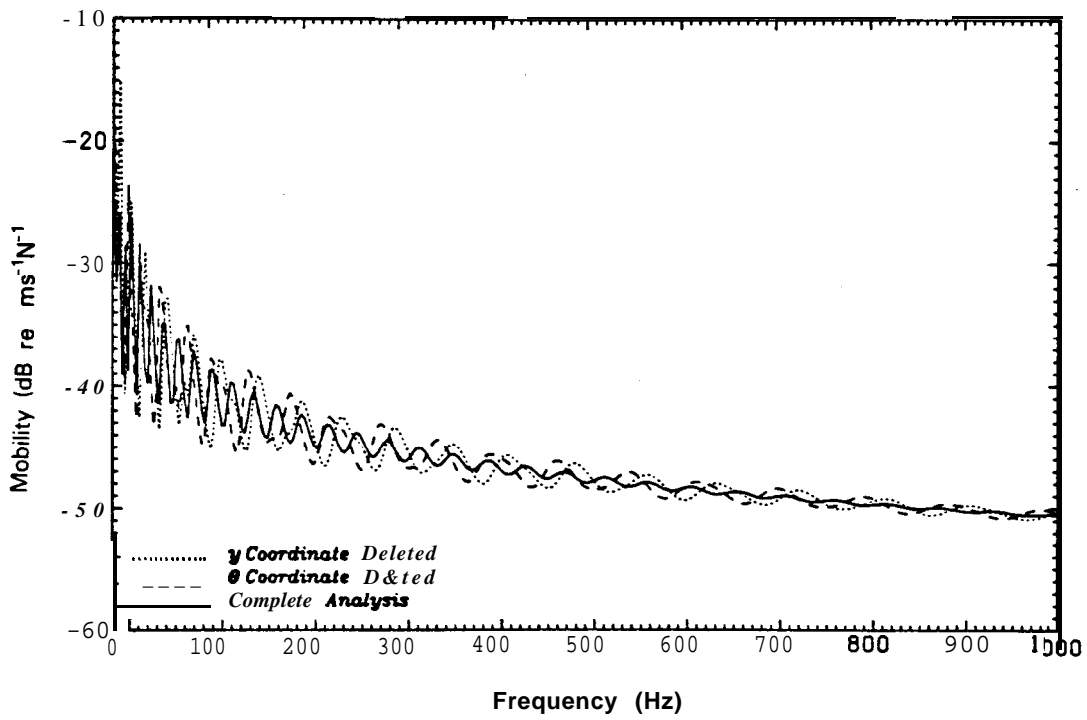


Fig.4.6(b) Example I- Driving-point response

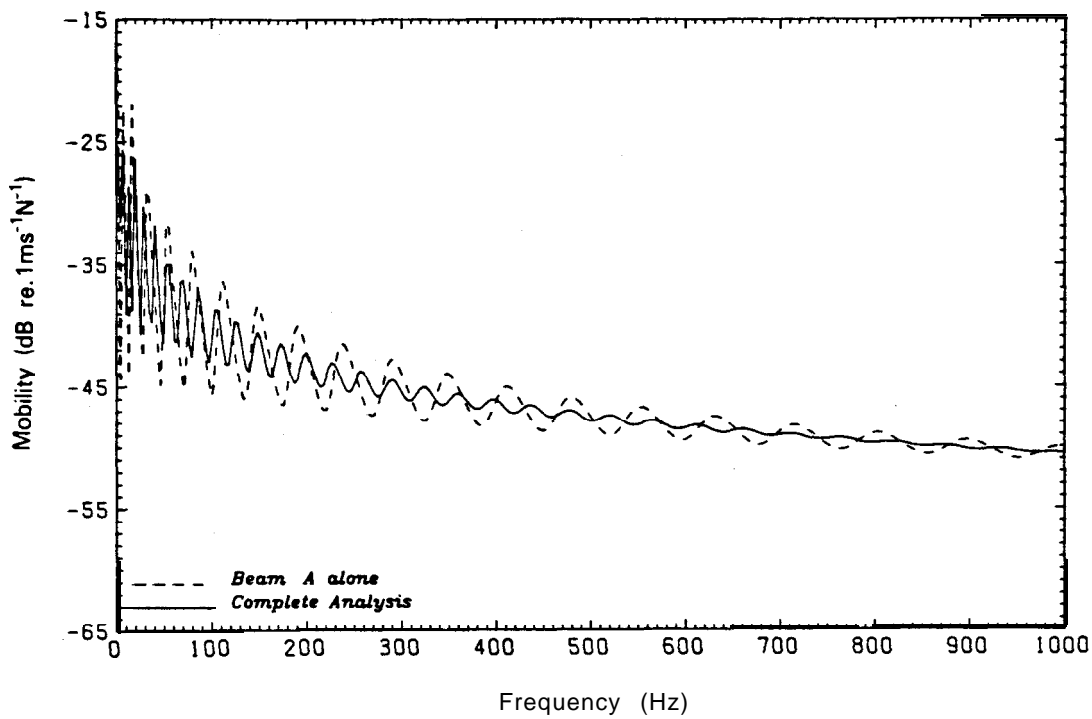


Fig.4.6(c) Example I - Driving-point response of coupled structure compared with Beam A alone

4.42 Example II

The subsystems of the test structure are identical to those of Example I, except that this time they are connected together at an angle of 10° , as shown in Fig.4.7. As in Example I, excitation is applied at the free end of Beam A, and responses are obtained at both the driving-point and the free end of Beam B. Here, a complete analysis requires the inclusion of all three coordinates at the joint. A plot of the energy transfer in each of the three coordinate directions is shown in Fig.4.8(a) for the frequency range 0 - 1000Hz. The transfer and driving-point responses are also shown in Figs.4.8(b) and 4.8(c).

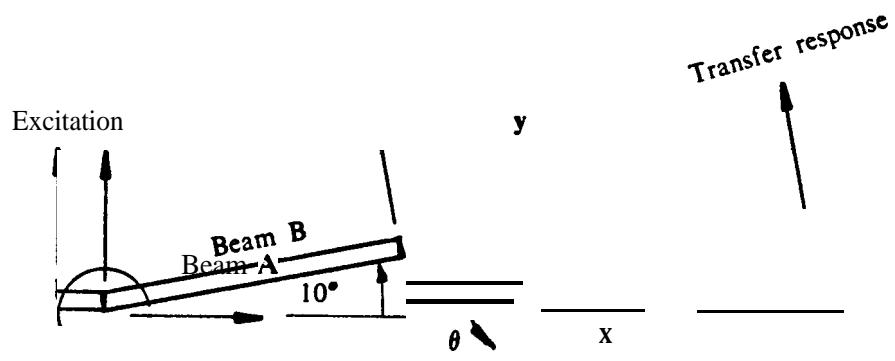


Fig.4.7 Test structure for Example II

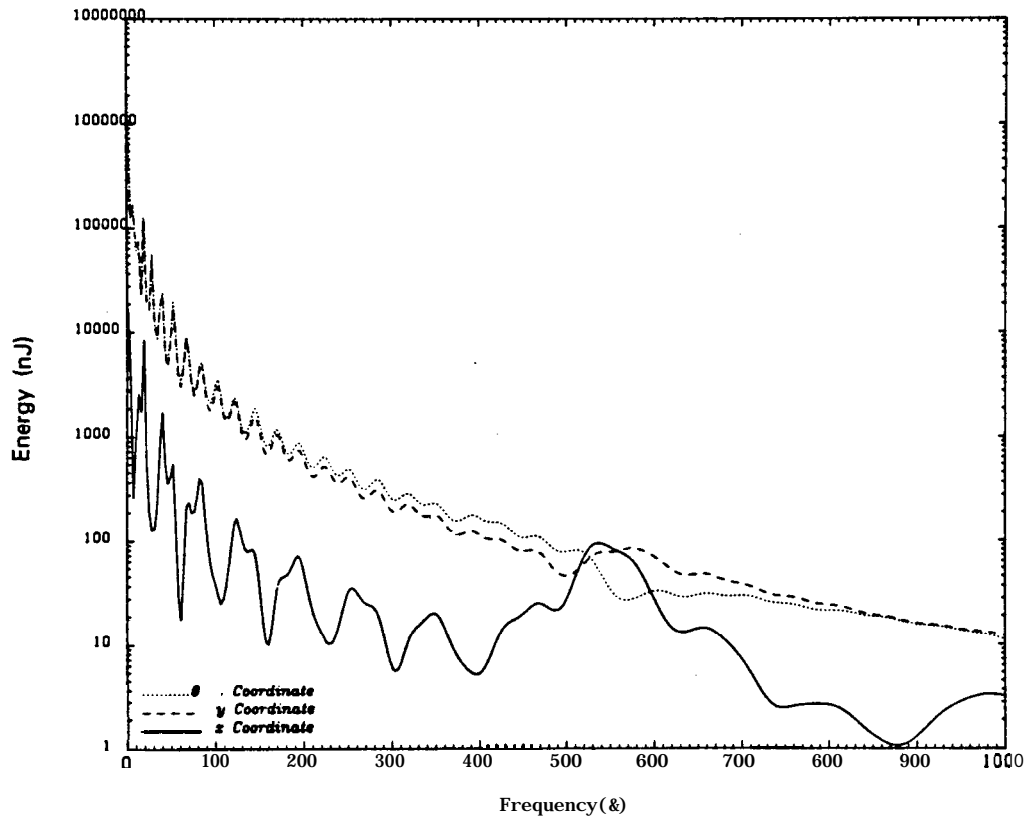


Fig.4.8(a) Example II - Energy transfer in coordinate directions

Examination of Fig.4.8(a) shows that, except for the frequency range 450 -650Hz approx., the energy transfer in the x coordinate direction is much smaller than that in the y and θ coordinate directions. Also, the energy transfer in the y and θ coordinate directions are of about the same magnitude. On the basis of the energy transfer we would expect that the elimination of the x coordinate will not severely affect the accuracy of the responses except in the 450 -650Hz range. Fig.4.8(b) shows that outside this particular frequency range the x coordinate may indeed be excluded from the analysis without any serious loss of accuracy in the transfer response calculation. Fig.4.8(c) also shows that the driving-point responses follow a similar trend to those in Example 1. The exclusion of coordinates has a smaller effect on the driving-point response as the frequency increases. The explanation given for Example 1 applies here.

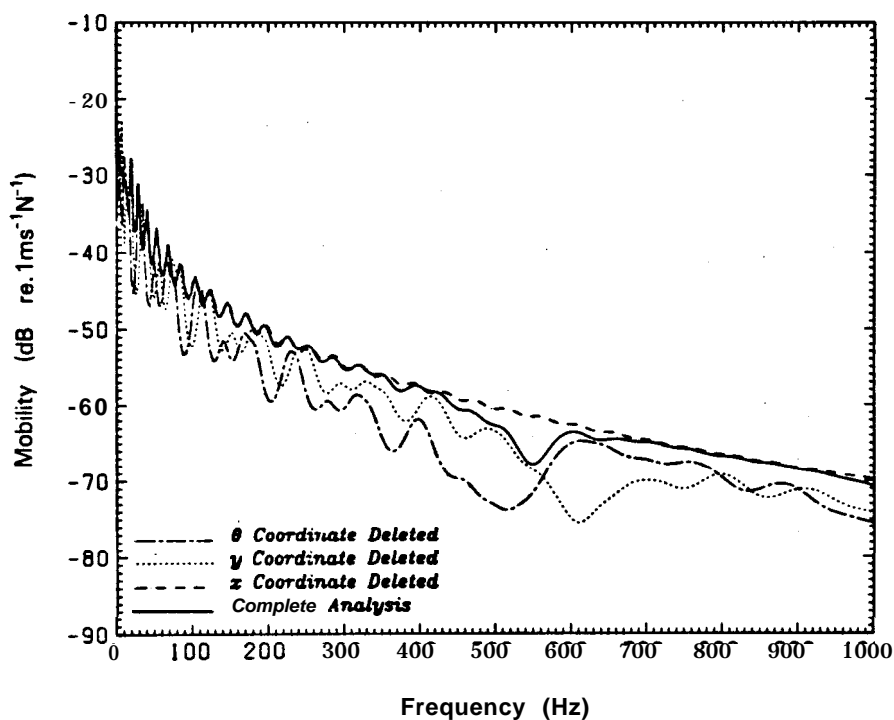


Fig.4.8(b) Example II - Transfer response

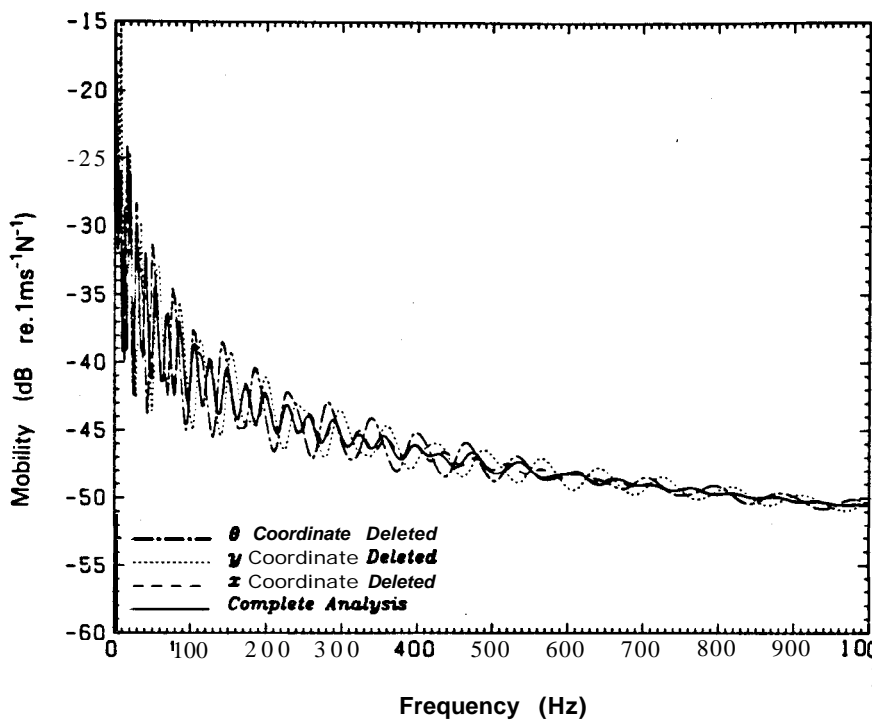


Fig.4.8(c) Example II - Driving-point response

4.4.3 Example III

The test structure here is shown in Fig.4.9. It is composed of two plane frames which have been joined together at one point and at right-angles to form a three-dimensional structure. An exciting force of unit amplitude is applied in the plane of Substructure A as shown in Fig.4.9.

The energy flow via each of the six coordinates at the joint is shown in Fig.4.10 for the frequency range 0 - 100Hz. Examination of this Figure shows that the relative magnitudes of energy transfer in the six coordinate directions are heavily frequency-dependent. This frequency dependence makes an assessment of the relative importance of the coordinates rather more difficult than the case of Examples I and II. However, a study of the energy transfer plot in conjunction with the response plots,

Fig.4.1 1(a),(b),(c),(d), shows that within any frequency range the effect of leaving out any coordinate from the analysis is directly related to the relative magnitude of the energy transfer in that coordinate direction.

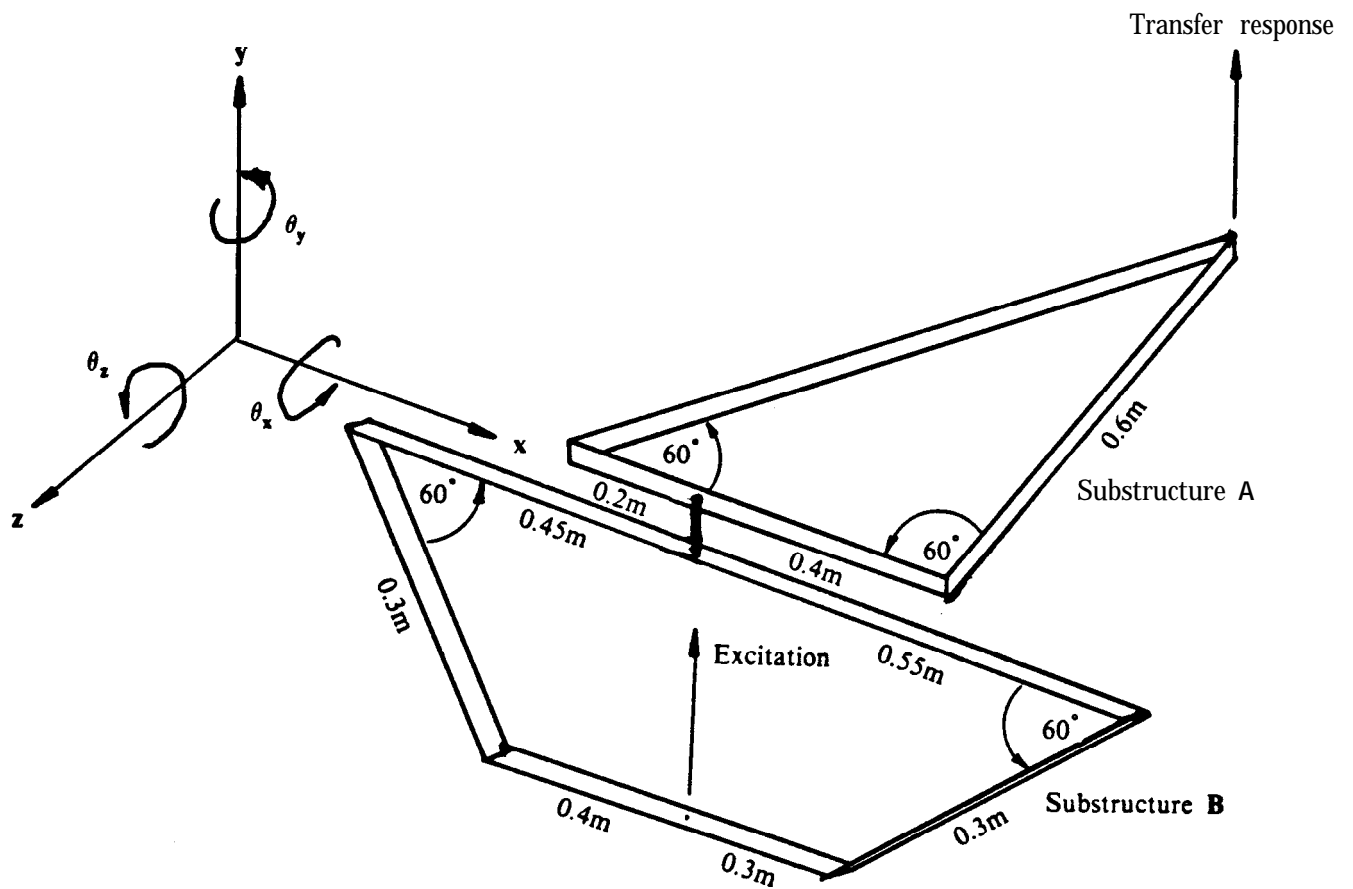


Fig.4.9 Test structure for Example III

Data

Cross-sectional Area = $2.0 \times 10^{-4} \text{ m}^2$
 Second moment of area, $I_x = 1.6667 \times 10^{-9} \text{ m}^4$
 „ „ $I_y = 6.6667 \times 10^{-9} \text{ m}^4$
 Density of beam material = 7850 kg m^{-3}
 Modulus of Elasticity, $E = 20.7 \times 10^{10} \text{ Nm}^{-2}$
 Shear Modulus, $G = 7.96 \times 10^{10} \text{ Nm}^{-2}$
 Damping loss factor, $\eta = 0.01$
 Timoshenko shear coefficient = 0.8497
 Torsional constant = 4.5776×10^{-9}

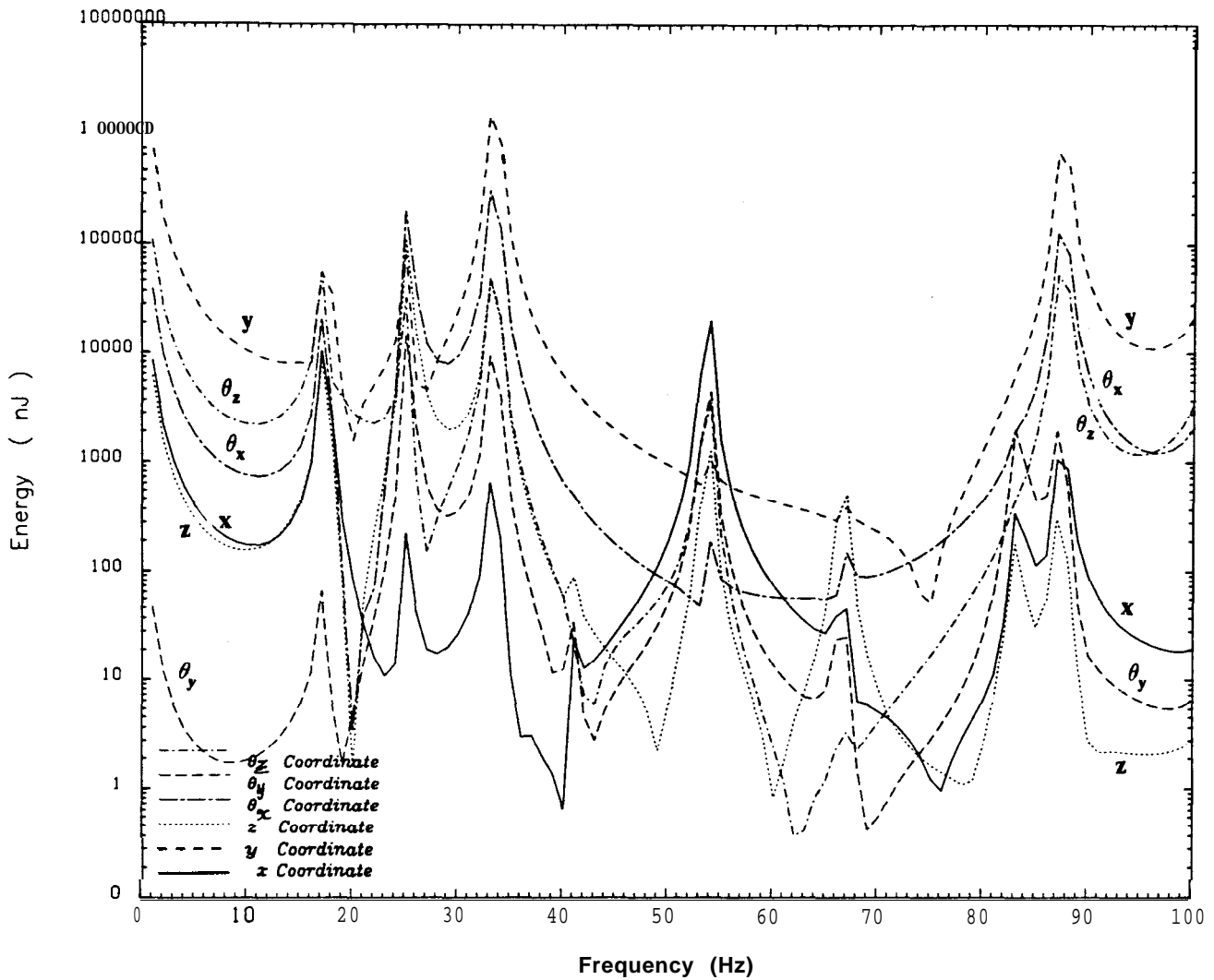


Fig.4.10 Example III - Energy flow in various coordinate directions

The energy transfer in the y coordinate is by far the largest. Thus, when the y coordinate is excluded there is a very severe degradation of the computed responses, Figs.4.11 (b) and 4.11(d). We must note however that although y is by far the most important coordinate, Figs.4.12(a) and 4.12(b) show that a single-coordinate coupling analysis is inadequate for most of the frequency range. In the vicinity of the last resonance (88Hz approx.) very much less energy is transferred in the x, z and θ_y coordinate

directions than in the other three. Thus, when any of these coordinates is excluded the responses are still close to those for the complete analysis in that frequency range. Indeed, Figs.4.12(a) and 4.12(b) show that an analysis based on the y, θ_x and θ_z coordinates alone is sufficient in this frequency range. The energy transfer in the x coordinate direction increases very sharply around the fourth resonance (54Hz approx.). Consequently, as may be seen from Figs.4.11(a) and 4.11(c) a marked degradation of the responses occurs around this mode. For the second resonance (25Hz approx.) the energy transfer is high for all coordinates except x; and, as may be seen from Figs.4.11 (a),(b),(c),(d), the exclusion of any coordinate except x results in some loss of accuracy of the responses.

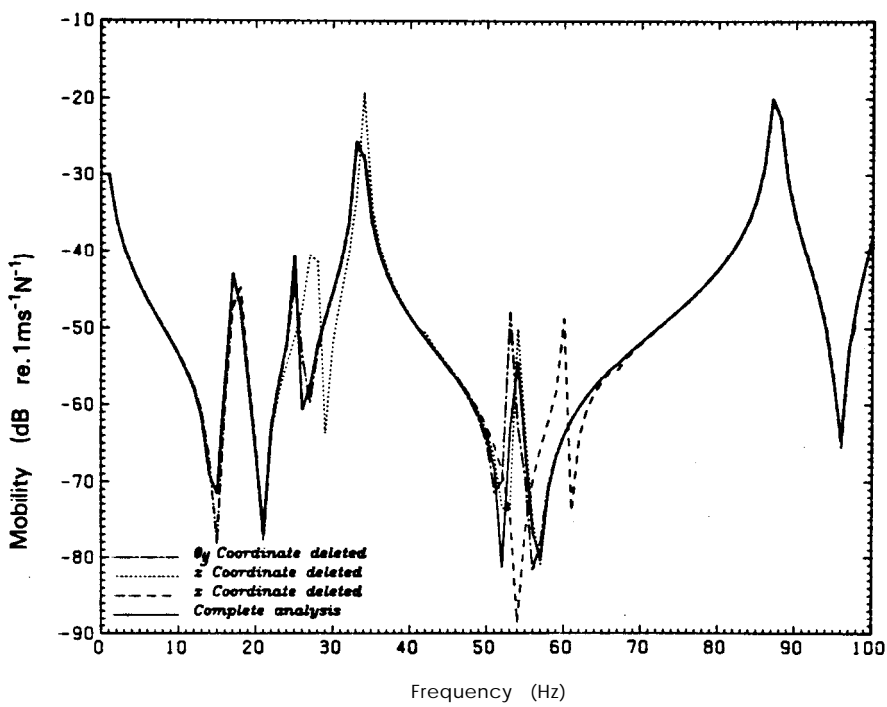


Fig.4.11(a) Example III - Driving-point response with various coordinates deleted

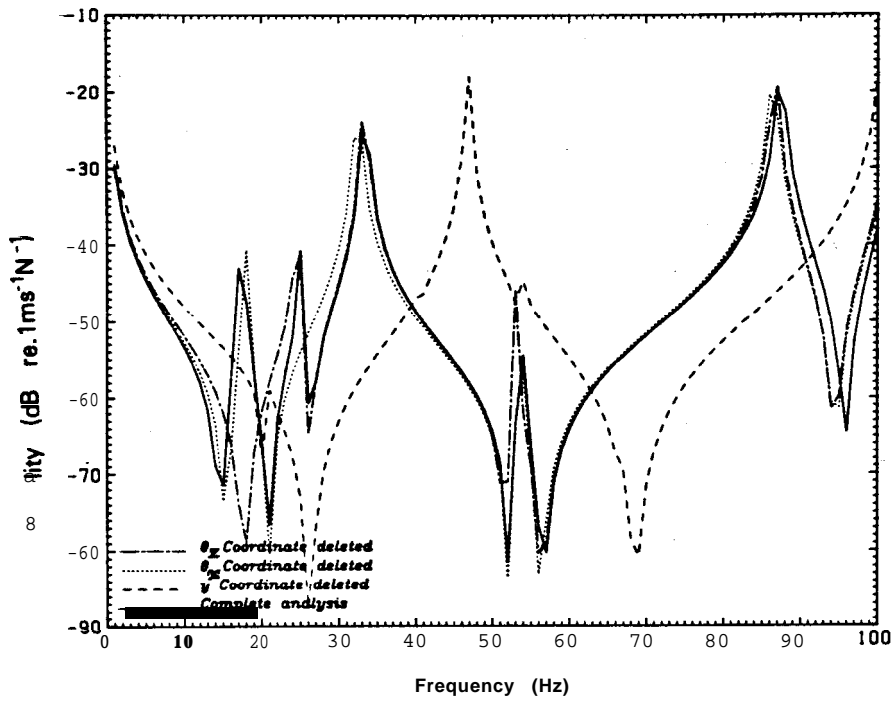


Fig.4.1 l(b) Example III - Driving-point responses with various coordinates deleted

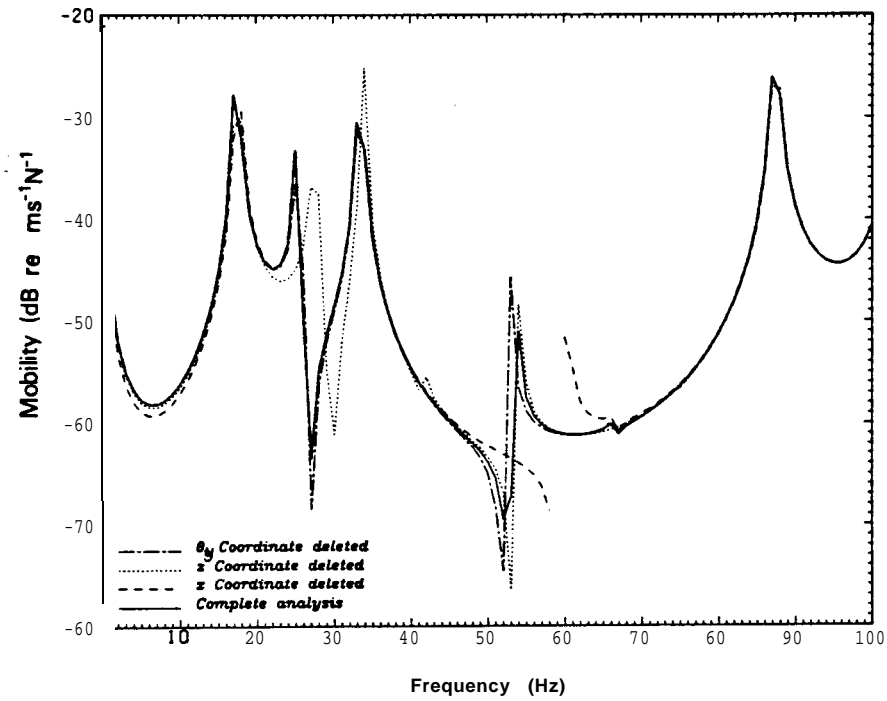


Fig.4.1 l(c) Example III - Transfer responses with various coordinates deleted

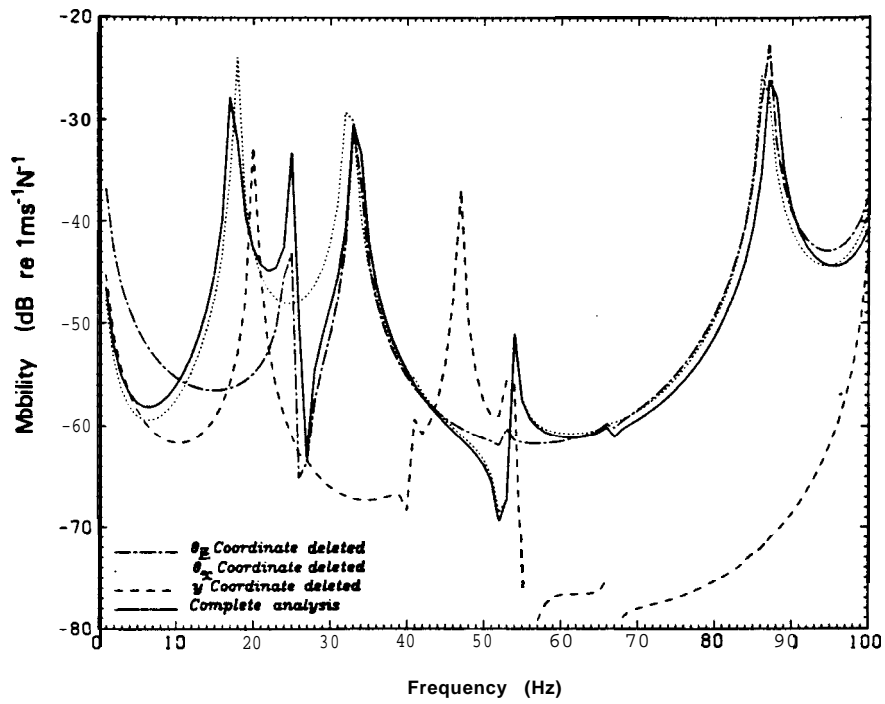


Fig.4.1 l(d) Example III - Transfer responses with various coordinates deleted

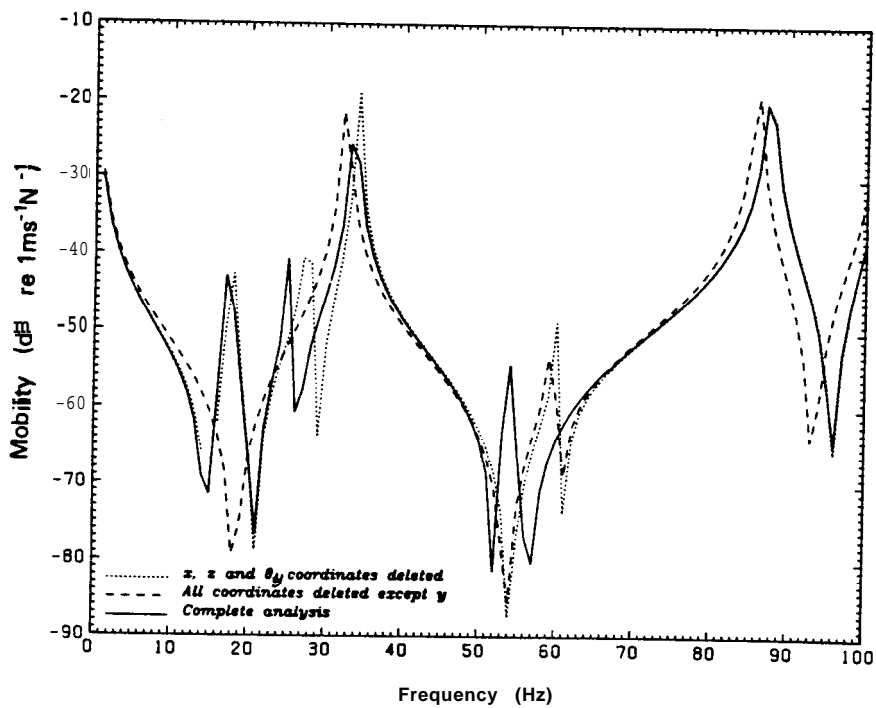


Fig.4.12(a) Example III - Driving-point responses with various combinations of coordinates deleted

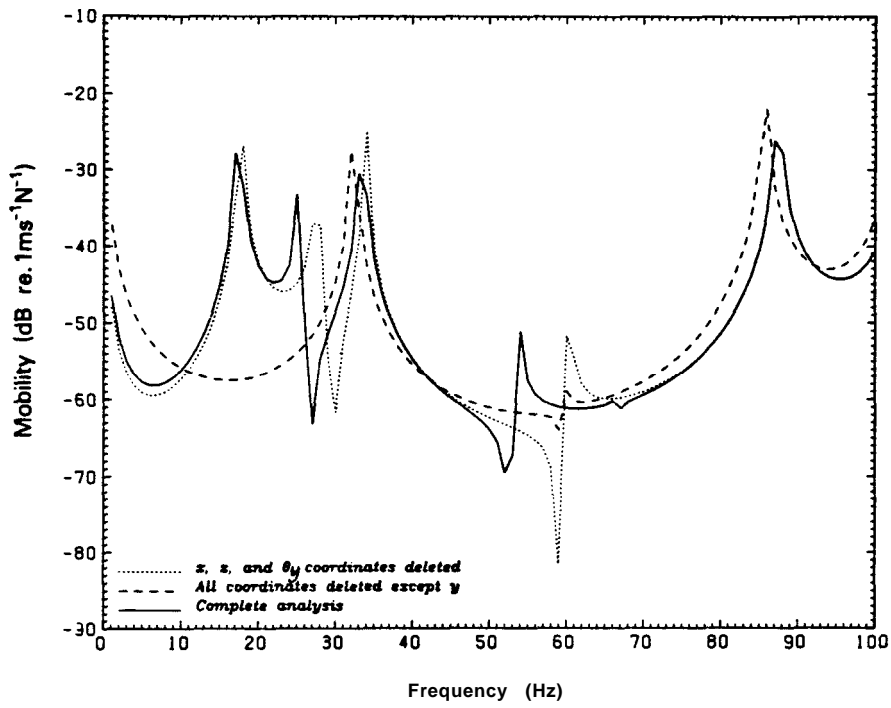


Fig.4.12(b) Example III - Transfer responses with various combinations of coordinates deleted

4.4.4 Example IV

The test structure for this example is a plane frame consisting of two substructures which are connected together at two points, Fig.4.13. The exciting force is in the plane of the structure, and therefore a complete analysis requires the inclusion of three coordinates at each joint.

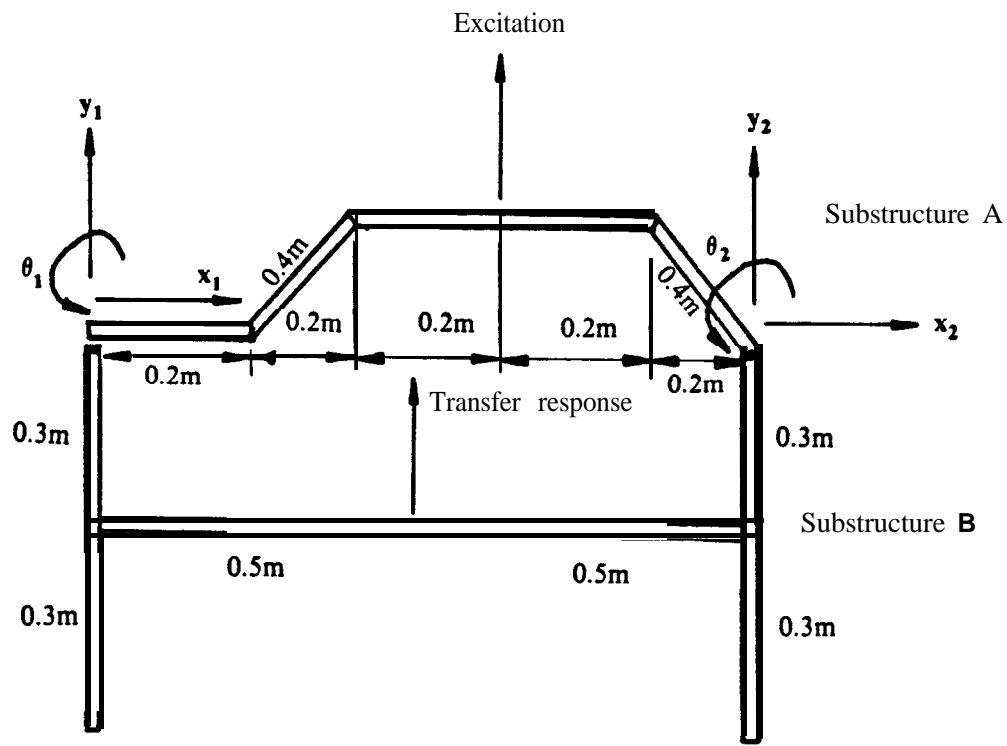


Fig.4.13 Test structure for Example IV

Data

Cross-sectional Area = $2.0 \times 10^{-4} \text{ m}^2$
 Second moment of area, $I_{xx} = 1.6667 \times 10^{-8} \text{ m}^4$
 Density of beam material = 7650 kg m^{-3}
 Modulus of Elasticity, $E = 20.7 \times 10^{10} \text{ Nm}^{-2}$
 Shear Modulus, $G = 7.96 \times 10^{10} \text{ Nm}^{-2}$
 Damping loss factor, $\eta = 0.01$
 Timoshenko shear coefficient = 0.6497

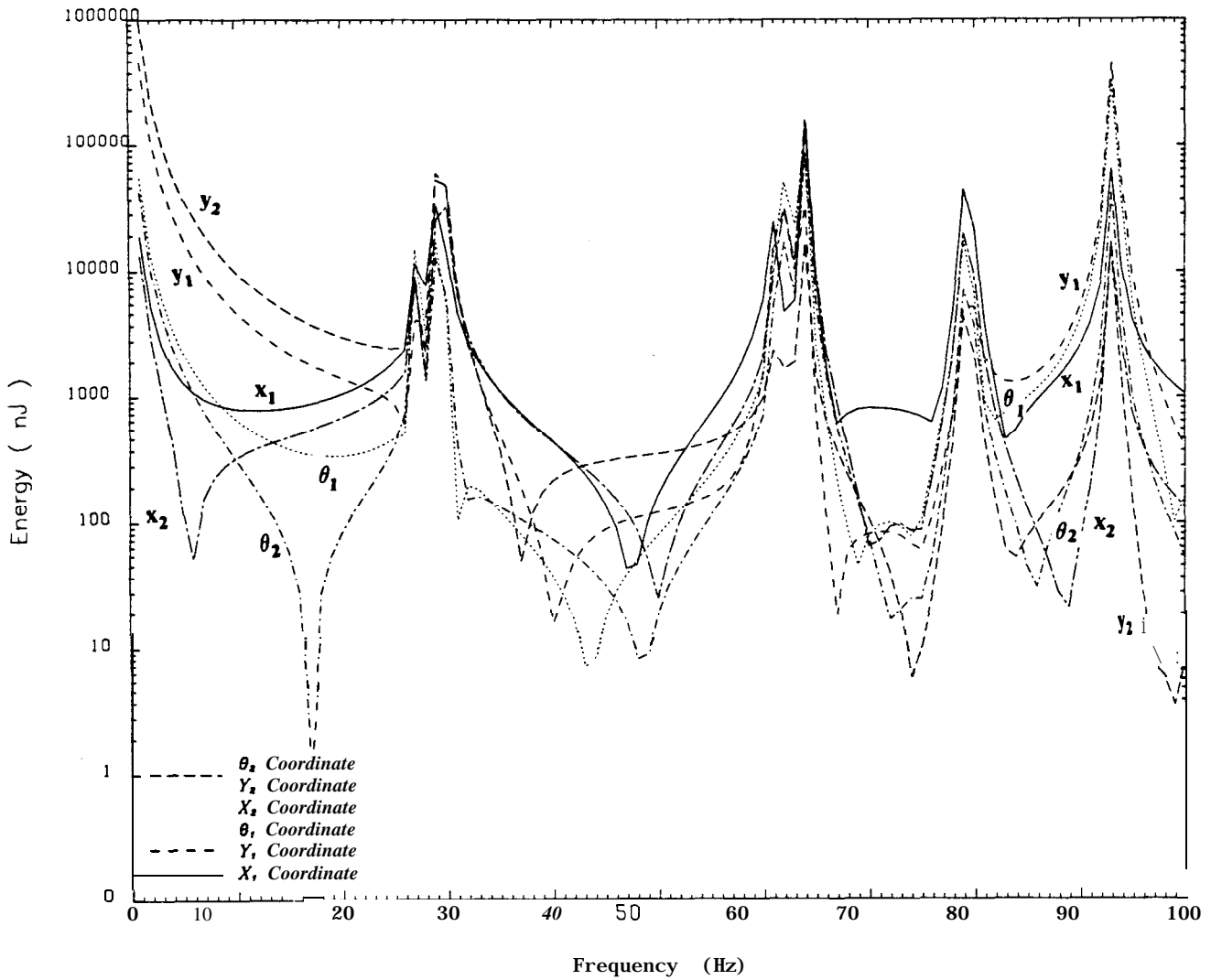


Fig.4.14 Example IV - Energy flow in various coordinate directions

The energy transfer in each of the coordinate directions is shown in Fig.4.14. As with Example III, it is seen that the relative magnitudes of energy transfer in the coordinate directions vary with frequency. However, in this example the energy transfer is more evenly distributed among the coordinates. The inference that may be made after examining the energy plot, is that no single coordinate (or group of coordinates) is so unimportant

that it may be left out of the analysis. A study of the response plots, Figs.4.15(a),(b),(c),(d), shows that this inference is correct. It is seen that the elimination of any one of the six coordinates results in some degradation of the coupled responses. The extent to which the responses differ from those of the complete analysis may be predicted from the energy transfer plot. For example, around the fifth resonance (93Hz approx.) the energy transfer in each of the x_1 , y_1 and θ_1 coordinate directions is greater than those in the other three directions. Consequently, when any of these coordinates is deleted the fifth mode is missed altogether. See Figs.4.15(a) and 4.15(b).

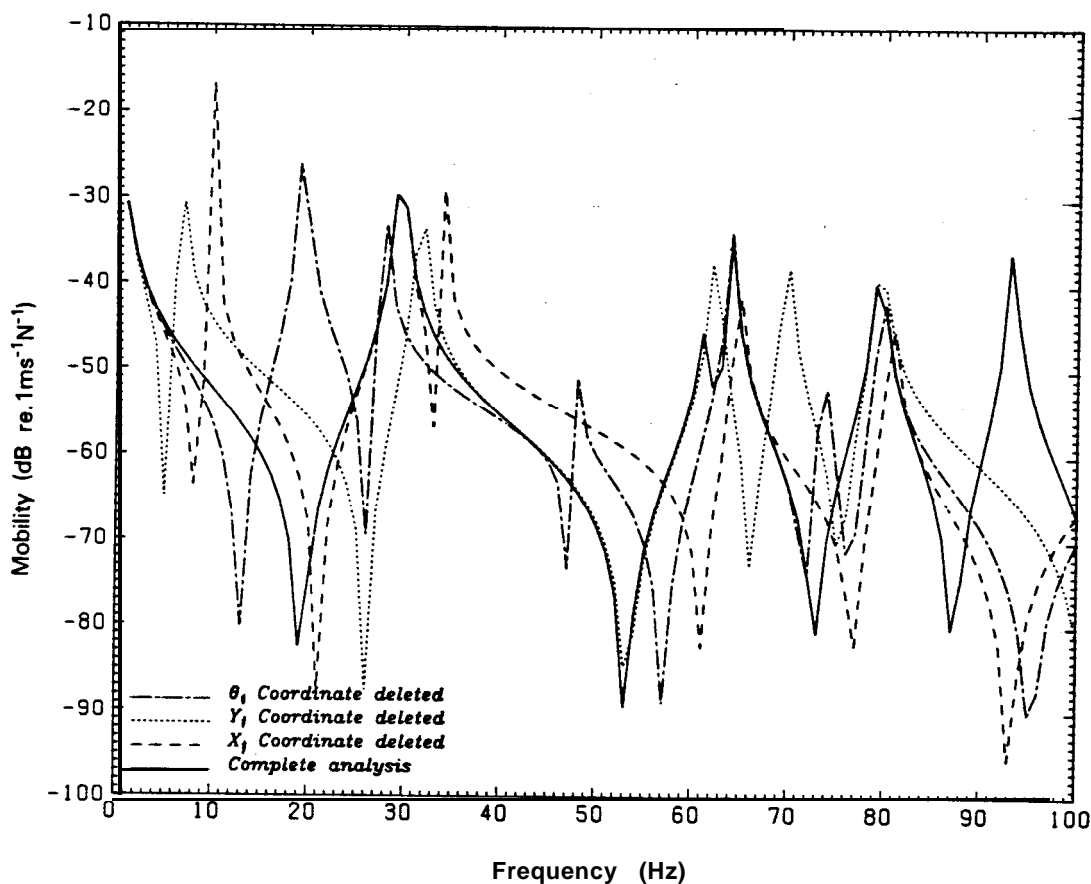


Fig.4.15(a) Example IV ~ Driving-point responses with various coordinates deleted

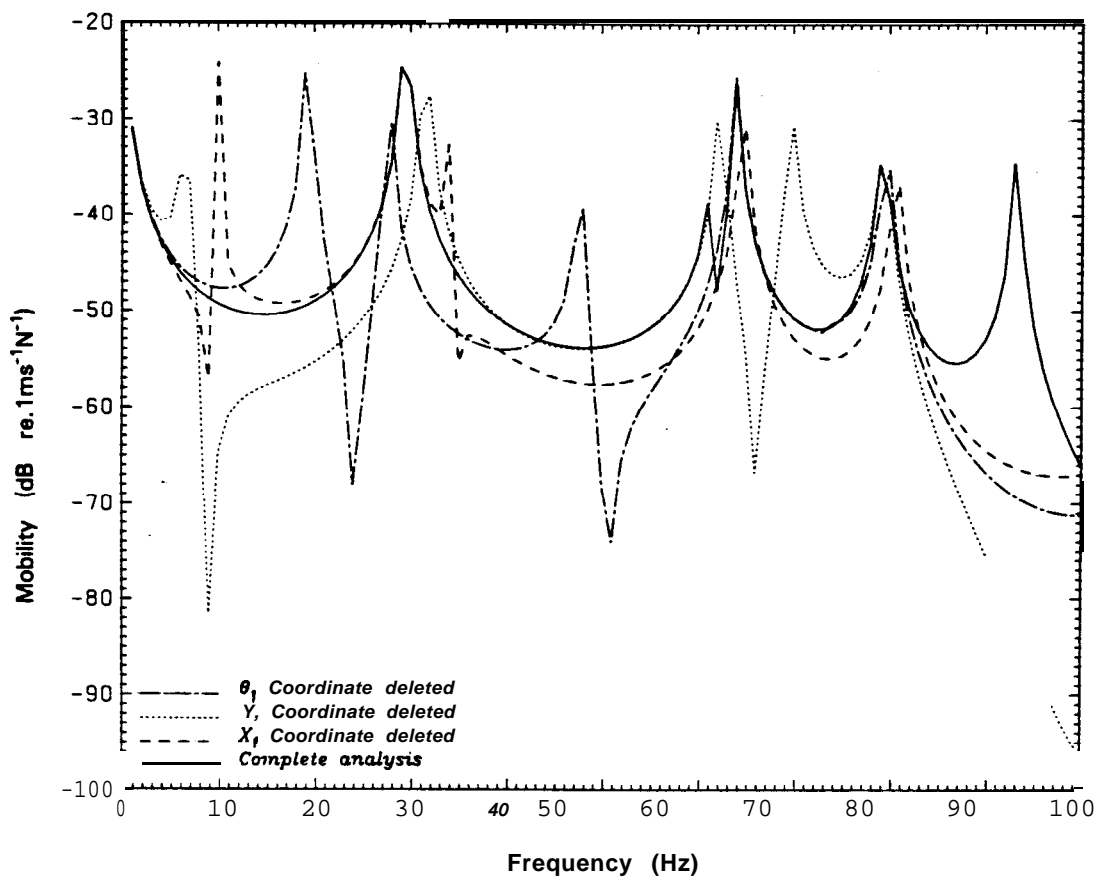


Fig.4.15(b) Example IV - Transfer responses with various coordinates deleted

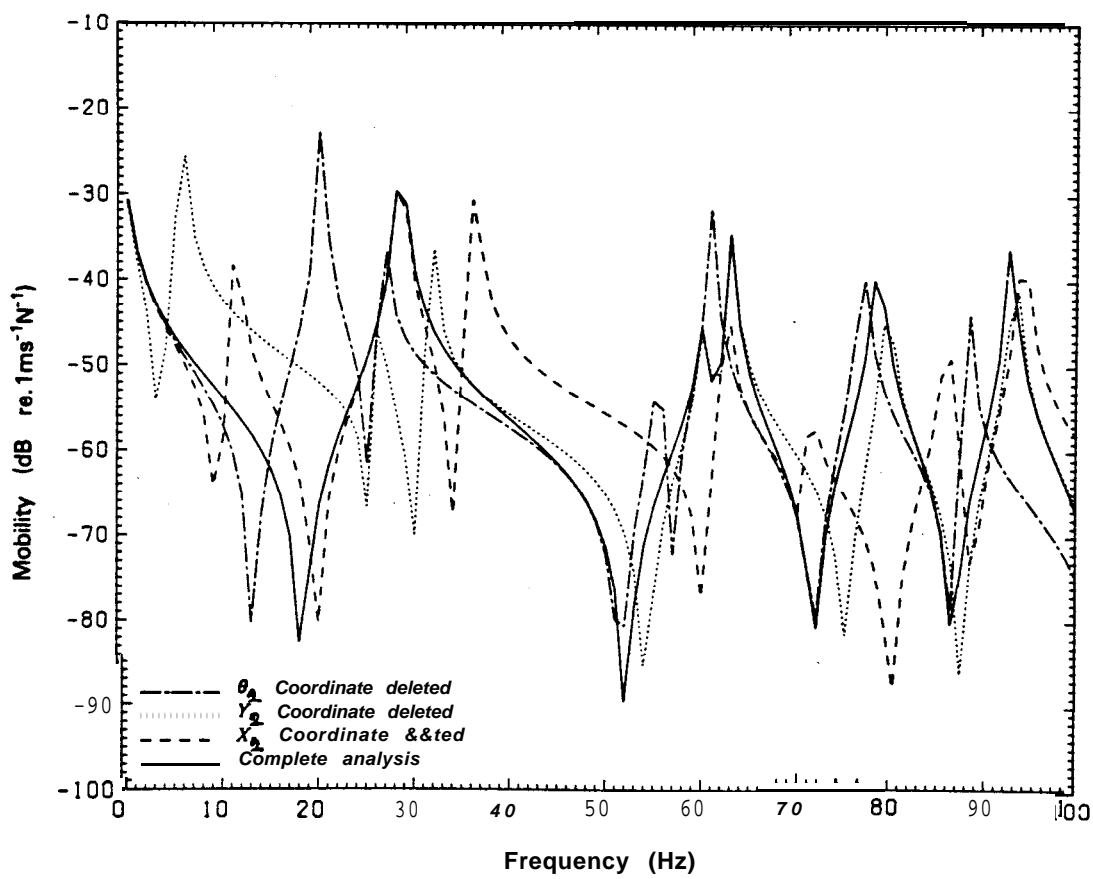


Fig.4.15(c) Example IV - Driving-point responses with various coordinates deleted

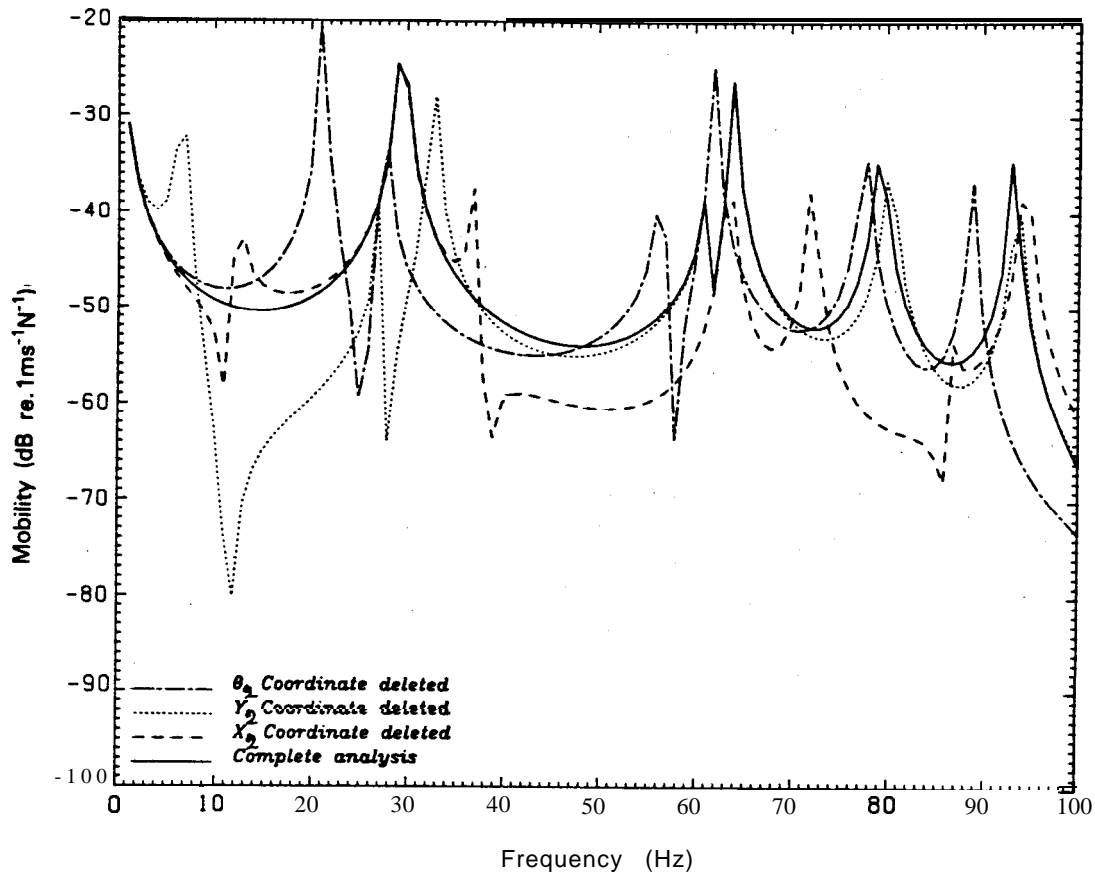


Fig.4.15(d) Example IV - Transfer responses with various coordinates deleted

4.5 Discussion

The four structures analysed in §4.4 were chosen to represent a spectrum of cases from which the underlying assumption of the proposed method can be verified. Examples I and II are relatively simple cases in which the assessment of the relative importance of coordinates is clear-cut. One important fact brought out by both examples is that, for very highly-damped structures vibrating at high frequency, the exclusion of coordinates at the joints will sometimes have very little effect on driving-point response calculations. The three-dimensional structure in Example III and the two-dimensional structure in Example IV represent situations where the relative importance of the coordinates is not very **obvious**. Even in these cases there

is still a direct correlation between the energy transfer in any coordinate direction, and the effect on the responses of excluding the coordinate from the analysis. Clearly, the examples presented here lend strong support to the basic assumption of the proposed method. It must be mentioned, though, that sometimes the only conclusion to be drawn from an application of the method is that none of the coordinates at the joints is so unimportant that it may be omitted from the analysis.

The practical application of the method may present some difficulties. In order to calculate the energy transfer in the various coordinate directions one is required to know the frequency response properties of the subsystems, as well as the responses (or internal transmitted forces) when the subsystems are assembled. This amounts to being required to know the results of the complete analysis before the analysis is carried out. One possible way round this difficulty is to carry out a preliminary analysis over selected parts of the frequency range. On the basis of the results any unimportant coordinates may be excluded, and the analysis repeated for the whole of the frequency range. However, this could lead to erroneous conclusions in situations where the relative importance of coordinates varies with frequency, as in some of the examples presented here.

There are a number of instances where the application of the method is not restricted by the difficulty discussed above. These include the situation where a particular Impedance Coupling calculation has produced inadequate results, and one wants to find a reason for this. The method may also be found useful in a theoretical study prior to the coupling analysis of a real structure. In this case one would apply the method to a similar theoretical structure, made up of simple components like beams, springs, masses, etc.

The results from this preliminary analysis would then form the basis for deciding which coordinates to include in the analysis of the real structure.

One area in which the proposed method could be employed is the interpretation of frequency response data in order to decide what vibration control measures are necessary. Quite often one is required to compare rotational and translational mobility data. Such a comparison is difficult because rotational and translational mobilities have quite different units. The results presented in this chapter suggest that this comparison could be done on the basis of energy transfer. Another possible application of the method proposed in this chapter is vibration path identification. By processing the frequency response data to obtain the energy transfer in each of the coordinate directions along various transmission paths one should be able to assess the relative importance of the vibration transmission paths in the structure. The potential applications of the proposed method warrant further study.

Chapter 5

AN EVALUATION OF THE POWER FLOW APPROACH TO VIBRATION ISOLATION PROBLEMS

5.1 Introduction

The object of vibration isolation is to reduce vibration levels, and the criterion for defining the effectiveness of a vibration isolation exercise depends on the particular type of problem. Traditionally, two types of isolation problems are considered:

(i) The requirement to reduce the transfer of vibration from a machine to the foundation or supporting structure on which it is mounted. In this case the effectiveness of the isolation exercise is defined in terms of the reduction in the magnitude of the dynamic forces transmitted from the machine to the foundation.

(ii) The requirement to isolate a piece of sensitive equipment from the vibration of its supporting structure. The main objective of isolation in this type of problem is to reduce the amplitude of the motion transmitted to the sensitive equipment.

In recent publications [13,14,15], a vibration isolation method has been proposed which aims at minimising the time-average power flow to the structure which is being isolated. The main attraction of the method appears to be the fact that it combines both force and motion in a single concept. However, the proposal to measure the effectiveness of vibration isolation in terms of the time-average power flow is based on the assumption that a reduction in **power** flow will always be accompanied by a reduction in the **magnitude** of transmitted force or motion, and thus an improvement in

isolation. There is a need to test this assumption, and in this chapter an evaluation of the proposed method is presented.

The discussion is centred around a single-stage vibration isolation system as represented in Fig.5.1. The system consists of a rigid machine of mass M_m mounted on a flexible foundation of mobility Y_f , via a **massless** spring of stiffness K . An external sinusoidal force of constant amplitude and frequency acts on the machine. Two simple approximations for the foundation characteristics are considered, namely, a simple one-degree-of-freedom system and a semi-infinite beam. The influence of some of the system parameters on the time-average power, transmitted force and motion response is investigated.

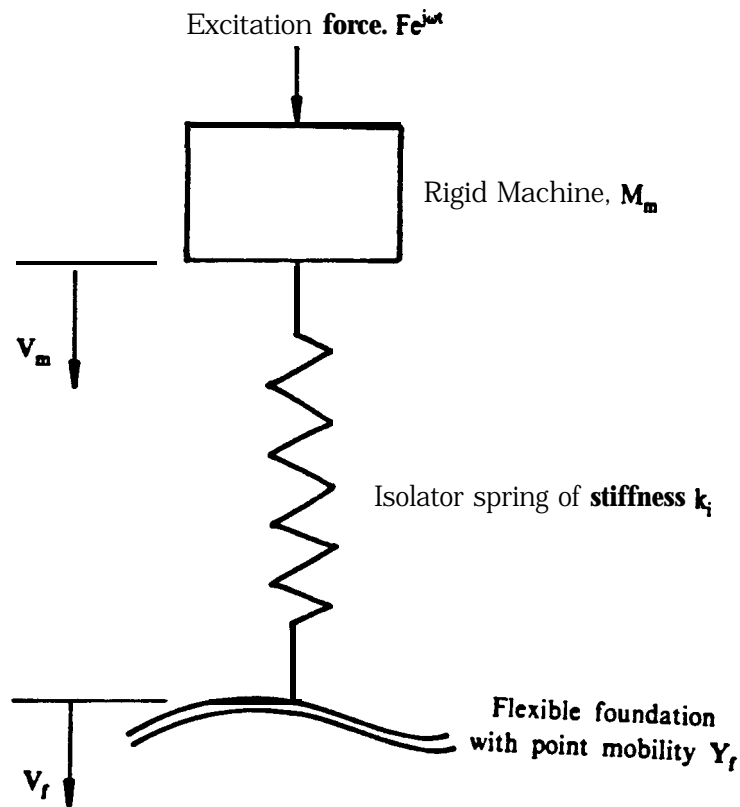


Fig.5.1 Single-stage vibration isolation system

5.2 Expressions for **time**-average power flow, velocity amplitudes and force transmitted to the foundation

The time-average power flow to the foundation of the isolation system shown in Fig.5.1 is [15]

$$P_{av} = \frac{1}{2}|F|^2 \frac{\text{Re}\{Y_f\}}{|1 - (\frac{\omega}{\omega_0})^2 + j\omega M_m Y_f|^2} \quad (5.1)$$

where $\omega_0^2 = K_i/M_m$

The amplitude of the foundation's velocity response is

$$|V_f| = \frac{|Y_f||F|}{|1 - (\frac{\omega}{\omega_0})^2 + j\omega M_m Y_f|} \quad (5.2)$$

and that of the machine is

$$|V_m| = \frac{|(Y_f + j\frac{\omega}{k_i})||F|}{|1 - (\frac{\omega}{\omega_0})^2 + j\omega M_m Y_f|} \quad (5.3)$$

The magnitude of the force transmitted to the foundation is

$$|F_T| = \frac{|F|}{|1 - (\frac{\omega}{\omega_0})^2 + j\omega M_m Y_f|} \quad (5.4)$$

5.3 Influence of changes in the machine-isolator subsystem

By inspection of equations (5.1), (5.2) and (5.4), it is seen that provided the foundation mobility is not altered, any change in the machine-isolator subsystem which results in a reduction of the power flow to the foundation will be accompanied by a reduction in velocity amplitude and transmitted force.

The foregoing conclusion may also be arrived at by the following argument. For the purposes of dynamic analysis we may separate the machine-isolator subsystem from the foundation, and impose force balance and motion compatibility at the connection point so as to ensure dynamic equivalence to the coupled system, Fig.5.2 . The time-average power flow to the foundation is then given by the following alternative expressions:

$$P_{av} = \frac{1}{2} |F_T|^2 \text{Re}\{Y_f\} \quad (5.5)$$

and

$$P_{av} = \frac{1}{2} |V_f| \frac{\text{Re}\{Y_f\}}{|Y_f|^2} \quad (5.6)$$

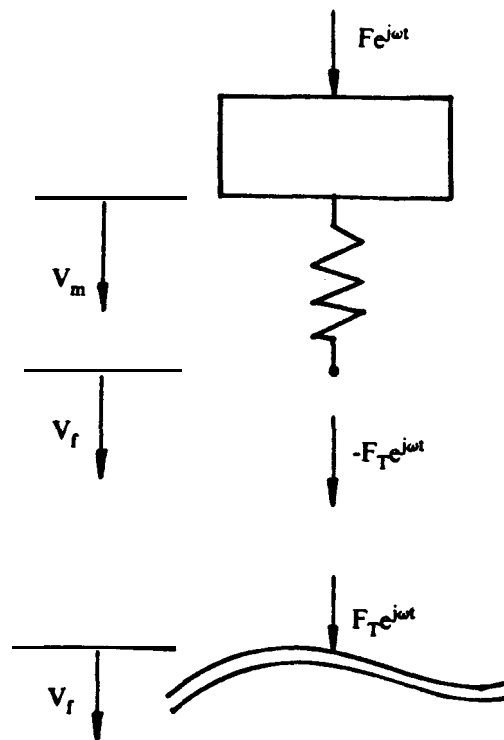


Fig.5.2 Vibration isolation system separated into components parts

It is immediately obvious from equations (5.5) that if the characteristics of the foundation are kept constant, then the power flow is directly proportional to the square of the transmitted force amplitude. In view of equation (5.6) a similar remark applies to the foundation velocity amplitude.

5.4 Influence of changes in the characteristics of the foundation

In order to investigate the influence of changes in the characteristics of the foundation it is necessary to assume a form for the foundation mobility. Two assumed forms for the foundation characteristics will be considered in turn, namely, a one-degree-of-freedom spring-mass-damper system and a semi-infinite beam.

5.4.1 One-degree-of-freedom approximation for foundation behaviour

We shall assume that the foundation behaves like a spring-mounted mass with hysteretic damping, i.e

$$Y_f = \frac{j\omega}{K_f - \omega^2 M_f + jK_f \eta_f} \quad (5.7)$$

where M_f , K_f and η_f are the mass, stiffness and damping loss factor respectively.

Our attention will be restricted to an investigation of the influence of the damping loss factor of the foundation. The influence of the foundation characteristics depends quite heavily on the frequency of excitation, and we shall now consider two cases.

5.4.1.1 Case where the excitation frequency coincides with the natural frequency of the machine-isolator subsystem.

If $\omega = \omega_0$, equations (5.1), (5.2) and (5.4) become

$$P_{av} = \frac{1}{2}|F|^2 \frac{Re\{Y_f\}}{\omega^2 M_m^2 |Y_f|^2} \quad (5.3)$$

$$|V_f| = \frac{|F|}{\omega M_m} \quad (5.9)$$

and
$$|F_T| = \frac{|F|}{\omega M_m |Y_f|} \quad (5.10)$$

Equation (5.9) shows that at this frequency the magnitude of the foundation velocity is independent of the foundation mobility. Therefore $|V_f|$ remains constant as the damping loss factor of the foundation subsystem is varied, Fig.5.3(a).

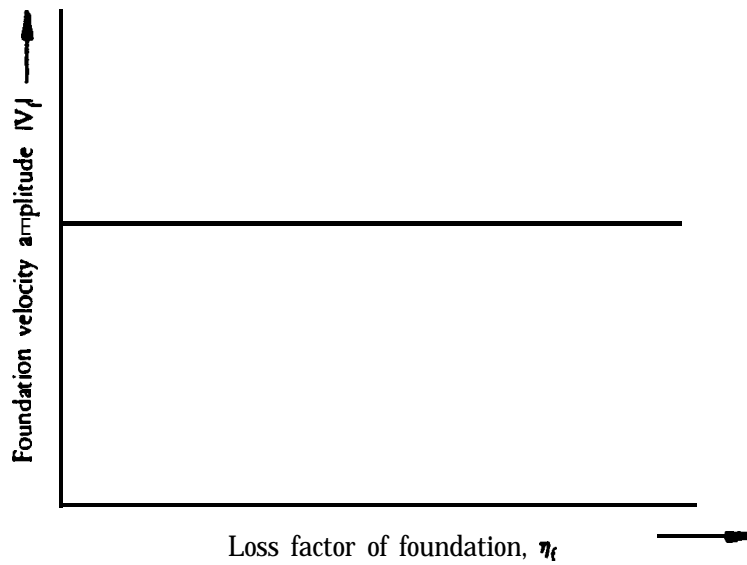


Fig.5.3(a) Variation of foundation velocity with damping

The modulus of mobility, $|Y_f|$, decreases as the loss factor of the foundation is increased and, consequently, in view of equation (5.10), the magnitude of the transmitted force increases as shown in **Fig.5.3(b)**.

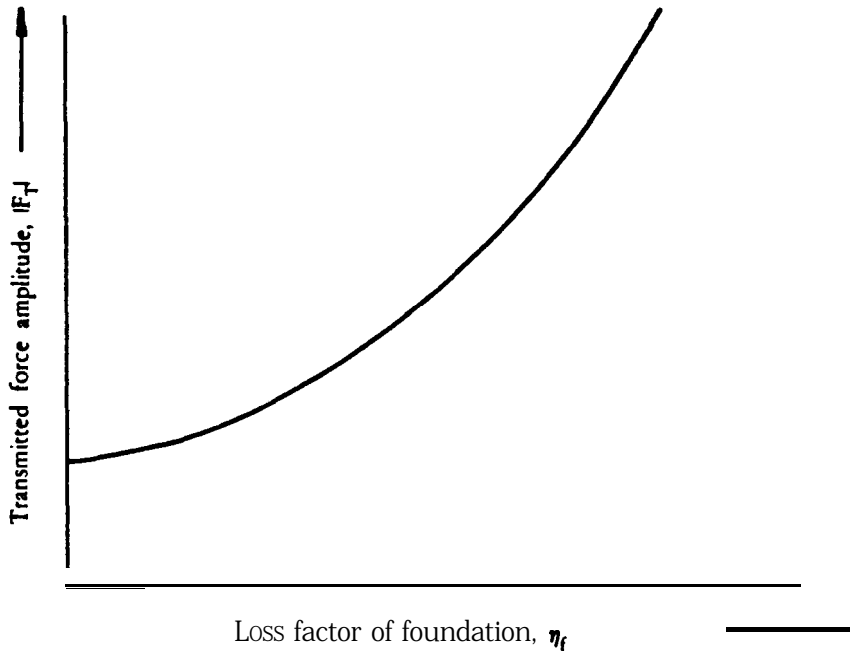


Fig.5.3(b) Variation of transmitted force with foundation damping

The time-average power flow to the foundation is proportional to the ratio $\text{Re}\{Y_f\}/|Y_f|^2$ as may be seen from equation (5.8).

Now,
$$\frac{\text{Re}\{Y_f\}}{|Y_f|^2} = \frac{K_f \eta_f}{\omega} \quad (5.11)$$

and therefore the time-average power varies linearly with the damping loss factor as shown in **Fig.5.3(c)**.

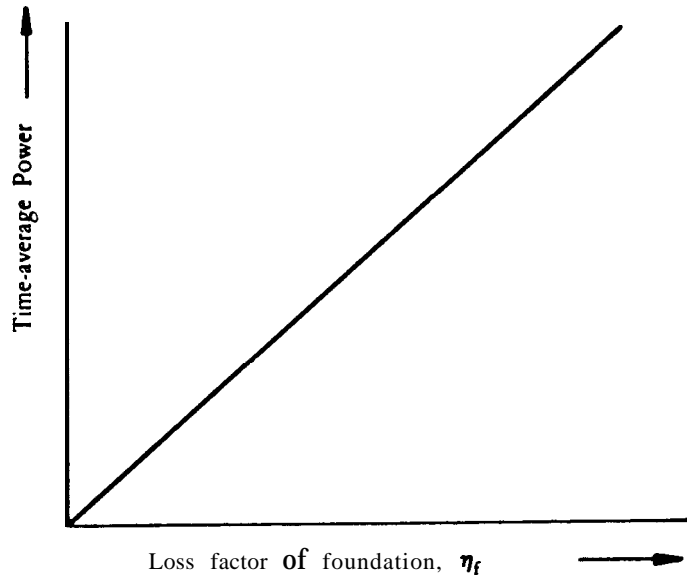


Fig.5.3(c) Variation of time-average power with foundation damping

Figs.5.3(b) and (c) show that a reduction of the power flow due to a change in the level of damping will be accompanied by a reduction of the force transmitted to the foundation. However, the foundation velocity amplitude will remain unchanged, according to Fig.5.3(a). Therefore at this excitation frequency, $\omega = \omega_0$, the amplitude of the foundation velocity cannot be attenuated by reducing the time-average power if this reduction is brought about by altering the foundation damping.

5.4.1.2 Case where excitation frequency is much greater than the natural frequency of the machine-isolator subsystem.

Consider the situation where $(\omega/\omega_0)^2 \gg 1$, and $\omega^2 < K_f/M_f$. The loci of the complex quantities of interest in equations (5.1), (5.2) and (5.4) are shown in Fig.5.4(a). (The influence of damping on the mobility of the simple oscillator with hysteretic damping is set out graphically in Appendix 2.) By inspection of equation (5.1), (5.2) and (5.4), and with the help of Fig.5.4(a), the influence of foundation damping may be determined. The power flow, velocity amplitude, and transmitted force are shown graphically in Figs.5.4(b),(c) and (d) respectively.

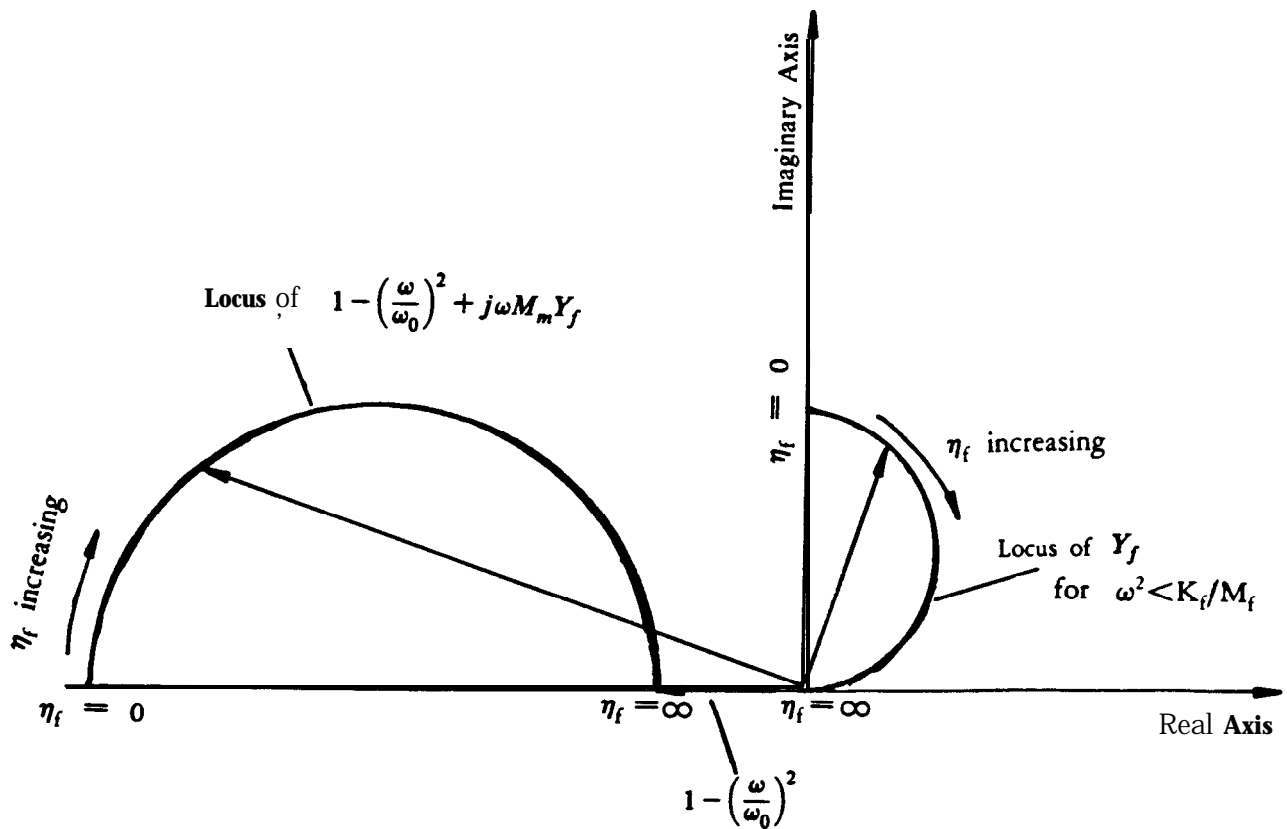


Fig.5.4(a) Loci of various complex quantities as damping is varied

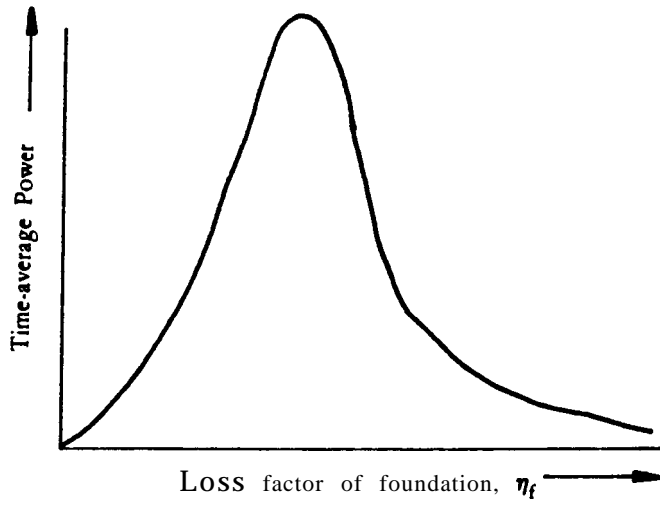


Fig.5.4(b) Variation of time-average power with loss factor

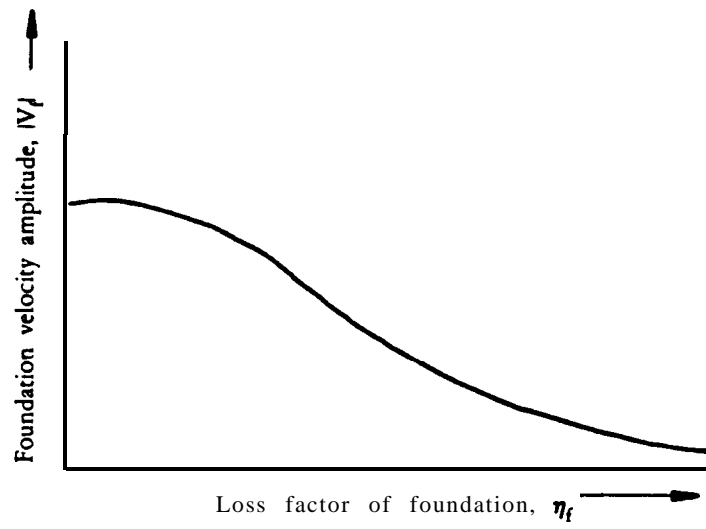


Fig.5.4(c) Variation of foundation velocity with damping

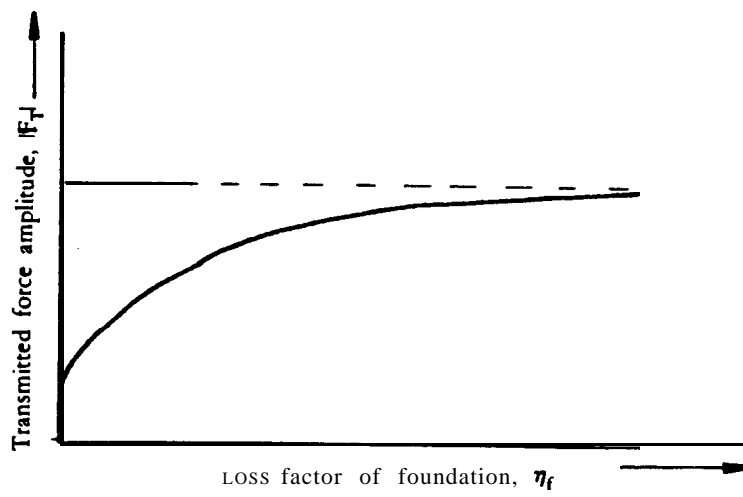


Fig.5.4(d) Variation of transmitted force with damping

It is seen that any reduction in power flow achieved by varying the amount of damping in the foundation will result in an increase of either the transmitted force or the velocity amplitude. Therefore an improvement in vibration isolation cannot necessarily be obtained by using alterations in the foundation damping to reduce power flow.

5.4.2 Semi-infinite beam approximation for foundation characteristics

Very often, when the modulus of the driving-point mobility of a damped complex structure is plotted against frequency on a log-log scale, the graph is found to be approximately a straight line in the high frequency range. In such cases the modulus of the mobility may be written approximately as

$$|Y(\omega)| = A \omega^b \tag{5.12}$$

where A and b are real constants.

The phase characteristic corresponding to a mobility modulus of this form is [47]

$$\phi(\omega) = \frac{b\pi}{2} \tag{5.13}$$

and the mobility is then given by

$$Y(\omega) = A \omega^b [\cos(\frac{b\pi}{2}) + j \sin(?)] \tag{5.14}$$

A semi-infinite beam is an example of a structure whose mobility modulus

exhibits straight line characteristics when plotted on a log-log scale. The mobility of a semi-infinite beam is [48]

$$Y = (EI\bar{m}^3\omega^2)^{-\frac{1}{4}}(1-j) \quad (5.15)$$

This may be written in the same form as equation (5.14), with A and b given by

$$A = \left(\frac{EI\bar{m}^3}{4}\right)^{-\frac{1}{4}} \quad \text{and } b = -\frac{1}{2} \quad (5.16)$$

We shall now consider the power flow to a foundation which possesses the characteristics of a semi-infinite beam, restricting our attention to the influence of the flexural stiffness, EI, of the beam.

We shall first dispose of the case where the frequency of excitation coincides with the natural frequency of the machine-isolator subsystem. In this case $1-(w/w_0)^2 = 0$, and equations (5.1), (5.2) and (5.4) may be written as

$$P_{av} = \frac{1}{2}|F|^2 \frac{\text{Re}\{Y_f\}}{\omega^2 M_m^2 |Y_f|^2} = \frac{|F|^2}{4M_m^2} \left(\frac{EI\bar{m}^3}{\omega^6}\right)^{\frac{1}{4}} \quad (5.17)$$

$$|V_f| = \frac{|F|}{\omega M_m} \quad (5.18)$$

and

$$|F_T| = \frac{|F|}{\omega M_m |Y_f|} = \frac{|F|}{\sqrt{2}M_m} \left(\frac{EI\bar{m}^3}{\omega^2}\right)^{\frac{1}{4}} \quad (5.19)$$

The time-average power flow and the transmitted force amplitude are

proportional to the fourth root of the flexural stiffness according to equations (5.17) and (5.19). Thus, if the time-average power is reduced by altering the flexural stiffness of the foundation the transmitted force will decrease. However, equation (5.18) shows that the foundation velocity is independent of the flexural stiffness and, therefore, if an attenuation of the velocity is desired it cannot be obtained by reducing the power flow in this way.

The more general case where $\omega \neq \omega_0$ is not very easy to deal with analytically. Therefore we shall consider a specific example with the following parameters: $M_m = 20.0\text{kg}$, $\omega_0 = 200\pi$, $\bar{m} = 58.875\text{kg/m}$. The time-average power, velocity amplitude and transmitted force have been computed for a range of flexural stiffness values at excitation frequencies of $\omega = 0.5\omega_0$ and $\omega = 1.591\omega_0$, with an exciting force of unit amplitude. The results are shown graphically in Figs.5.5(a),(b),(c) and Figs.5.6(a),(b),(c). A study of the plots for each of these two particular cases would again show that if the flexural stiffness is altered in such a way that the power flow is reduced, a reduction of transmitted force or velocity amplitude is not always assured. Therefore, in the design of a foundation of this sort, the flexural stiffness which gives the least time-average power will not necessarily provide the best vibration isolation.

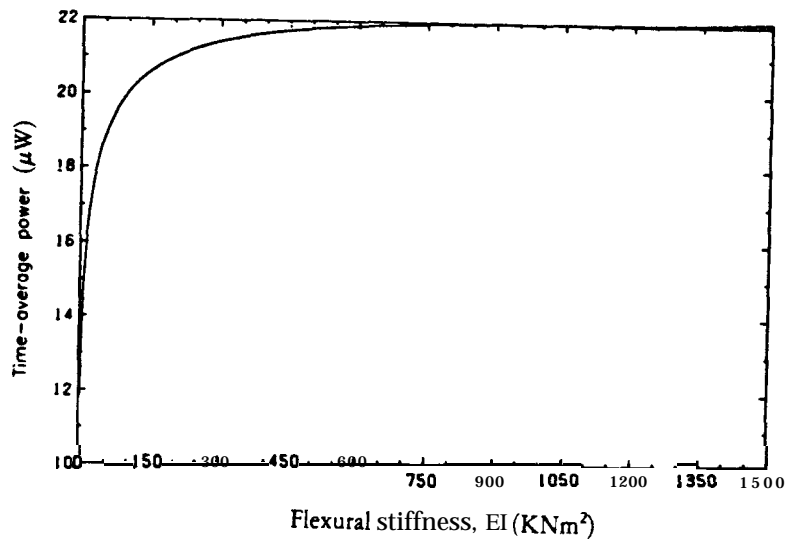


Fig.5.5(a) Time-average power flow to foundation ($\omega=0.5\omega_0$)

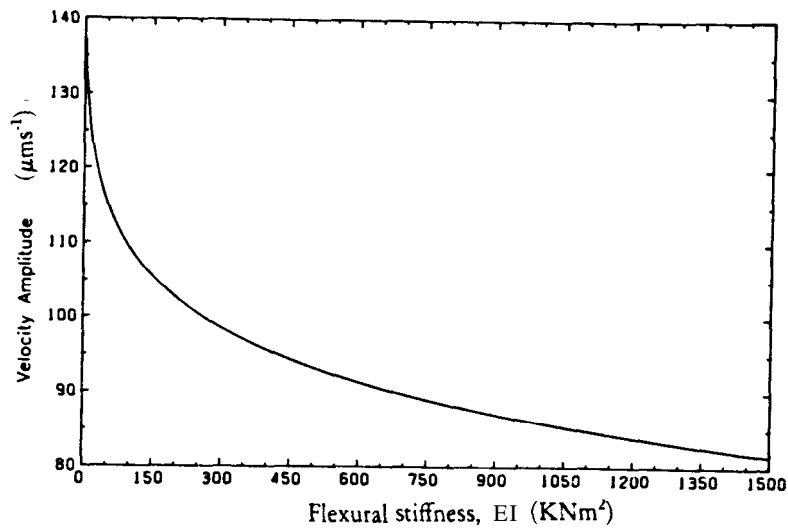


Fig.5.5(b) Amplitude of foundation velocity ($\omega=0.5\omega_0$)

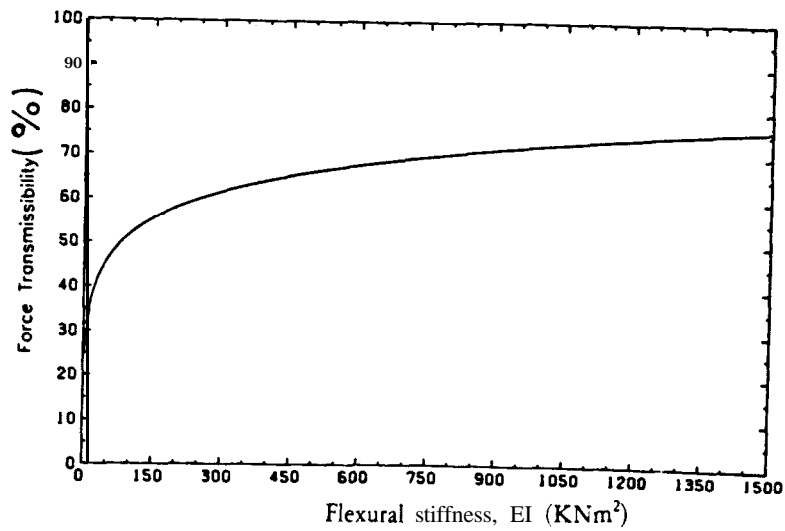


Fig.5.5(c) Force Transmissibility ($\omega=0.5\omega_0$)

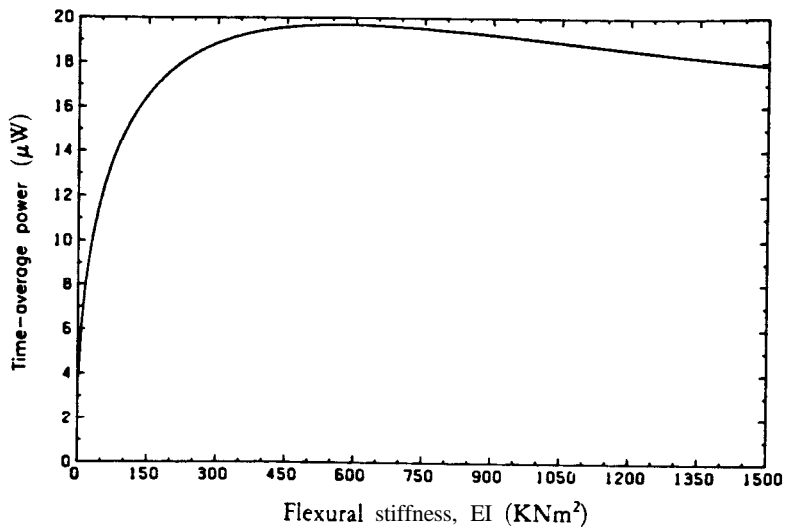


Fig.5.6(a) Time-average power flow to foundation ($\omega=1.591\omega_0$)

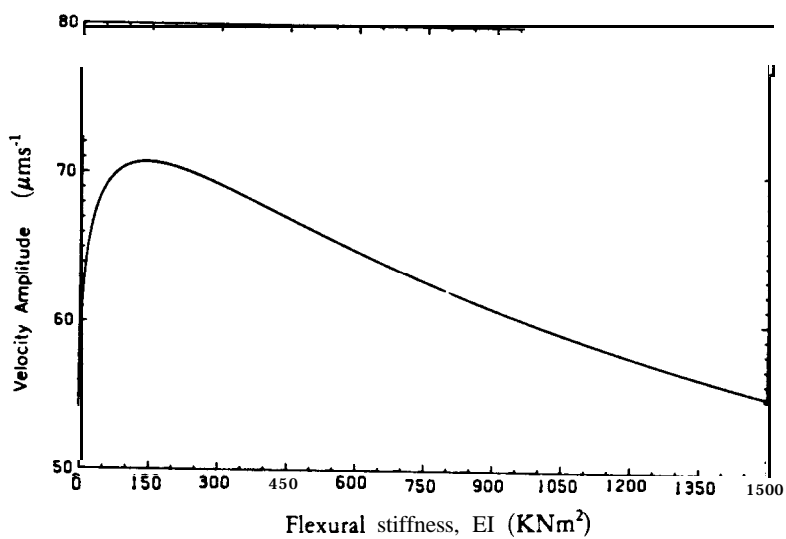


Fig.5.6(b) Amplitude of foundation velocity ($\omega=1.591\omega_0$)

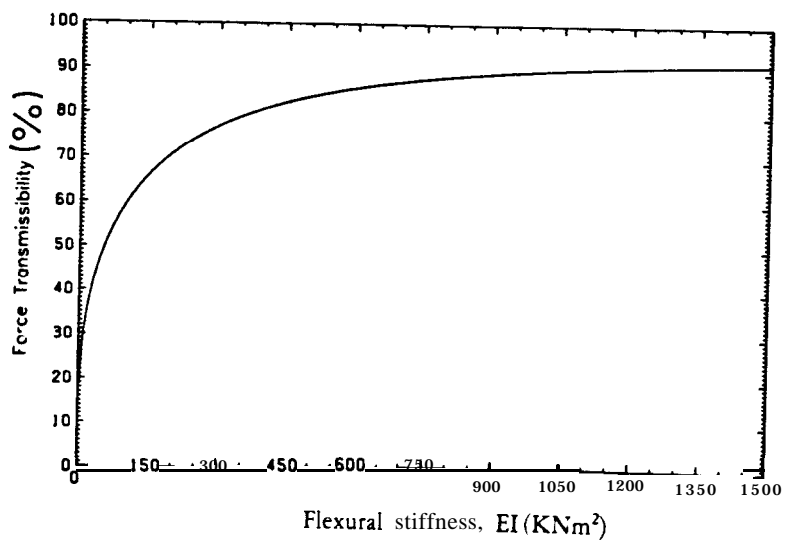


Fig.5.6(c) Force Transmissibility ($\omega=1.591\omega_0$)

5.5 Discussion

It was shown in §5.3 that provided the characteristics of the foundation are kept constant, the time-average power flow is directly proportional to the squares of foundation velocity and transmitted force amplitudes. This result is not as useful as it would appear because it is not applicable if the machine interacts with the foundation with more than one degree of freedom. Consider a vibrating system composed of two subsystems, A and B, linked together in n coordinate directions, Fig.5.7, with the external exciting forces applied to subsystem A alone.

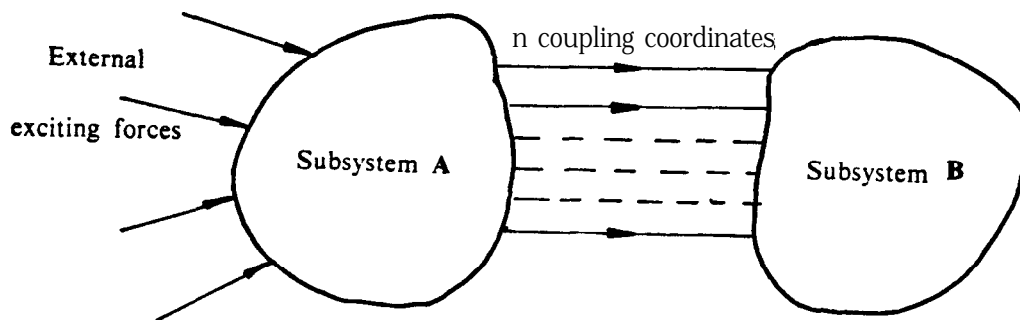


Fig.5.7 Subsystems linked in n coordinate directions

The time-average power flow to subsystem B may be written as

$$P_{av} = \frac{1}{2} \text{Re} \left(\{F\}^H [Y^{(B)}] \{F\} \right) \tag{5.20}$$

where $[Y^{(B)}]$ is the mobility matrix of B, relating to the n coupling coordinate directions, and $\{F\}$ is a vector of the forces transmitted to B.

This expression may be written more explicitly as

$$P_{av} = \frac{1}{2} |F_1|^2 \text{Re} \{ Y_{11}^{(B)} \} + \frac{1}{2} |F_2|^2 \text{Re} \{ Y_{22}^{(B)} \} + \dots + \frac{1}{2} |F_n|^2 \text{Re} \{ Y_{nn}^{(B)} \} \\ + \frac{1}{2} \sum_{r=1}^n \sum_{s=1, s \neq r}^n F_r^* F_s \text{Re} \{ Y_{rs}^{(B)} \} \tag{5.21}$$

This expression may also be written in terms of the velocity responses and the impedances of subsystem B:

$$P_{av} = \frac{1}{2}|V_1|^2 \text{Re}\{Z_{11}^{(B)}\} + \frac{1}{2}|V_2|^2 \text{Re}\{Z_{22}^{(B)}\} + \dots + \frac{1}{2}|V_n|^2 \text{Re}\{Z_{nn}^{(B)}\} + \frac{1}{2} \sum_{r=1}^n \sum_{s=1}^n V_r^* V_s \text{Re}\{Z_{rs}^{(B)}\} \quad (5.22)$$

Equation (5.21) is difficult to interpret on account of the fact that there are now many more transmitted forces to be considered. If the dynamic characteristics of subsystem A are altered in such a way that the time-average power flow is reduced, it is not certain that all the n transmitted forces will be simultaneously reduced. It is more likely that some of the forces will actually increase while others decrease in magnitude. There will then be the difficulty of deciding whether or not the alteration in subsystem A has improved or worsened the situation. The foregoing remarks also apply to the velocities, in view of equation (5.22).

The case where the reduction of time-average power is achieved by alterations in the characteristics of the foundation was considered in §5.4. It was necessary to assume a form for the dynamic characteristics of the foundation. Two such assumed forms were considered, namely, a one-degree-of-freedom system and a semi-infinite beam. The results show quite clearly that a reduction of the time-average power flow to the foundation will not always be accompanied by a decrease in the amplitudes of the force and velocity transmitted to the foundation. Therefore, we may conclude that the design of machinery support structures on the basis of power flow alone will not necessarily provide good vibration isolation.

The time-average power supplied to any subsystem of a vibrating structure is equal to the average rate at which energy is being lost in that subsystem. This power loss is made up of the dissipated power, P_{dis} (ie power converted to heat by damping mechanisms), and the power radiated into the surrounding air or other fluid medium, P_{rad} . It may be argued, on the basis of energy conservation, that if the power flowing to the subsystem is reduced then less power will be available for sound radiation. However, the effect of a reduction of time-average power will depend quite heavily on how the power reduction has been brought about. It is possible to conceive of a situation in which the power radiated remains unaltered even though the total power flow (equal to $P_{dis} + P_{rad}$) has been reduced. Consider the vibration problem shown schematically in Fig.5.8. Let us suppose that we are concerned about sound radiation from the receiver which is plate-like and supports only waves propagated via the transmission path. If, in an attempt to reduce the total time-average power flow, the power dissipated in the receiver alone is reduced, the result could well be an increase of the radiated power.

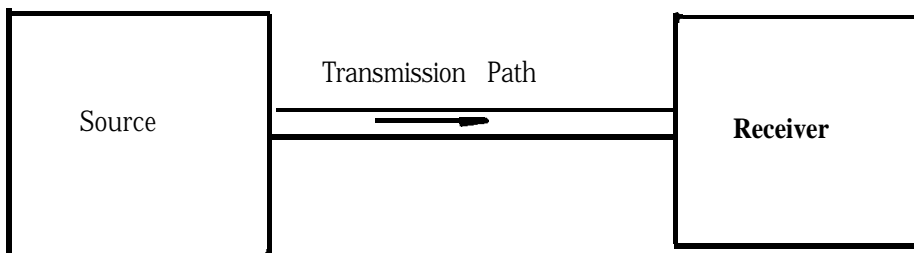


Fig.5.8 Schematic representation of vibration problem

The use of power flow considerations in sound radiation problems requires considerable caution and judgement. Even in situations where the analysis shows that an abatement of sound radiation will result from a reduction in the time-average power flow, care must be taken to ensure that all the significant transmission paths have been accounted for. It has been shown, for example, that for large resiliently-mounted engines at medium and high frequencies the sound transmission through the surrounding air can be more important than the transmission through a good resilient mount [49]. A vibration isolation exercise which is successful in reducing the structure-borne power could well result in more power being transmitted through the acoustic path.

The analysis presented here has been restricted to steady-state sinusoidal excitation at discrete frequencies, and we have been concerned with vibration responses in specific coordinate directions only. We have not considered situations where the excitation forces are random and distributed; nor have we considered spatial-average responses. These considerations belong to the realm of Statistical Energy Analysis (SEA). The literature on SEA suggests that the basic conclusion of this chapter is equally applicable where the excitation force field is random. The design of vibration isolation systems for random force excitation on the sole basis of a reduction in the power flow is not likely to be satisfactory unless the whole isolation problem is considered within the context of SEA. Outside the framework of SEA there is no simple relationship between power flow and vibration response.

Chapter 6

MEASUREMENT OF TIME-AVERAGE POWER FLOW ALONG A SIMPLE BEAM STRUCTURE

6.1 Introduction

The measurement of vibrational power flow in structures is of interest as a means of identifying vibration transmission paths. The instantaneous power flow across any section of a vibrating structure during steady-state forced vibration consists of an active component, which is the time-average power, and a reactive component which is sinusoidal and has twice the excitation frequency. For the purpose of identifying vibration transmission paths it is the active component of power which is of interest to us. By measuring the magnitude as well as the direction of the time-average power flow at various positions over a structure the major paths of energy transmission can be identified. A decision can then be made on the appropriate vibration control measures that are needed. These measures could involve, for example, the application of damping materials along the transmission paths to absorb the energy.

One of the methods available for the measurement of vibrational power flow is that due to Noiseux [27] who proposed a method for measuring the vibration intensity (time-average power flow per unit width of cross-section) in uniform beams and plates vibrating in flexure. **Suprisingly**, his method has received little attention until recently [28]. In this chapter we present the results of the measurement of vibration intensity along a

simple beam structure using Noiseux's technique. Signal processing was done with the Bruel & Kjaer Sound Intensity Analysing System Type 3360. The object of the tests was to check the accuracy of Noiseux's technique, and to assess its acceptability for routine measurements in simple beam structures.

6.2 Theory and measuring method

One way of describing the net flow of vibrational energy at a given point in a vibrating structure is by the vibration intensity vector, w . The magnitude and direction of the intensity vector are defined such that the time-average power flow per unit width in any given direction is equal to the projection of the intensity vector, w , on this direction. A formulation of the vibration intensity for a uniform undamped beam is now presented. This formulation follows that presented by Noiseux [27] up to the point where the vibration intensity transducer is considered.

Consider a uniform beam lying with its axis in the x direction and vibrating in flexure. The flow of energy along the beam is due to a bending moment, M , and a shear force, Q , as shown in Fig. 6.1.

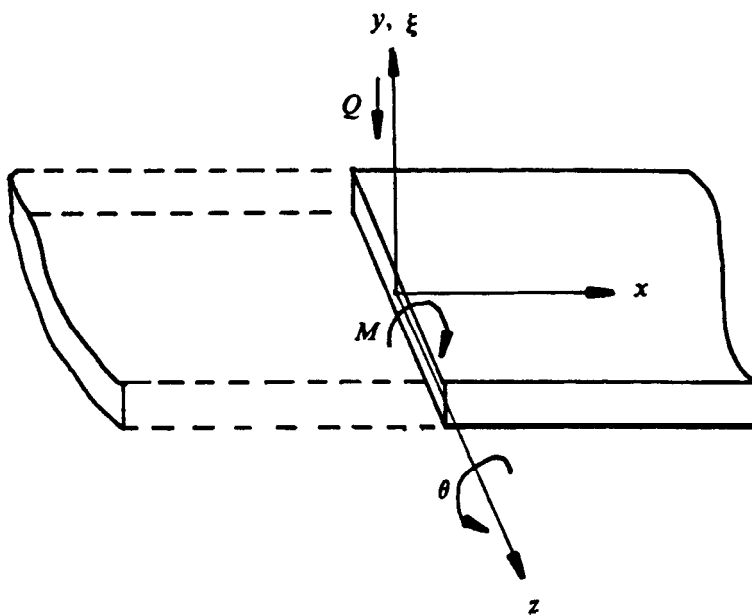


Fig.6.1 Shear force and bending moment acting on beam cross-section

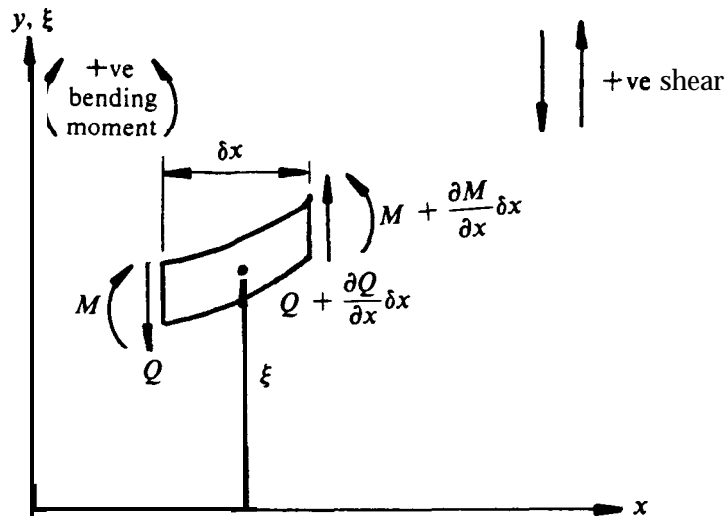


Fig.6.2 Dynamics of beam element – positive sign convention

The shear force and bending moment acting on the cross-section whose normal is in the +ve x direction are shown in Fig.6.1. Under the sign convention indicated in Fig.6.2, the Bernoulli-Euler beam theory gives the following bending moment-curvature relationship:

$$M = EI \frac{\partial^2 \xi}{\partial x^2} \quad (6.1)$$

while the shear force is given by

$$Q = -EI \frac{\partial^3 \xi}{\partial x^3} \quad (6.2)$$

where E is the modulus of Elasticity and I is the second moment of area. The rotation is related to the flexural displacement, ξ , by

$$e = \frac{\partial \xi}{\partial x} \quad (6.3)$$

and the angular velocity is

$$\theta = \frac{\partial}{\partial t} \left(\frac{\partial \xi}{\partial x} \right) \quad (6.4)$$

The total intensity in the +ve x direction along the beam is[†]

$$\begin{aligned} w_x &= \langle -Q\dot{\xi} \rangle_t + \langle -M\dot{\theta} \rangle_t \\ &= w_{xf} + w_{xm} \end{aligned} \quad (6.5)$$

where $\langle \dots \rangle_t$ denotes time-averaging, and the shear force and bending moment are calculated per unit width of the beam; w_{xf} and w_{xm} are the force and moment components of intensity respectively. For waves in the free-field (see Appendix 3), the partial derivative of equation (6.1) may be written as

$$\frac{\partial^2 \xi}{\partial x^2} = -k^2 \xi$$

so that
$$M = -EI k^2 \xi \quad (6.6)$$

where k is the wave number which is given by

$$k^4 = \frac{\omega^2 \bar{m}}{EI} \quad (6.7)$$

and \bar{m} is the mass per unit length of the beam.

It can be shown (see Appendix 3) that if the free-field solution alone is considered, the force and moment components of intensity are equal, ie $w_{xf} = w_{xm}$. Equation (6.5) may then be written as

$$\begin{aligned} w_x &= 2w_{xf} = 2w_{xm} \\ &= 2 \langle -M\dot{\theta} \rangle_t \end{aligned} \quad (6.8)$$

[†] Note that under the sign convention adopted here the rotation θ and the moment M are in opposite directions. The same relationship applies to ξ and Q .

and using equation (6.6) we have

$$w_x = 2 \langle B k^2 \xi \dot{\theta} \rangle_t \quad (6.9)$$

$$= 2 \langle B k^2 \dot{\theta} \int \int \ddot{\xi} dt^2 \rangle_t \quad (6.10)$$

where $B = EI = \frac{E h^3}{12}$ (evaluated per unit width) and h is the thickness of the beam.

For a pure sinusoidal vibration at an angular frequency, ω , the integral in equation (6.10) is equal to $-\ddot{\xi}/\omega^2$, so that

$$\begin{aligned} w_x &= - \langle \frac{2B k^2}{\omega^2} \dot{\theta} \ddot{\xi} \rangle_t \\ &= -2 \frac{\sqrt{B m}}{w} \langle \dot{\theta} \ddot{\xi} \rangle_t \end{aligned} \quad (6.11)$$

Thus the measurement of the vibration intensity boils down to the measurement of the rotational velocity and the transverse acceleration of the beam. The transducer used to measure these quantities is shown in Fig.6.3. It is modelled on the vibration intensity transducer used by *Bruel & Kjaer* [28], and consists of two accelerometers rigidly glued onto a small aluminium block.

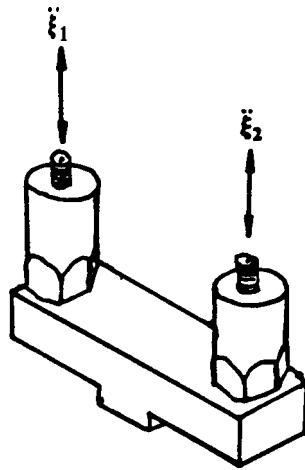


Fig.6.3 Vibration intensity transducer

The rotational velocity is obtained from the difference of the two measured accelerations:

$$\dot{\theta} = \int \left(\frac{\ddot{\xi}_2 - \ddot{\xi}_1}{\Delta r} \right) dt \quad (6.12)$$

where Δr is the distance between the accelerometers. The transverse acceleration, $\ddot{\xi}$, is found from the mean

$$\ddot{\xi} = \frac{1}{2}(\ddot{\xi}_2 + \ddot{\xi}_1) \quad (6.13)$$

Substitution of these into equation (6.11) yields

$$w_x = -\frac{2\sqrt{B\bar{m}}}{\omega} < \frac{1}{2}(\ddot{\xi}_1 + \ddot{\xi}_2) \int \left(\frac{\ddot{\xi}_2 - \ddot{\xi}_1}{\Delta r} \right) dt >_t \quad (6.14)$$

The implementation of this equation is done in the B&K 3360 Sound Intensity Analysing System, a block diagram of which is shown in Fig.6.4.

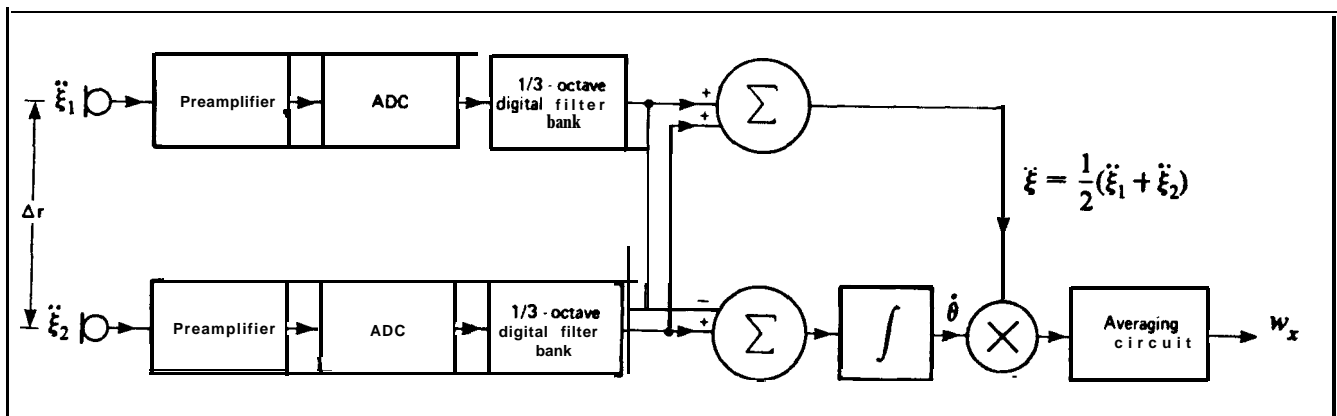


Fig.6.4 Signal processing in the B&K 3360 Sound Intensity Analysing System

6.3 Theoretical study of test structure

The most important feature of Noiseux's technique is the assumption that the force and moment components of intensity are equal. Indeed, the quantity that is actually measured in a test is the moment component, w_{xm} ; the total intensity is simply taken to be equal to $2w_{xm}$. For a uniform lossless beam the relationship $w_{xf}=w_{xm}$ is strictly true only if measurements are made in the free field. However, even where the measurements are not made in the free field it is found that the force and moment components of intensity are approximately equal under certain conditions. For example, if we consider the near field of a semi-infinite beam excited at the tip, the force and moment components of intensity are practically equal at distances greater than a half wavelength from the point of excitation. (See reference 27 and Appendix 3.) In order to ensure that our chosen test structure was amenable to the measuring technique a theoretical study was carried out.

6.3.1 The test structure and its model

The structure chosen for the study described in this chapter consisted of an aluminium beam one end of which was of 5-layer sandwich construction. The damping layers were of PVC and the constraining layers were of sheet steel. Details of the structure are given in Fig.6.5.

The test structure was modelled theoretically as a simple Bernoulli-Euler beam with constrained layer damping applied at one end. The frequency response data were computed using the program COUPLE1, and the computed and the measured driving-point mobilities are shown in Fig.6.6 and Fig.6.7 respectively. The exciting force is applied at the undamped end of the beam.

It is seen that at low frequencies the theoretical model describes the behaviour of the actual structure quite accurately. At higher frequencies the measured mobility differs from that computed for the model in its detail, but the general characteristics are similar. Because of the fact that viscoelastic materials have properties which vary with frequency, temperature and dynamic strain level [51], the model was not expected to compare with the measured characteristics more favourably than this and, in any case, an exact model is unnecessary for this kind of study. All that is required is for the model to have the same general dynamic behaviour as the real test structure.

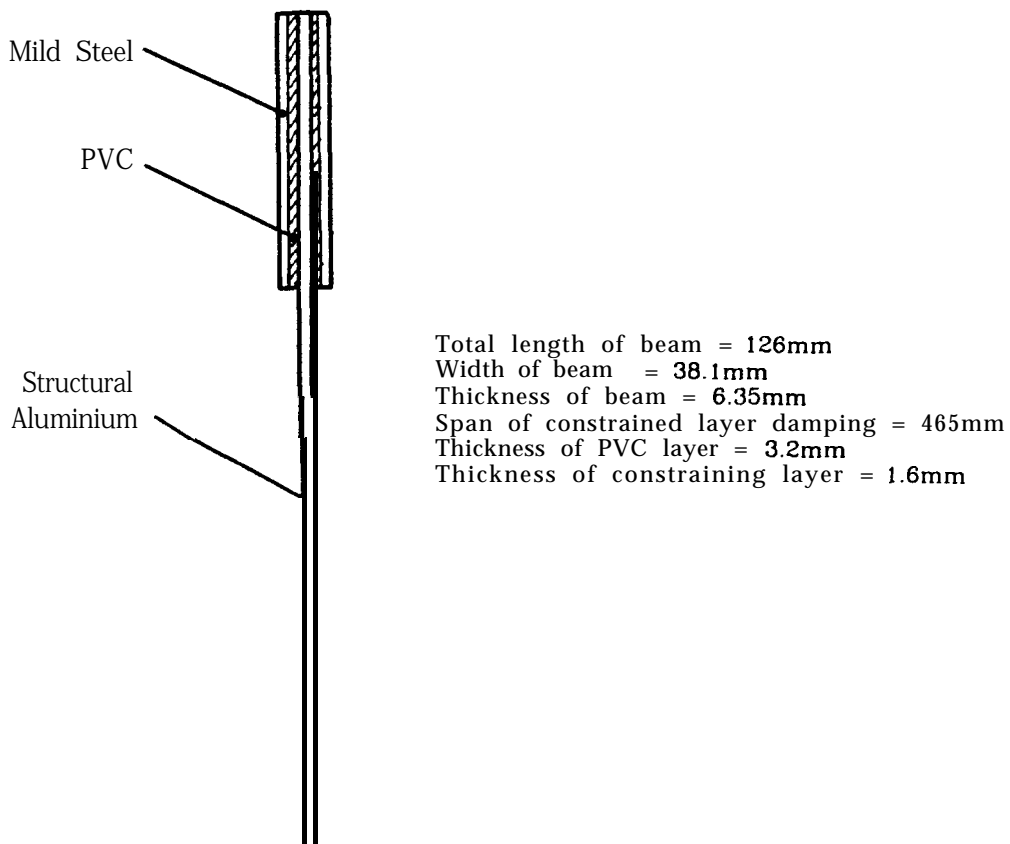


Fig.6.5 Details of test structure

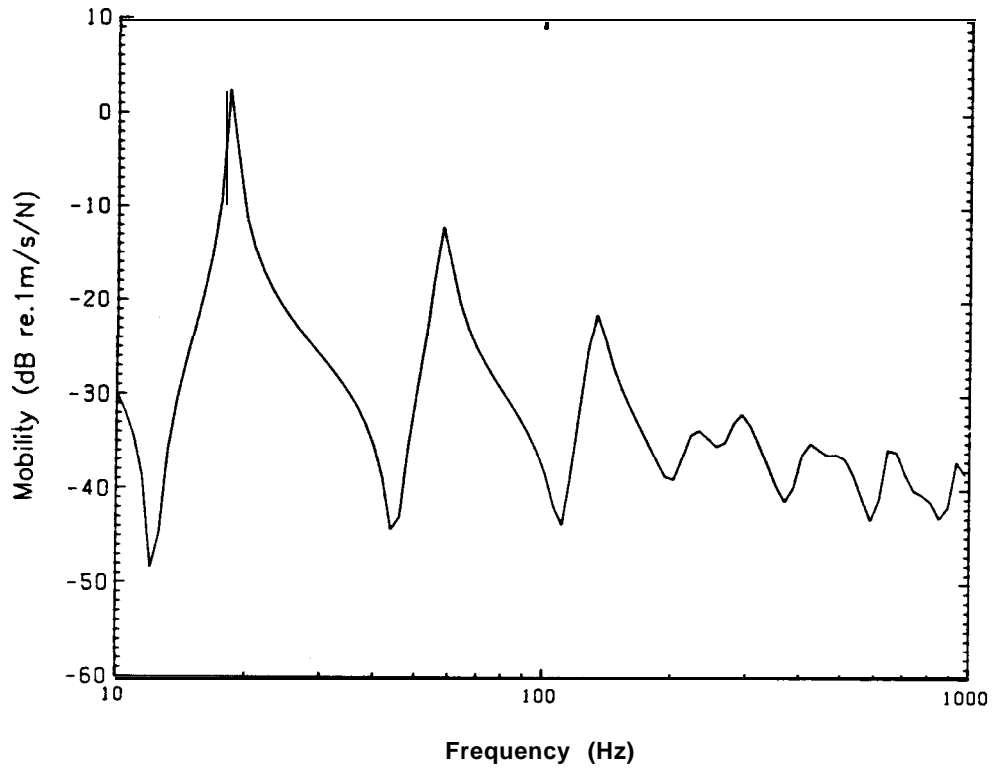


Fig.6.6 Computed driving-point mobility of test structure

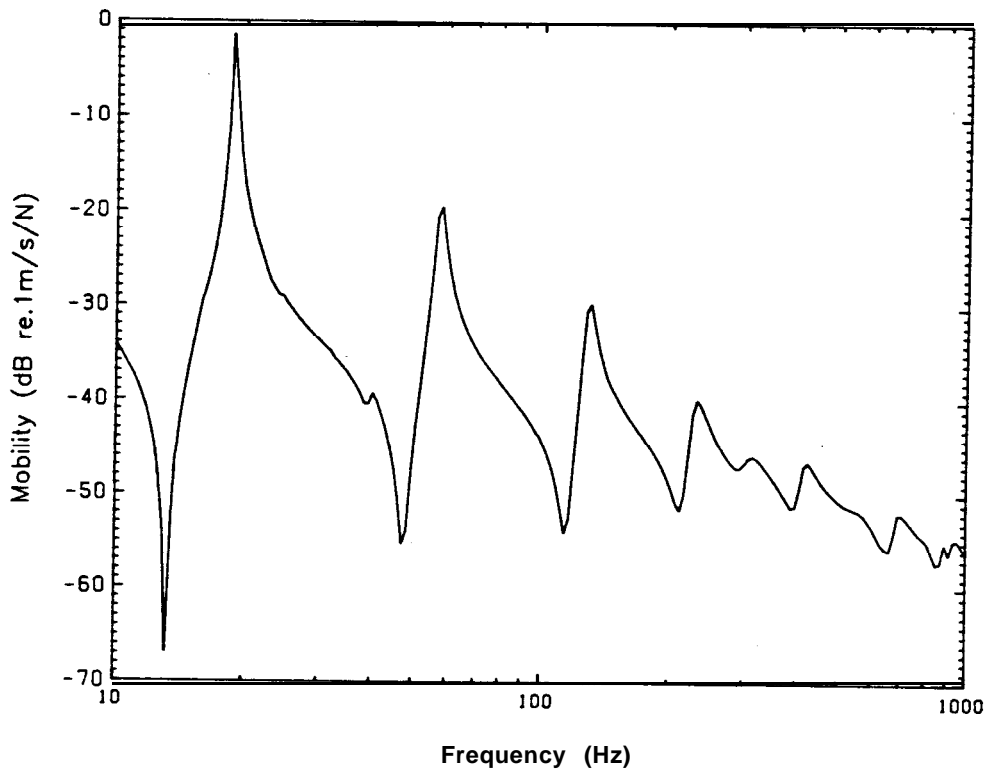


Fig.6.7 hieasured driving-point mobility of test structure

6.3.2 Computed results

The moment component of intensity, w_{xm} , was calculated as a percentage of the total intensity, w_x for various distances along the beam. The variation of the ratio w_{xm}/w_x with distance is shown graphically in Fig.6.6 for three excitation frequencies. Fig.6.9 also shows the variation of this ratio with frequency at various distances. Roughly speaking, these plots take the form that would be expected for a semi-infinite beam; see Appendix 3. The ratio w_{xm}/w_x increases from zero to an 'overshoot' value of about 60% before settling to a value of about 50%. The ratio then remains steady up to a certain distance from the sandwich portion of the beam. The span over which the ratio remains steady at 50% depends on the frequency; the higher the frequency, the longer the span.

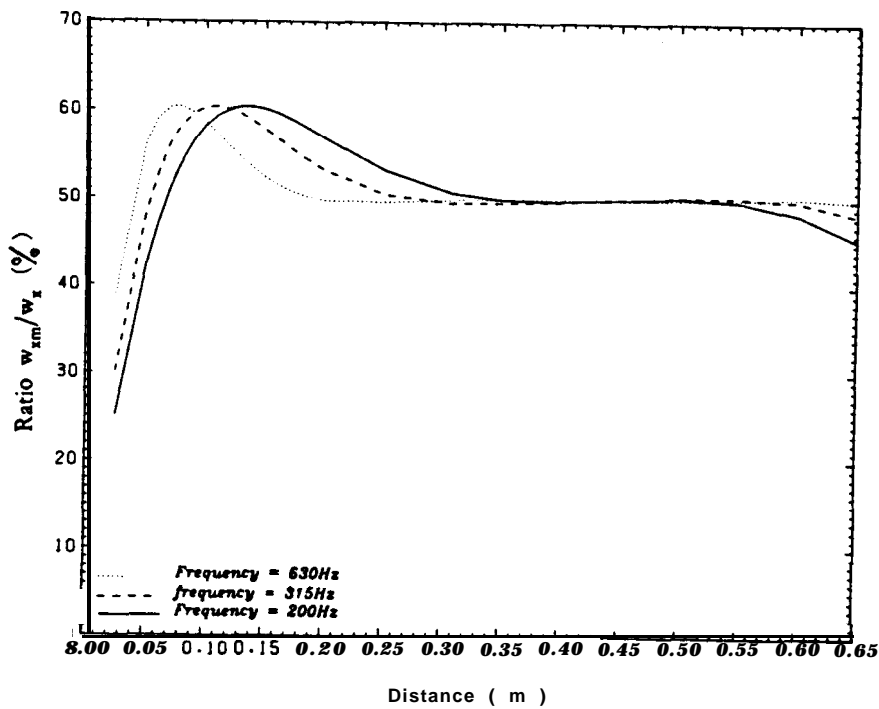


Fig.6.6 Computed variation of ratio w_{xm}/w_x with distance from driving-point

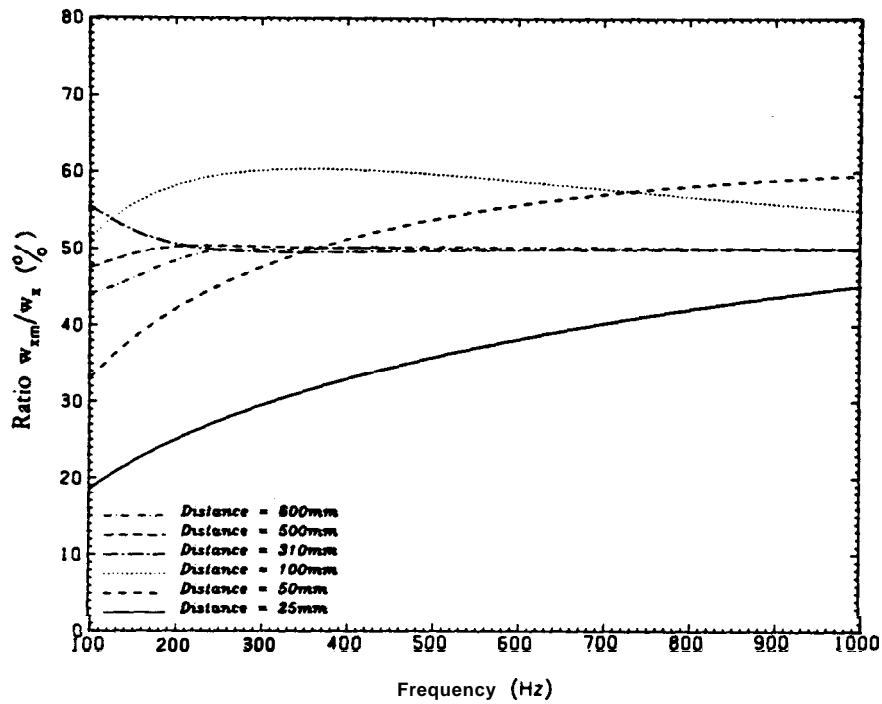


Fig.6.9 Computed variation of ratio w_{fm}/w_x with excitation frequency

6.4 Experimental results

6.4.1 Set-up for vibration intensity measurements

The set-up for the vibration intensity measurements is shown in Fig.6.10. The beam was suspended from its damped end, and the excitation was applied at the undamped end. The input force and the driving-point response were measured using the Solartron Frequency Response Analyser. The signals from the vibration intensity transducer were fed through charge amplifiers into the B&K Sound Intensity Analysing System Type 3360. The main component of

the B&K 3360 System is the Sound Intensity Analyser Type 2134. which is primarily designed for acoustic intensity measurements and is basically a digital frequency analyser with two input channels. The 3360 System measures sound intensity over the 3.2Hz-10KHz frequency range in octave and third octave bands, and displays the results in real time.

When the B&K 3360 is used for acoustic intensity measurements the computations are based on the two-microphone method [52], employing a finite difference approximation for calculating the particle velocity from the pressure gradient and hence the acoustic intensity. The use of the B&K 3360 for vibration intensity measurements is possible only because the mathematical expression for vibration intensity, as represented by equation (6.14), is of the same form as the corresponding expression for acoustic intensity.

The B&K 3360 displays results in octave and 1/3 octave bands, and since the experiments involved only pure tones, it was necessary to choose each excitation frequency to coincide with the center frequency of one of the 1/3 octave bands. During the calibration of the system various known signals were fed from an oscillator into the analyser, and the intensity readings were checked against the calculated values. The readings from the display unit were found to be exactly equal to the intensities calculated from the known signals.

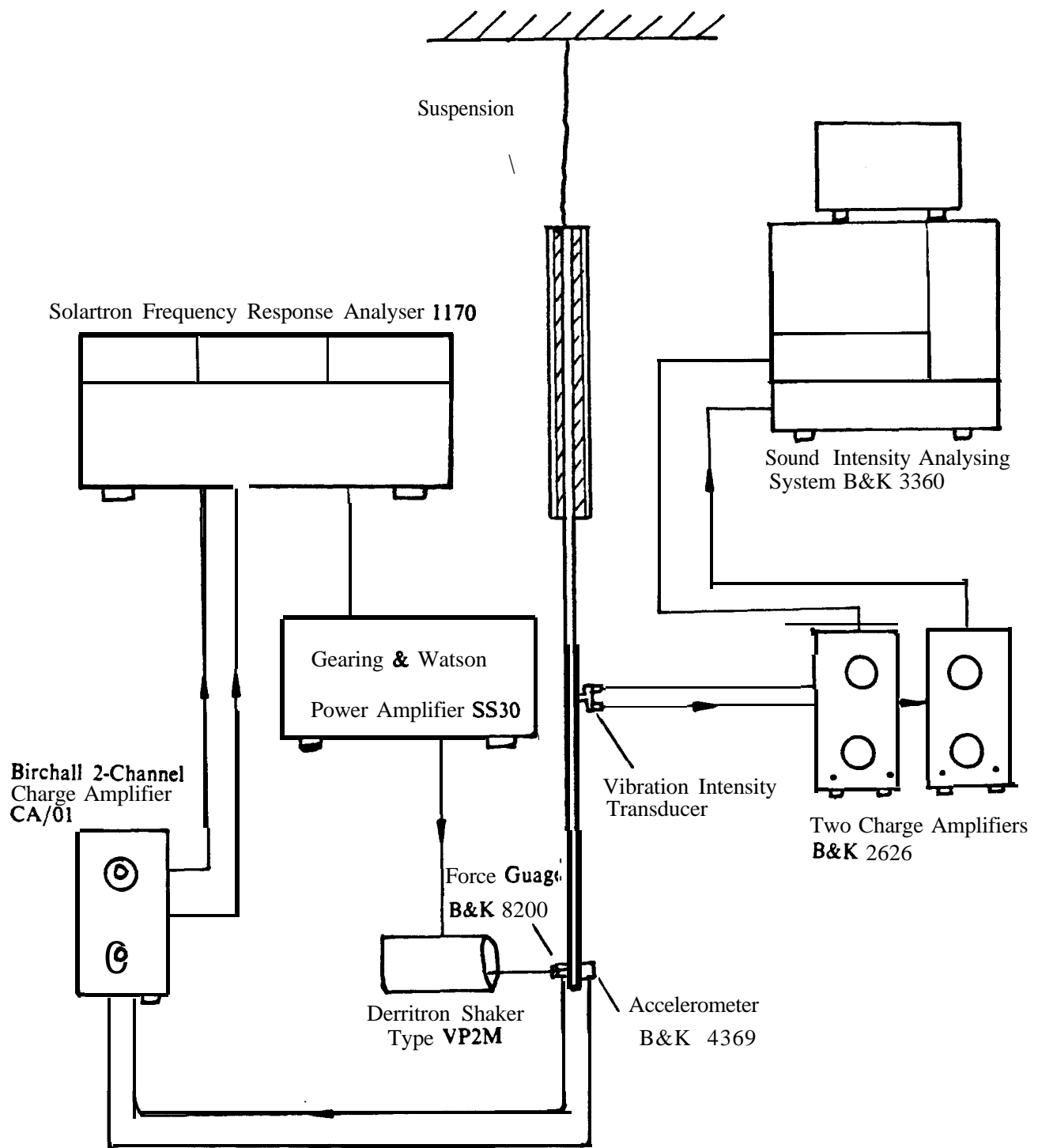


Fig.6. 0 Set-up for vibration intensity measurements

As a further check on the accuracy of the signal processing in the Intensity Analyser, a series of tests was carried out in which the structure was excited at a constant frequency, and the intensity was measured at a fixed point along the beam for various magnitudes of input intensity. The input intensity was calculated using equation (6.15) in §6.4.2, and one typical set of results is shown graphically in Fig.6.11. The ratio w_x/w_{in} was found to be approximately constant for each set of tests. This result provided further evidence of the accuracy of the Sound Intensity Analysing System. It also boosted our confidence in the measuring technique.

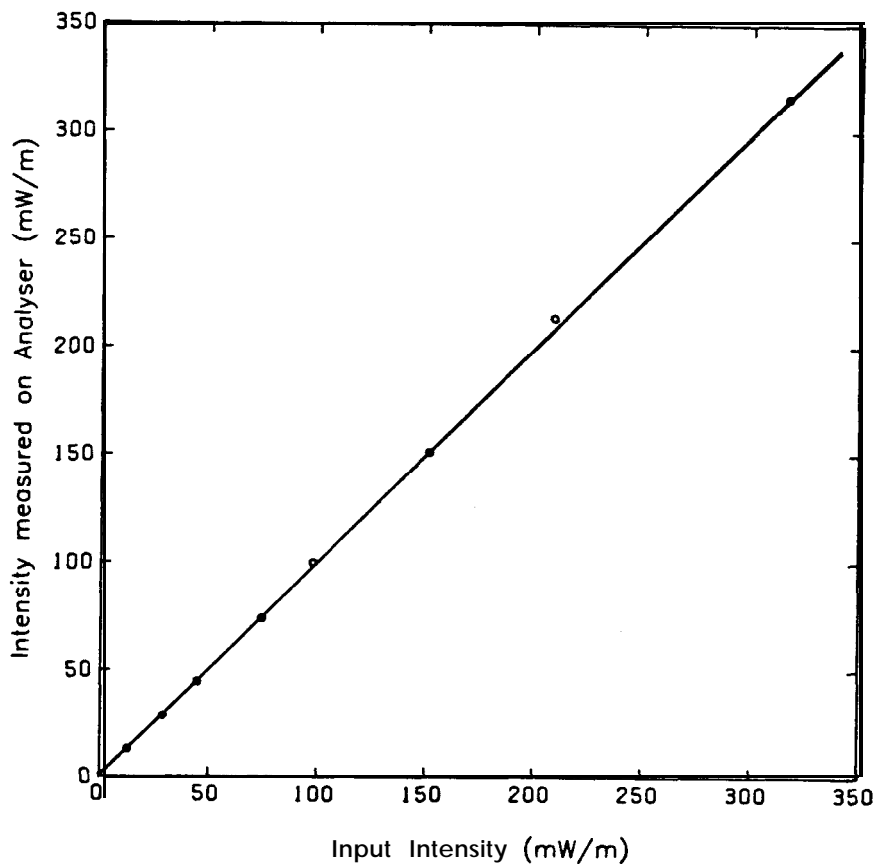


Fig.6.11. Measured variation of w_x with input intensity, w_{in}

6.4.2 Variation of intensity with distance from driving point

The structure was excited at a fixed frequency of 315Hz, and the intensity was measured at various distances from the point of excitation. The object of this test was to verify the theoretical predictions of §6.3.2. Ideally, the whole test should have been carried out with the input power held constant, but this was not practicable owing to the need to turn off the input when changing the position of the vibration intensity transducer. Therefore, in addition to the intensity, w_x , along the beam, the force and acceleration at the driving point were also measured, and the input intensity, w_{in} , was calculated. The measurement of input force and response represents an additional source of error which makes interpretation of results a bit more difficult. Fortunately, as will be argued later, this is not a significant source of error here. The variation of the ratio w'_{xm}/w_{in} is shown graphically in Fig.6.12, and may be seen to be similar in form to that for the ratio w_{xm}/w_x (from theoretical analysis), Fig.6.6, except that the deviations from the mean value of 50% are wider.†

The input intensity was calculated using the expression

$$w_{in} = \frac{1}{2\omega b} |a| |F| \sin \theta \quad (6.15)$$

where b is the width of the beam, F is the input force, a the acceleration, and θ the phase angle between force and acceleration. The transducers used for the measurements were new. Since calibration facilities were not readily available the manufacturers' sensitivity data was used. However, a mass calibration test [35] yielded an inertance scale factor of unity which helped to boost confidence in the manufacturers' data.

† w'_{xm} is the measured moment component of intensity. The damping between the driving point and the point of intensity measurement is negligibly small. Therefore the total intensity, w_x , at any location should be equal to the input intensity, w_{in} , hence the comparison between the ratios w'_{xm}/w_{in} (from measurement) and w_{xm}/w_x (from theoretical analysis).

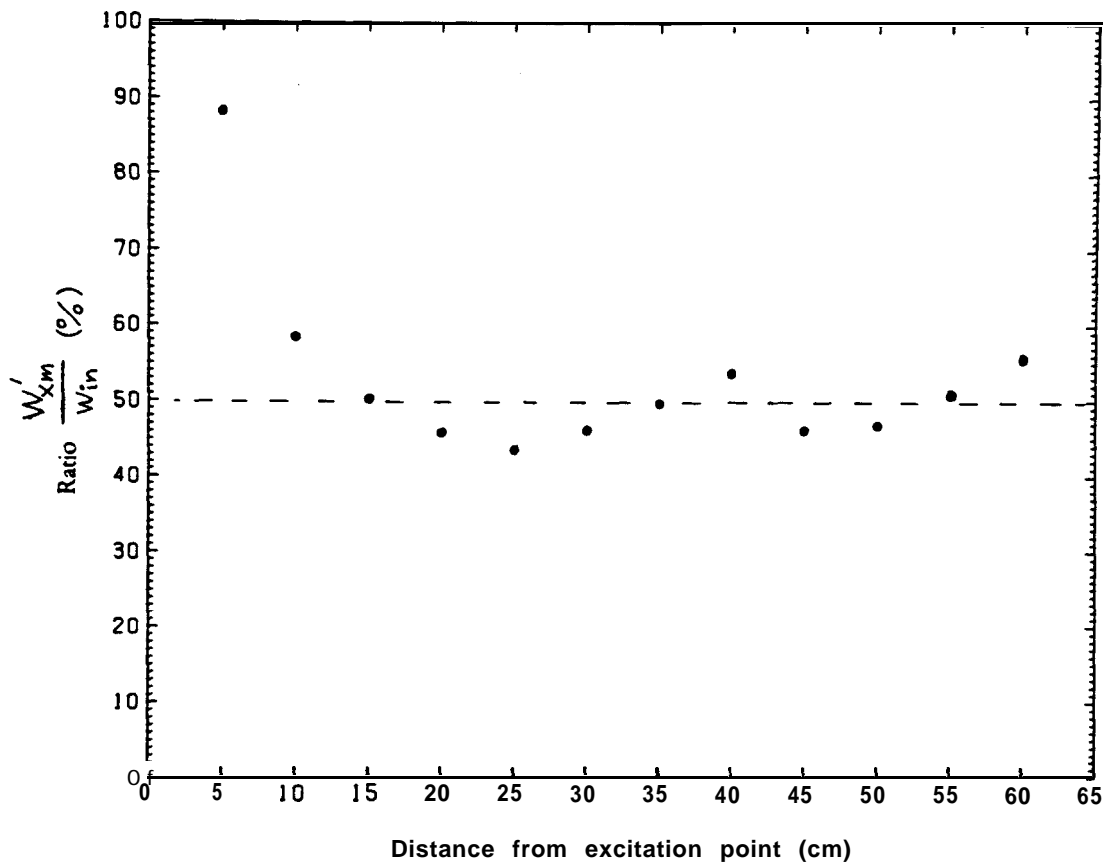


Fig.6.12 Measured variation of intensity with distance from driving-point

The main source of error in input power measurements is the phase angle. If θ is very small, $\sin\theta$ is very sensitive to errors. The error sensitivity of $\sin\theta$ decreases as θ increases from zero to 90° and so the influence of phase angle errors depends on the size of the angle being measured. In this particular test the phase angle was of the order of 20° (with small variations as the intensity transducer was moved from one measurement point to another). A phase angle error of the order of 3% (well within the accuracy of the Solartron 1170) will produce a corresponding error of less than 3% in the input intensity. Thus in this particular case the effects of errors in the measurement of input power are unlikely to be significant. The

slight deviations of the ratio $\frac{w'_{xwm}}{w_{in}}$ from the expected value of 50% are due to errors in the measurement of vibration intensity, w_x , along the beam.

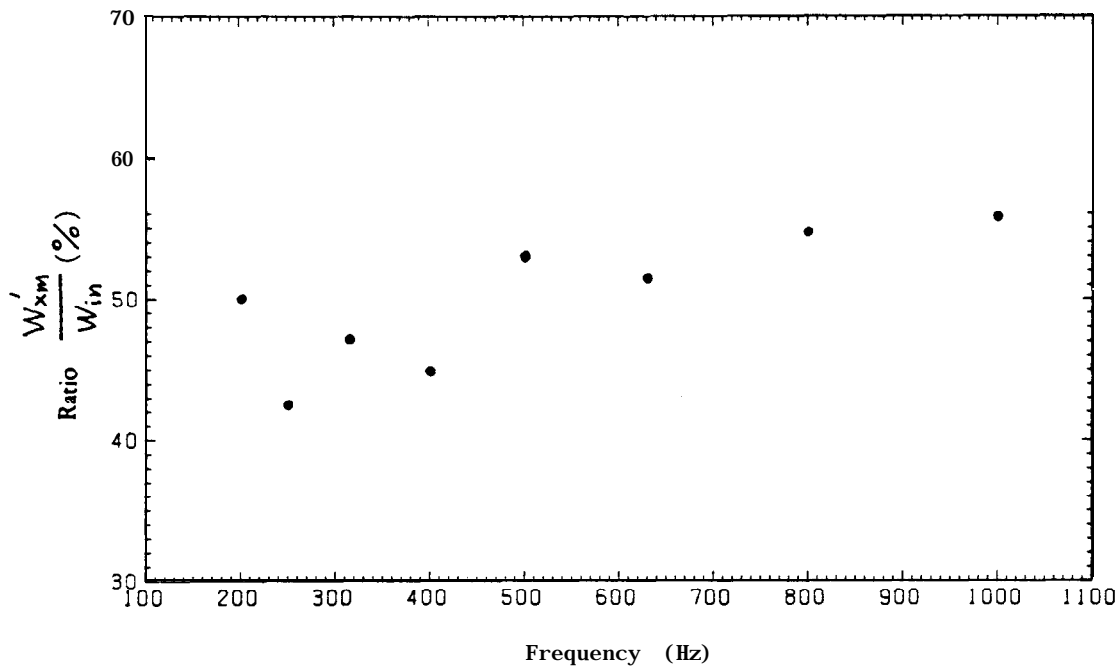


Fig.13 Measured variation of intensity with excitation frequency

6.4.3 Variation of intensity with excitation frequency

The vibration intensity was measured at a fixed point along the beam for various excitation frequencies. Again, the object was to verify the results of the theoretical study. Unfortunately, owing to the need to choose the excitation frequencies to coincide with the **center** frequencies of the **1/3** octave bands on the Analyser display unit, the number of possible excitation frequencies was very limited. Furthermore, at high frequencies the wavelength will be very small, and the base area of the transducer will have

to be very small in order to obtain reasonably accurate results. During the tests it was observed that at high frequencies (greater than about 1200Hz) the signals from the intensity transducer were quite noisy, and this was thought to be due to the flexibility as well as the base area of the intensity transducer. It was therefore decided to limit the tests to frequencies below 1000Hz.

The variation of the ratio w'_{xm}/w_{in} is shown in Fig.6.13 for a measurement 50cm from the driving point. Examination of the corresponding curve in Fig.6.9 shows that, theoretically, the ratio w'_{xm}/w_{in} should remain constant at about 50%. Fig.6.13 shows that for all the eight frequencies for which measurements were made the ratio remains within 20% of the expected value. This comparison is quite good, considering that in this test the phase angles were such that errors in the determination of input intensity could not be discounted.

6.5 Discussion

The errors in the experimental results presented in the foregoing sections may be classified into two broad groups as follows:

- (i) errors arising from the inherent limitations of the measuring technique; and
- (ii) errors caused by the difficulty of measuring the required kinematic quantities accurately.

We shall now discuss these sources of error with a view to assessing the suitability of the method for routine application to beam structures.

The main inherent source of error is the assumption that the force and

moment components of intensity are equal. This assumption is satisfied exactly only if the free-field solution alone is considered. However, there are many situations where the relationship $w_{xt} = w_{xm}$ is approximately true even in the nearfield. An example of this is a semi-infinite beam if measurements are made at a distance greater than a half-wavelength from the tip; see Appendix 3. The results of the theoretical study of our test structure lead us to the view that in practice the assumption that $w_{xt} = w_{xm}$ is not as restrictive as it appears. This view is reinforced by the results of computations carried out for a number of finite beams. A typical set of results is shown in Fig.6.14.

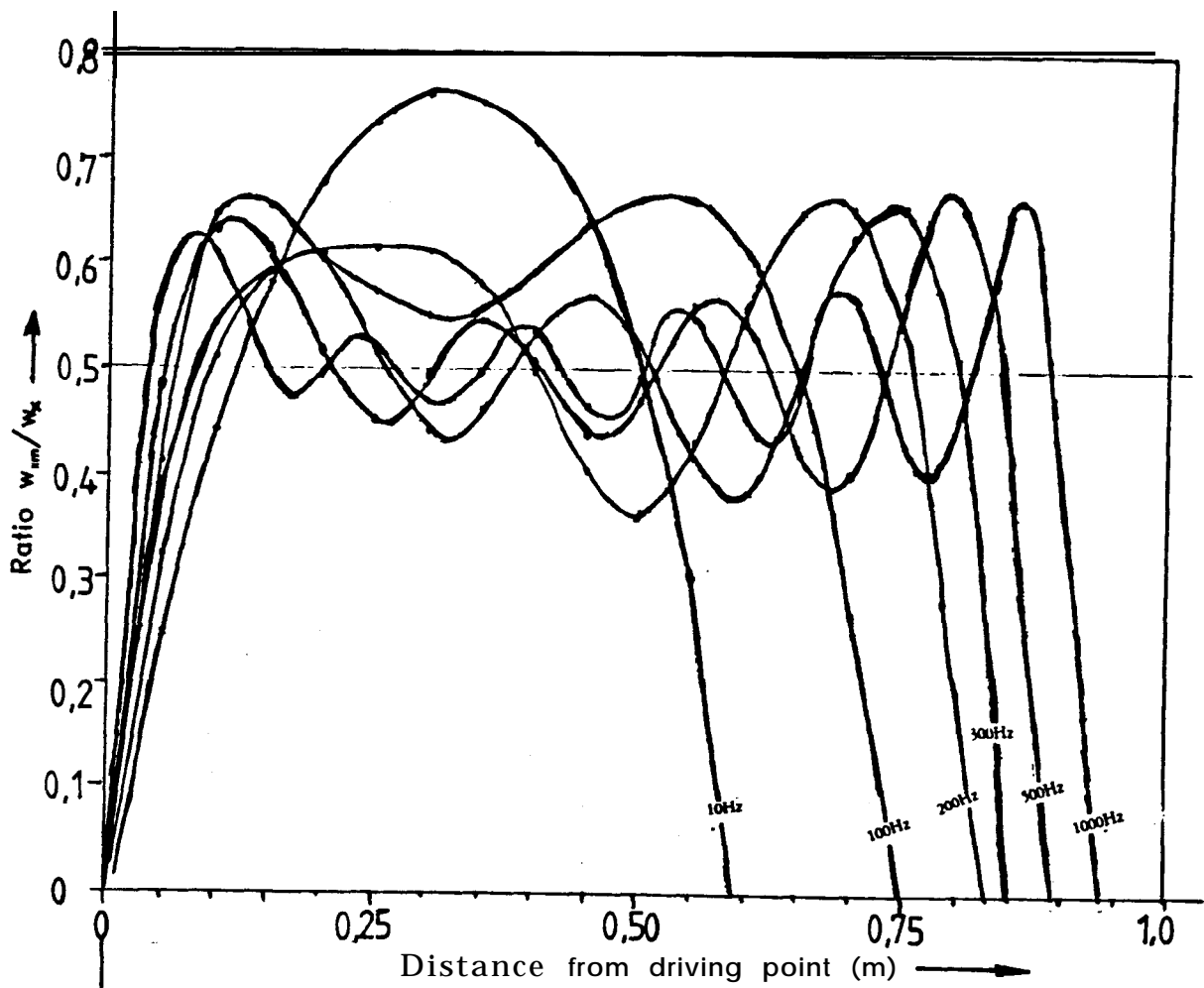


Fig.6.14 Computed variation of ratio w_{xm}/w_x along finite beam

Fig.6.14 shows the variation of the ratio w_{xm}/w_x with distance for a beam 1m long and of 40mm x 10mm cross-section, excited by a force at the tip. The beam is of mild steel and a damping loss factor of 0.01 is assumed. It is seen from the figure that provided the measurements are made at a high enough frequency and at a distance not too close to the ends of the beam, reasonable estimates of the vibration intensity can be obtained by assuming $w_{xt} = w_{xm}$. The higher the frequency the longer the span over which reasonable measurements can be made. It is important to note that beyond a certain distance from the driving-point the ratio w_{xm}/w_x becomes negative. Therefore, measurement beyond this distance will result in errors in the direction as well as the magnitude of the intensity.

Equation (6.11) shows that the measurement of intensity reduces to the determination of the rotational velocity, $\dot{\theta}$, and the transverse acceleration, $\ddot{\xi}$. The accuracy of vibration intensity measurements depends on how precisely these quantities can be measured. Transverse acceleration can be measured very accurately with an ordinary linear accelerometer. However, the rotational velocity cannot be measured easily because rotational transducers for routine vibration measurements are not yet available. In our experiments, the transverse and rotational motions were determined from the mean and difference of the signals from two ordinary linear accelerometers mounted on a block. One shortcoming of this method is that an error in one of the measuring channels will result in errors in both ξ and θ . When these are subsequently used in the calculation of intensity the error is further compounded. Small accelerometer sensitivity errors and phase mismatch of the measuring channels will have a significant effect on the accuracy of the vibration intensity. There will also be problems when measurements are made near nodes and antinodes. In the vicinity of an antinode the rotation is

small, and consequently the signals from the two accelerometers will be nearly equal. Signal processing involving the difference of two quantities which are nearly equal is prone to errors. A similar remark applies to the transverse acceleration in the vicinity of a node.

A number of mobility measurements were made in an attempt to assess the extent to which the shortcomings of the vibration intensity transducer have affected the accuracy of the intensity measurements. The accuracy of transverse measurements was checked against a measurement made with an ordinary accelerometer. The transfer mobilities measured by the two methods are shown in Fig.6.15. It is seen that the intensity transducer compares very well with the ordinary accelerometer.

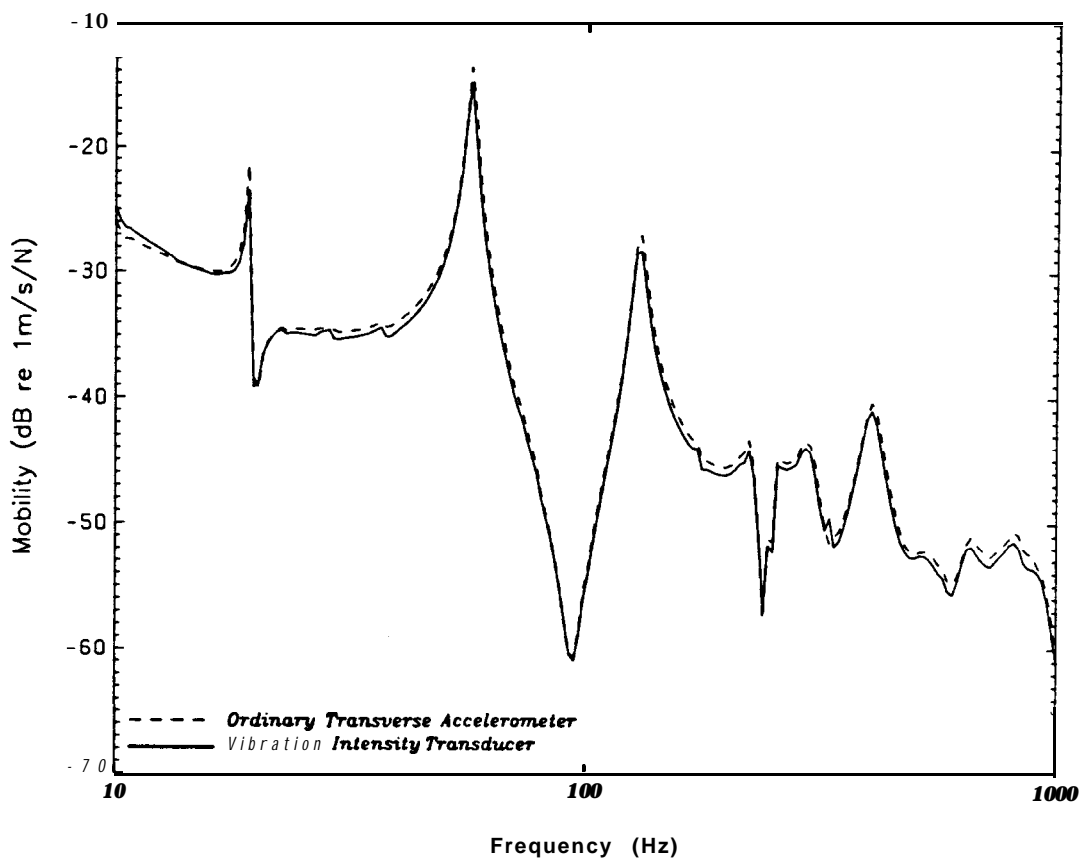


Fig.6.15 Comparison of transverse mobility measurements

In the case of rotation the measurements were compared with those of a new rotational accelerometer which is still under development? Since the rotational accelerometer has not yet been calibrated properly it cannot be used to judge the accuracy of the vibration intensity transducer. Nevertheless, one cannot fail to note the fact that the comparison between the measurements obtained from these two quite different transducers is fairly good. This observation, together with the fact that the intensity transducer measures transverse motion quite accurately, suggests that in our vibration intensity measurements errors caused by the shortcomings of the intensity transducer were not very severe.

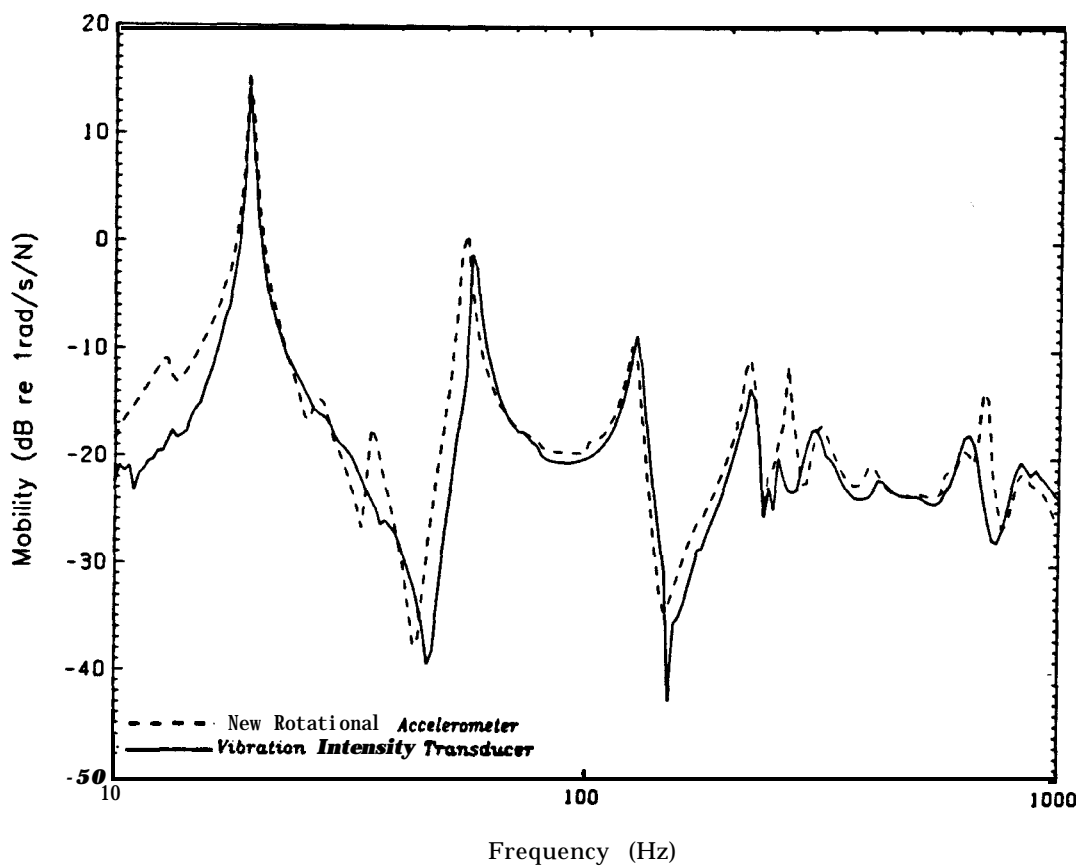


Fig.6.16 Comparison of rotational mobility measurements

† A new rotational accelerometer is currently being tested. It is, in fact, an ordinary accelerometer which has been modified so that it is sensitive to rotation rather than translation. That the accelerometer is sensitive to rotation has been established. What is now required is a suitable method for calibrating it.

The main conclusion which may be drawn from all our theoretical and experimental results is that Noiseux's method for vibration intensity measurements is quite accurate as far as beam structures are concerned. The requirement that measurements be made in the free field is not very restrictive. In practice, accurate results will be obtained provided that measurements are not made too close to the boundaries and sources of excitation. A more likely source of error is the measurement of rotation. Efforts to find a simple and accurate method for the measurement of rotation should continue.

Chapter 7

CONCLUSIONS

Various aspects of the flow of vibrational power in structures have been considered in this thesis. The main conclusions will now be discussed with some suggestions for further research.

In Chapter 2 the basic power and energy relations for vibrating systems were discussed with a study of spring-mass-damper systems, drawing on well-known concepts in Electrical Engineering. By studying the dependence of **time-average** power, velocity amplitude and force transmissibility on frequency and damping for the simple oscillator, it was shown that an increase of the time-average power does not necessarily lead to a higher amplitude of vibration response, and vice versa. A brief study of the undamped dynamic vibration absorber system also showed that a reduction in the instantaneous power flow to any part of a vibrating system could be accompanied by an increase **of** its amplitude of vibration. The conclusion to be drawn from these observations is that vibrational power flow is not a suitable sole indicator of vibration response levels.

The general procedure for calculating the power flow to the components of a connected structure was indicated in Chapter 3. It was shown that the basic Impedance Coupling relation cannot be derived by considering power balance alone. This result is evidence that power flow data are of a less general nature than frequency response data. The flow of energy in the various coordinate directions at the joints between connected structures was also discussed. This discussion set the scene for the proposal, in Chapter 4, of a method for assessing the relative importance of coordinates when the Impedance Coupling technique is used in the vibration analysis of connected

structures. The method is based on the assumption that the relative importance of any coordinate is determined by the magnitude of the energy transferred in the direction of that coordinate. The proposed method was tried on a range of test structures, and it was found that there was always a direct correlation between the magnitude of energy transfer in any coordinate direction and the effect on the responses of excluding that particular coordinate from the analysis. The conclusion that may be drawn from this is that the underlying assumption of the proposed method is sound and that the method works.

The frequency response data for the structures studied in Chapter 4 were generated theoretically. One way of carrying this study further would be to apply the method to structures whose data have been determined experimentally. The object would be to find out whether or not measured frequency response data are accurate enough to be used in the application of the method. Two possible applications of the proposed method which require further study were mentioned in Chapter 4. The first is the comparison of rotational and translational mobility data, a comparison which is difficult because of the different units involved. It is being suggested that this comparison could be done on the basis of energy transfer. The other application is the assessment of the relative importance of various vibration transmission paths in a structure. This assessment could be based on a computation of the energy transfer via each of the groups of coordinate directions involved.

An evaluation was presented in Chapter 5 of a method proposed in the literature for designing vibration isolation systems. The proposed method aims at reducing the time-average power flow to the foundation. By studying the simple machine-isolator-foundation problem, it was shown that the method is applicable only where the machine interacts with the foundation with one

degree of freedom, and any reduction of power flow is brought about by altering the characteristics of the machine-isolator subsystem alone. A number of examples were considered where a reduction of the time-average power flow results in an increase of the amplitude of the force and motion transmitted to the foundation. The method is not applicable where the machine interacts with the foundation in more than one coordinate direction. This is because power, being a single scalar quantity, cannot be directly related to response amplitudes except in situations where the motion response can also be represented by a single quantity. The conclusion is that the design of vibration isolation systems on the sole basis of a reduction of time-average power flow does not guarantee successful isolation and, therefore, the proposed method must be applied with great caution.

Several methods have been proposed in the literature for the measurement of vibrational power flow in structures. The method due to Noiseux has been used for measuring the vibration intensity (time-average power flow per unit width of cross-section) in a simple beam structure. The experimental and theoretical results presented in Chapter 6 lead to the conclusion that Noiseux's method is quite accurate as far as beam structures are concerned. The requirement that measurements be made in the free-field is not very restrictive in practice, and problems with the method are more likely to arise from the difficulty of measuring rotational motion accurately.

Noiseux's method is also applicable to uniform plates, and it is suggested that a theoretical and experimental study be carried out along similar lines to those in Chapter 6. There is also a need to carry out an experimental study of the practical use of vibration intensity measurements in vibration path identification. However, such a study should be preceded by efforts to find an accurate method for the routine measurement of rotational motion. In our experiments rotation was obtained from the difference of the signals

from two linear accelerometers. Further studies are required to assess the accuracy of the two-accelerometer method of measuring rotation. Efforts to develop a simple rotational accelerometer should also be stepped up.

It has been intended to provide an answer to the following question: Is the power flow method any better than the well-established methods based on frequency response data? In order to answer this question it is helpful to consider briefly the nature of the information contained in the two types of data. Frequency response data are of a very general nature in the sense that they represent the input-output (force-motion) characteristics of a structure for the particular coordinates under consideration. The main application of frequency response data is in the construction of mathematical models of test structures for use in further vibration analysis. One such analysis is the prediction of the dynamic characteristics of a complex structure by using the models of its component parts. Mathematical models may also be used to predict the response of structures to various combinations of excitation forces and to study the effects of modifications.

In comparison with frequency response data, power flow data are less general because they relate to the particular excitation forces prevailing. The information obtainable from power flow depends on the particular form in which the data is presented. Perhaps the least useful form arises when the data is given as a single scalar quantity representing the total time-average power flow to a structure. It is not possible to obtain from this data any detailed information about the dynamic characteristics of the structure; nor is it possible to learn much about the excitation forces. A more useful form of power flow data is a set of vibration intensity vectors giving the magnitude and direction of the time-average power flow per unit width at a number of points over a structure. In this form, the data could

be used to determine the locations of high energy dissipation and to identify vibration sources and transmission paths. At the present time it may be argued that methods based on power flow data do not offer any significant advantage over the more traditional methods. However, the use of power flow and energy in vibration problems outside the context of Statistical Energy Analysis is in its infancy and, therefore, a definitive comparison with other methods is premature. The potential of power flow methods is quite considerable and lies mainly in the area of diagnostics. Unlike mobility properties, power flow characteristics may be obtained from measurements made when a structure is in service and is vibrating as a result of forces prevailing under operating conditions. In such a case, power measurements could provide information about the relative strengths of excitation sources as well as the paths by which vibration is being transmitted. It may be argued that if the mathematical model of a structure has been formulated, the forces causing the vibration may be determined by using measurements of the actual vibration levels of the structure in service. However, the determination of excitation forces in this way is very difficult in practice. But for the immense measurement difficulties, power flow could provide an easier way of assessing the relative magnitudes of excitation forces. As measurement techniques improve we can expect to see a gradual realisation of the potential of power flow methods.

In parts of this thesis arguments have been put forward against the use of power flow in certain vibration problems. The intention has not been to suggest that methods based on power flow and energy are inferior to other more traditional methods. There are certainly many uses for power flow data, as exemplified by the method proposed in Chapter 4. Further research is required to identify other ways in which power and energy may be used in vibration problems. What is being urged here is that any proposed applications should be based on results that have been proved analytically or experimentally and not merely assumed.

REFERENCES

1. R. H. LYON and G. MAIDANIK 1962 *Journal of the Acoustical Society of America*, Vol.34, No.5, pp623-639 Power flow between linearly coupled oscillators
2. P.W. SMITH and R.H. LYON 1965 *NASA Contractor Report CR-160* Sound and Structural Vibration
3. E.E. UNGAR 1967 *Trans. ASME Journal of Engineering for Industry*, 89, pp626-632 Statistical Energy Analysis of Vibrating Systems
4. E.E. UNGAR and J.E. MANNING 1968 In: *Dynamics of Structural Solids ASME, New York* Analysis of Vibratory Energy Distribution in Composite Structures
5. R.H. LYON 1970 *The Shock and Vibration Digest Vol.2, No.6* pp2-11 What good is Statistical Energy Analysis anyway?
6. L. CREMER, M. HECKL and E.E. UNGAR 1973 *Structure-borne Sound* 2nd Edition Springer-Verlag N. York
7. F.J. FAHY 1974 *The Shock and Vibration Digest Vol.6, No. 7* pp14-33 Statistical Energy Analysis - A Critical Review
8. R.H. LYON 1975 *Statistical Energy Analysis of Dynamical Systems: Theory and Applications* MIT Press
9. J. WOODHOUSE 1981 *Journal of the Acoustical Society of America* 69 (6), pp1695-1709 An Approach to the Theoretical Background of Statistical Energy Analysis applied to Structural Vibration
10. G. MAIDANIK 1981 *Journal of Sound and Vibration* 78 (3), pp4 17-423 Extension and Reformulation of Statistical Energy Analysis with use of Room Acoustics Concepts
11. J. WOODHOUSE 1981 *Applied Acoustics* 14, pp445-469 An Introduction to Statistical Energy Analysis of Structural Vibration
12. B.L. CLARKSON, R.J. CUMMINS, D.C.G. EATON and J.P. VESSAZ 1981 *European Space Agency Journal*, Vol.5, No.2 pp137-152 Prediction of High Frequency Structural Vibration using Statistical Energy Analysis (SEA)
13. H. G. D. GOYDER and R. G. WHITE 1980 *Journal of Sound and Vibration* 68(1), pp59-75. Vibrational Power Flow from Machines into Built-up Structures, Part 1: Introduction and Approximate Analysis of Beam and Plate-like Foundations.
14. H. G. D. GOYDER and R. G. WHITE 1980 *Journal of Sound and Vibration* 68(1), pp77-96. Vibrational Power Flow from Machines into Built-up Structures, Part 2: Wave Propagation and Power Flow in Beam-stiffened Plates.

15. H. G. D. GOYDER and R. G. WHITE 1960 *Journal of Sound and Vibration* **68(1)**, pp97-117 Vibrational Power Flow from Machines into Built-up Structures, Part 3: Power Flow through Isolation systems.
16. R. J. PINNINGTON and R. G. WHITE 1961 *Journal of Sound and Vibration* **75(2)**, pp179-197. Power Flow through Machine Isolators to Resonant and Non-resonant Beams.
17. J.W. VERHEIJ 1982 *Doctoral Thesis of the University of Technology, Delft, The Netherlands* Multi-path Sound Transfer from Resiliently Mounted Shipboard Machinery
18. L. FROMMER and A. MURRAY 1945 *Journal of the Iron & Steel Institute* Vol.151, pp45-53. The Influence of the Heat Treatment of Steel on the Damping Capacity at Low Stresses
19. W.J. MCGONNAGLE 1961 *Nondestructive Testing* McGraw-Hill Book Company Inc., New York
20. J.M.W. BROWNJOHN and G.H. STEELE 1980 *B.Sc Report, Department of Mechanical Engineering, University of Bristol* Nondestructive Testing using Measurements of Structural Damping
21. I. G. KAVADIAS 1982 *M.Sc Dissertation, Mechanical Engineering Department, Imperial College* Measurement of Local Damping in Structures
22. J.M.W BROWNJOHN, G.H STEELE, P CAWLEY and R.D ADAMS 1980 *Journal of Sound and Vibration* **73(3)**, pp461-468 Error in Mechanical Impedance Data obtained with Impedance Heads.
23. G. E. OTTESEN and T. E. VIGRAN 1979 *Applied Acoustics* **12**, pp243-252 Measurement of Mechanical Input Power with Applications to Wall Structures.
24. P. B. SWIFT and D. A. BIES 1975 *90th Meeting of the Acoustical Society of America, San Francisco, Nov. 1975*. Steady-state measurement of Loss Factors.
25. D. A. BIES and S. HAMID 1980 *Journal of Sound and Vibration* **70(2)**, pp187-204. In-situ Determination of Loss and Coupling Loss Factors by the Power Injection Method.
26. F. J. FAHY 1969 *Journal of Sound and Vibration* **10(3)**, pp517-518. Measurement of Mechanical Power Input to a Structure.
27. D. U. NOISEUX 1970 *Journal of the Acoustical Society of America* **47**, pp238-247. Measurement of Power Flow in Uniform Beams and Plates.
28. P. RASMUSSEN 1982 *Bruel and Kjaer technical paper* Measurement of Vibration Intensity
29. G. PAVIC 1976 *Journal of Sound and Vibration* **49(2)**, pp221-230. Measurement of Structure Borne Wave Intensity, Part 1: Formulation of the Methods.

30. H. G. D. GOYDER 1980 *Journal of Sound and Vibration* **68(2)**, pp209-230. Methods and Application of Structural Modelling from Measured Structural Frequency Response Data.
31. G. PAVIC 1976 *Ph. D Thesis, University of Southampton, England*. Techniques for the Determination of Vibration Transmission Mechanisms in Structures.
32. F. J. FAHY and R. PIERRI 1977 *Journal of the Acoustical Society of America* **62(5)**, pp1297-1298. Application of Cross-Spectral Density to a Measurement of Vibration Power Flow between Connected Plates.
33. J. W. VERHEIJ 1980 *Journal of Sound and Vibration*, **70(1)**, pp133- 139 Cross-Spectral Density Methods for Measuring structure Borne Power Flow on Beams and Pipes.
34. R.E.D. BISHOP and D.C. JOHNSON 1960 *The Mechanics of Vibration* Cambridge University Press
35. D.J. EWINS *Journal of the Society of Environmental Engineers* Dec. 1975 - June 1976 Measurement and Application of Mechanical Impedance Data:
Part I. Introduction and Ground Rules
Part II. Measurement Techniques
Part III. Interpretation and Application of Measured Data
36. R.E.D. BISHOP, G.M.L. GLADWELL and S. MICHAELSON 1965 *The Matrix Analysis of Vibration* Cambridge University Press
37. J.W. STRUTT (BARON RAYLEIGH) 1945 *The Theory of Sound* Dover Publications, New York
(See Vol. I §80)
38. E.A. GUILLEMIN 1963 *Theory of Linear Physical Systems* John Wiley & Sons, N.York (Chapters 5 and 8)
39. D.J. EWINS, J.M.M. SILVA and G. MALECI 1980 *The Shock and Vibration Bulletin* **50 (2)** Vibration Analysis of a Helicopter plus an Externally-attached Structure
40. J. ANTONIO 1980 *MSc Disertation, Mechanical Engineering Department, Imperial College* Vibration Analysis of Connected Structures
41. M.G. SAINSBURY and D.J. EWINS August 1974 *Journal of Engineering for Industry* Vibration Analysis of a Damped Machinery Foundation using the Dynamic Stiffness Coupling Technique
42. D.J. EWINS September 1979 *Journal of the Society of Environmental Engineers* Whys and Wherefores of Modal Testing
43. E.J. SKUDRZYK 1958 *Journal of the Acoustical Society of America* Vol.30, No.12, pp1140-1152 Vibration of Systems with a Finite and an Infinite Number of Resonances

44. E.J. SKUDRZYK 1968 The Pennsylvania State University Press *Simple and Complex Vibratory Systems*
45. M.G. SAINSBURY May 1975 *User's Guide for the Structural Dynamic Analysis Computer Program COUPLE 1* Dynamics Group, Mechanical Engineering Department, Imperial College
(Manual in 3 parts. Program modified in 1981 under the name COUPLE2)
46. M.G. SAINSBURY September 1976 *Experimental and Theoretical Techniques for the Vibration Analysis of Damped Complex Structures* Doctoral Thesis, Imperial College.
47. H. W. BODE 1947 *Network Analysis and Feedback Amplifier Design* D Van Nostrand Company Inc. New York. (Cited in ref. 15) Chapter 14
48. M. A. HECKL 1961 *Compendium of Impedance Formulas* Bolt Beranek and Newman Inc. Report No. 774.
49. M. A. HECKL 1976 *Proceedings of the International Symposium on Shipboard Acoustics* The different ways of sound transmission in and around resilient mounts.
50. *Bruel & Kjaer* 1982 Instruction manual, Sound Intensity Analysing System Type 3360
51. P. GROOTENHUIS 1970 *Journal of Sound and Vibration*, 1 1(4), pp421– 433
The Control of Vibrations with Viscoelastic Materials
52. F.J. FAHY 1977 *Journal of the Acoustical Society of America*, Vol.62, No. 4, pp1057–1 059 Measurement of Acoustic Intensity using the Cross-spectral Density of Two Microphone Signals
53. L.E. KINSLER, A.R. FREY, A.B. COPPENS and J.V. SANDERS 1982 *Fundamentals of Acoustics* Third Edition. John Wiley & Sons

APPENDIX 1

DETERMINATION OF VARIOUS AREAS UNDER INSTANTANEOUS POWER CURVE

Determination of E_{neg}

The area labelled E_{neg} in Fig.1A is the same as the cross-hatched area in Fig. 1 B.

Fig. 1A

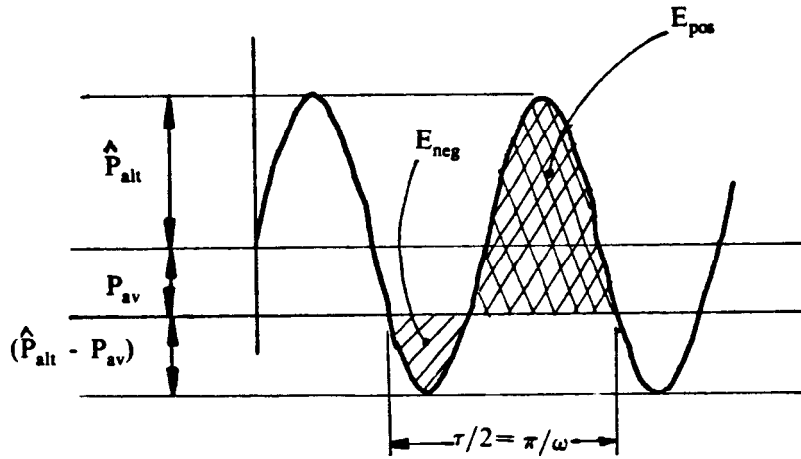
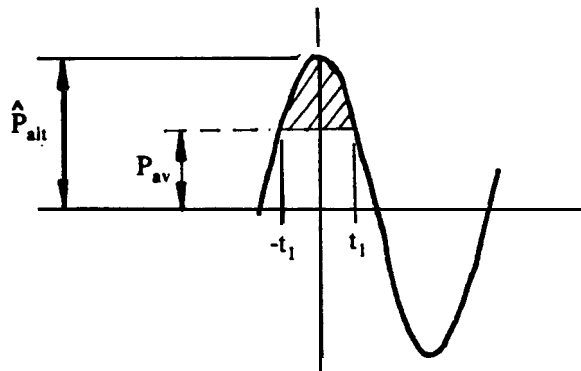


Fig. 1B



The curve in Fig. 1B is of the form $\hat{P}_{alt} \cos 2\omega t$. The time t , is given by

$$t_1 = \frac{1}{2\omega} \cos^{-1}\left(\frac{P_{av}}{\hat{P}_{alt}}\right)$$

The total area under the curve from $-t_1$ to t_1 , is

$$A = 2 \int_0^{t_1} \hat{P}_{alt} \cos 2\omega t \, dt$$

$$= \frac{\hat{P}_{alt}}{\omega} \sin 2\omega t_1$$

Now, $\sin 2\omega t_1 = \sqrt{1 - \cos^2 2\omega t_1} = \sqrt{1 - \left(\frac{P_{av}}{\hat{P}_{alt}}\right)^2}$

Therefore

$$A = \frac{\hat{P}_{alt}}{\omega} \sqrt{1 - \left(\frac{P_{av}}{\hat{P}_{alt}}\right)^2}$$

Also, the area of the unshaded portion under the curve is

$$P_{av} \times 2t_1 = \frac{P_{av}}{\omega} \cos^{-1}\left(\frac{P_{av}}{\hat{P}_{alt}}\right)$$

Therefore the area of the shaded portion is

$$E_{neg} = \frac{\hat{P}_{alt}}{\omega} \sqrt{1 - \left(\frac{P_{av}}{\hat{P}_{alt}}\right)^2} - \frac{P_{av}}{\omega} \cos^{-1}\left(\frac{P_{av}}{\hat{P}_{alt}}\right)$$

$$= \frac{\hat{P}_{alt}}{\omega} (\sin \phi - \phi \cos \phi)$$

where $\phi = \cos^{-1}\left(\frac{P_{av}}{\hat{P}_{alt}}\right)$

Determination of E_{pos}

The area E_{pos} may be determined by using the fact that

$$E_{pos} - E_{neg} = P_{av} \frac{\tau}{2}$$

and therefore

$$E_{pos} = P_{av} \frac{\tau}{2} + E_{neg}$$

$$= P_{av} \frac{\pi}{\omega} + \frac{\hat{P}_{alt}}{\omega} (\sin \phi - \phi \cos \phi)$$

$$= \frac{\hat{P}_{alt}}{\omega} \pi \cos \phi + \frac{\hat{P}_{alt}}{\omega} (\sin \phi - \phi \cos \phi)$$

$$= \frac{\hat{P}_{alt}}{\omega} ((\pi - \phi) \cos \phi + \sin \phi)$$

APPENDIX 2

THE INFLUENCE OF DAMPING ON THE MOBILITY OF THE SIMPLE OSCILLATOR

The mobility of the simple 1-degree-of-freedom spring-mass system with hysteretic damping is

$$Y = \frac{j\omega}{k - \omega^2 M + jk\eta}$$

where M, k and η are respectively the mass, stiffness and hysteretic damping loss factor.

The real and imaginary parts of the mobility are

$$Re\{Y\} = \frac{\omega k \eta}{(k - \omega^2 M)^2 + k^2 \eta^2}$$

$$Im\{Y\} = \frac{\omega(k - \omega^2 M)}{(k - \omega^2 M)^2 + k^2 \eta^2}$$

Consider a plot of the mobility on the complex plane. We wish to trace the locus of the mobility as the damping loss factor is increased from zero to infinity, with the frequency being kept constant. We assume that the locus is circular with centre at $(0, \omega/2(k - \omega^2 M))$ and radius $\omega/2(k - \omega^2 M)$. If this assumption is true then the following condition must hold:

$$Re^2 + \left(Im - \frac{\omega}{2(k - \omega^2 M)}\right)^2 = \left(\frac{\omega}{2(k - \omega^2 M)}\right)^2$$

where $Re = Re\{Y\}$, and $Im = Im\{Y\}$

The above condition is equivalent to

$$R e^2 + I m^2 = I m. \frac{\omega}{(k - \omega^2 M)}$$

Now

$$\begin{aligned} R e^2 + I m^2 &= \left(\frac{\omega k \eta}{(k - \omega^2 M)^2 + k^2 \eta^2} \right)^2 + \left(\frac{\omega(k - \omega^2 M)}{(k - \omega^2 M)^2 + k^2 \eta^2} \right)^2 \\ &= \frac{\omega^2 k^2 \eta^2 + \omega^2 (k - \omega^2 M)^2}{[(k - \omega^2 M)^2 + k^2 \eta^2]^2} \\ &= \frac{\omega^2}{(k - \omega^2 M)^2 + k^2 \eta^2} \\ &= I m. \frac{\omega}{(k - \omega^2 M)} \end{aligned}$$

as was to be shown.

The locus of the mobility is shown in Figures 2A, 2B and 2C for the three possible excitation cases.

Fig.2A
Excitation
below Resonance

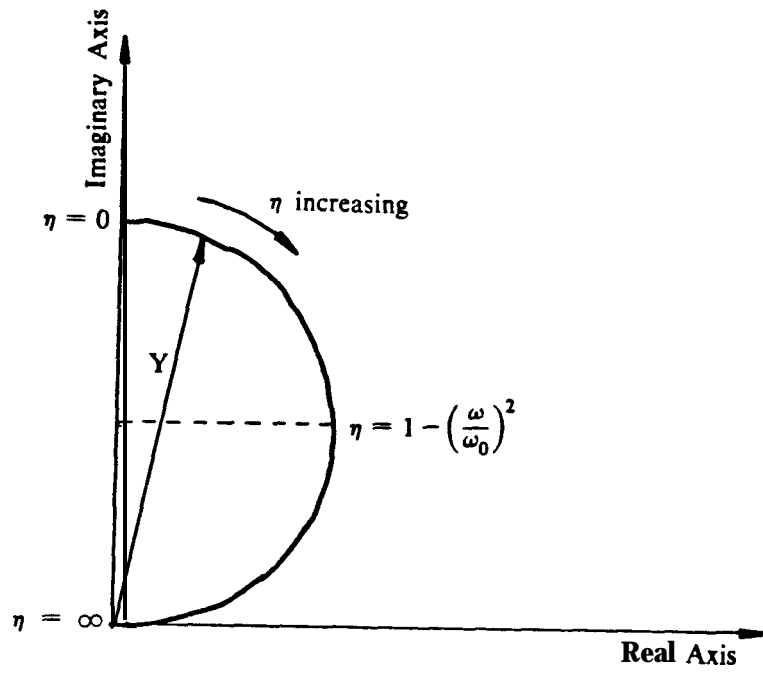


Fig.2B
Excitation
at Resonance

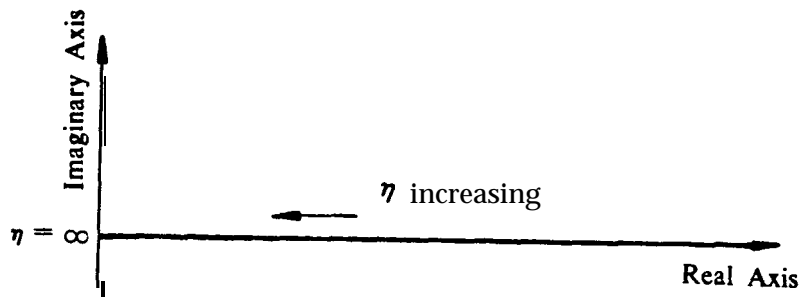
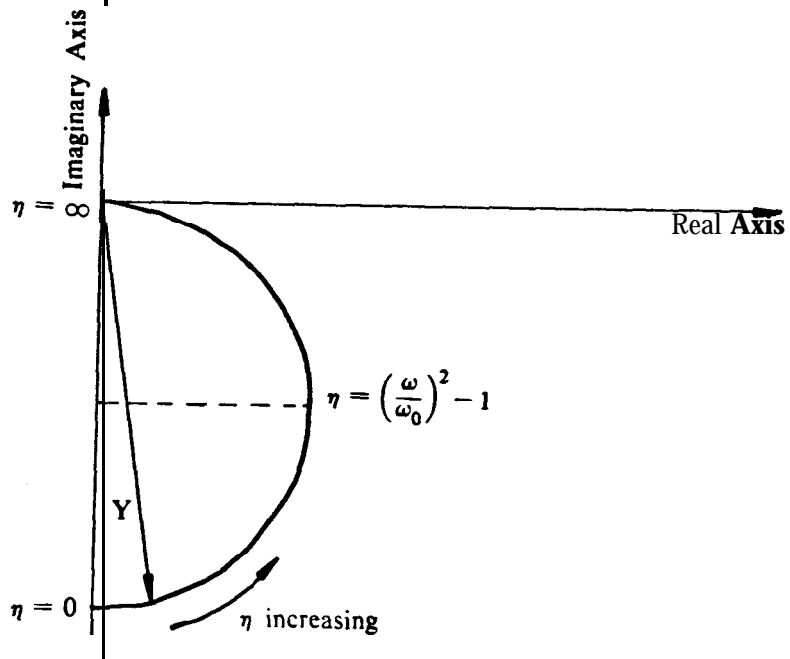


Fig.2C
Excitation
above Resonance



APPENDIX 3

ANALYSIS OF VIBRATION INTENSITY IN UNIFORM BEAMS

For a uniform undamped beam vibrating in flexure at a frequency ω , the complex representation of the transverse displacement is [53]

$$\xi(x, t, \omega) = e^{j\omega t} [A_1(\omega)e^{-jkx} + A_2(\omega)e^{jkx} + B_1(\omega)e^{-kx} + B_2(\omega)e^{kx}] \quad (3-1)$$

where A_1 , A_2 , B_1 and B_2 are complex constants and k is the wavenumber.

Free-field solution

The free-field solution is represented by the first two terms of equation (3-1):

$$\xi(x, \omega) = A_1(\omega)e^{-jkx} + A_2(\omega)e^{jkx} \quad (3-2)$$

where the time factor $e^{j\omega t}$ has been omitted.

The transverse velocity is

$$v = \frac{\partial \xi}{\partial t} = j\omega [A_1(\omega)e^{-jkx} + A_2(\omega)e^{jkx}] \quad (3-3)$$

and the shear force associated with the wave is

$$\begin{aligned} Q &= -EI \left(\frac{\partial^3 \xi}{\partial x^3} \right) \\ &= -k^3 EI e^{j\omega t} j [A_1(\omega)e^{-jkx} - A_2(\omega)e^{jkx}] \end{aligned} \quad (3-4)$$

where E is the Modulus of Elasticity and I is the second moment of area.

Thus the force component of the intensity is'

$$\begin{aligned} w_{xf} &= -\frac{1}{b} \langle \text{Re}\{Q\} \text{Re}\{v\} \rangle, \\ &= -\frac{1}{2b} \text{Re}\{Qv^*\} \\ &= \frac{1}{2} E I_0 k^3 \omega (|A_1|^2 - |A_2|^2) \end{aligned} \quad (3-5)$$

where b is the width of the beam and I , is the second moment of area per unit width.

The rotational velocity is

$$\begin{aligned} \dot{\theta}_x &= \frac{\partial}{\partial t} \left(\frac{\partial \xi}{\partial x} \right) \\ &= j\omega [-jk A_1(\omega) e^{-jkx} + jk A_2(\omega) e^{jkx}] \\ &= k\omega [A_1(\omega) e^{-jkx} - A_2(\omega) e^{jkx}] \end{aligned} \quad (3-6)$$

and the bending moment associated with the wave is

$$\begin{aligned} iu &= EI \frac{\partial^2 \xi}{\partial x^2} \\ &= -EI k^2 [A_1(\omega) e^{-jkx} + A_2(\omega) e^{jkx}] \end{aligned} \quad (3-7)$$

Thus the moment component of the intensity is

$$\begin{aligned} w_{xm} &= -\frac{1}{2b} \text{Re}\{M \dot{\theta}^*\} \\ &= \frac{1}{2} E I_0 k^3 \omega (|A_1|^2 - |A_2|^2) \end{aligned} \quad (3-8)$$

The force and moment components of the intensity are therefore equal.

†Note that under the sign convention adopted (see Chapter 6) the shear force Q is in the -ve y direction, and hence a negative sign is introduced in the expression for the force component of intensity. A similar remark applies to the moment component of intensity.

Semi-infinite beam

Consider an undamped semi-infinite beam excited at one end $x=0$. Since there are no reflected waves travelling in the -ve x direction the complex amplitude of the transverse displacement is

$$\xi(x, \omega) = A_1 e^{-jkx} + B_1 e^{-kx} \tag{3-9}$$

and the amplitude of the transverse velocity is

$$v(x, \omega) = j\omega [A_1 e^{-jkx} + B_1 e^{-kx}] \tag{3-10}$$

Now

$$\frac{\partial^3 \xi}{\partial x^3} = k^3 [jA_1 e^{-jkx} - B_1 e^{-kx}] \tag{3-11}$$

and therefore the shear force associated with the wave is

$$Q = -EI \left(\frac{\partial^3 \xi}{\partial x^3} \right) = -EI k^3 [jA_1 e^{-jkx} - B_1 e^{-kx}] \tag{3-12}$$

The force component of the intensity is then

$$\begin{aligned} wxf &= -\frac{1}{2b} \operatorname{Re} \{ Q v^* \} \\ &= -\frac{1}{2b} \operatorname{Re} \{ -EI k^3 [jA_1 e^{-jkx} - B_1 e^{-kx}] (-j\omega) [A_1^* e^{jkx} + B_1^* e^{-kx}] \} \\ &= -\frac{EI_0 k^3 \omega}{2} \operatorname{Re} \{ (jA_1 e^{-jkx} - B_1 e^{-kx}) (jA_1^* e^{jkx} + jB_1^* e^{-kx}) \} \\ &= \frac{EI_0 k^3 \omega}{2} \operatorname{Re} \{ -|A_1|^2 - j|B_1|^2 e^{-2kx} - jB_1 A_1^* e^{-kx} e^{jkx} - B_1^* A_1 e^{-kx} e^{-jkx} \} \\ &= \frac{EI_0 k^3 \omega}{2} \operatorname{Re} \{ |A_1|^2 + e^{-kx} [jB_1 A_1^* e^{jkx} + B_1^* A_1 e^{-jkx}] \} \end{aligned} \tag{3-13}$$

Now write $A_1 = |A_1| e^{j\phi_A}$ and $B_1 = |B_1| e^{j\phi_B}$

so that $B_1 A_1^* = |A_1 B_1| e^{j(\phi_B - \phi_A)} = |A_1 B_1| e^{j\phi}$

and $B_1^* A_1 = |A_1 B_1| e^{-j(\phi_B - \phi_A)} = |A_1 B_1| e^{-j\phi}$

where $\phi = (\phi_B - \phi_A)$

Then equation (3-13) may be written as

$$\begin{aligned}
 w_{xf} &= \frac{EI_0 k^3 \omega}{2} R e \{ |A_1|^2 + e^{-kx} |A_1 B_1| (j e^{j(kx+\phi)} + e^{-j(kx+\phi)}) \} \\
 &= \frac{EI_0 k^3 \omega}{2} (|A_1|^2 + e^{-kx} |A_1 B_1| [\cos(kx + \phi) - \sin(kx + \phi)])
 \end{aligned} \tag{3-14}$$

The bending moment associated with the wave is

$$M = EI \frac{\partial^2 \xi}{\partial x^2} = -EI k^2 [A_1 e^{-jkx} - B_1 e^{-kx}] \tag{3-15}$$

and the rotational velocity is

$$\dot{\theta}_x = \frac{\partial}{\partial t} \left(\frac{\partial \xi}{\partial x} \right) = \omega k [A_1 e^{-jkx} - j B_1 e^{-kx}] \tag{3-16}$$

The moment component of the intensity is therefore given by

$$\begin{aligned}
 w_{xm} &= -\frac{1}{2b} R e \{ M \dot{\theta}_x \} \\
 &= \frac{EI_0 k^3 \omega}{2} R e \{ [A_1 e^{-jkx} - B_1 e^{-kx}] [A_1 \dot{e}^{jkx} + j B_1 \dot{e}^{-kx}] \} \\
 &= \frac{EI_0 k^3 \omega}{2} R e \{ |A_1|^2 - j |B_1|^2 e^{-2kx} - B_1 A_1 \dot{e}^{-kx} e^{jkx} + j B_1 A_1 e^{-kx} e^{-jkx} \} \\
 &= \frac{EI_0 k^3 \omega}{2} R e \{ |A_1|^2 - e^{-kx} |A_1 B_1| [e^{j(kx+\phi)} - j e^{-j(kx+\phi)}] \} \\
 &= \frac{EI_0 k^3 \omega}{2} (|A_1|^2 - e^{-kx} |A_1 B_1| [\cos(kx + \phi) - \sin(kx + \phi)])
 \end{aligned} \tag{3-17}$$

The total intensity is then

$$w_x = w_{xf} + w_{xm} = EI_0 k^3 \omega |A_1|^2 \tag{3-18}$$

If the only excitation present is a force F at x=0, then

$$A_1 = B_1 = \frac{F}{2EI_0 k^3} (1 + j)$$

and the total intensity is

$$w_x = \frac{\omega |F|^2}{2E I_0 k^3} \tag{3-19}$$

and the components of the intensity are

$$w_{xf} = \frac{w_x}{2} [1 + e^{-kx} (\cos kx - \sin kx)] \tag{3-20}$$

and

$$w_{xm} = \frac{w_x}{2} [1 - e^{-kx} (\cos kx - \sin kx)] \tag{3-21}$$

The variation of the ratios $\frac{w_{xf}}{w_x}$ and $\frac{w_{xm}}{w_x}$ is shown in Fig.3A. It is seen that at distances greater than a half-wavelength ($x > \frac{\pi}{k}$) from the tip of the beam the two components of the intensity are practically equal.

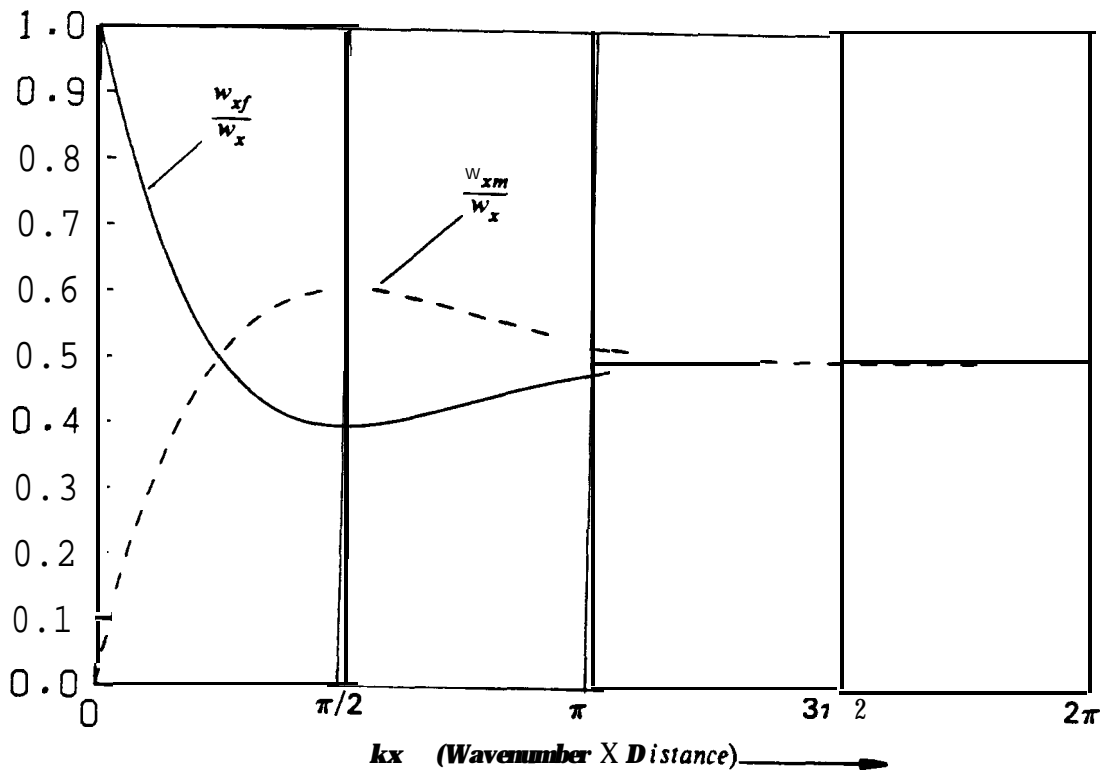


Fig.3A. Variation of components of intensity for semi-infinite beam